Downloaded from orbit.dtu.dk on: Dec 19, 2017

Technical University of Denmark

Optics and Fluid Dynamics Department annual progress report for 1999

Hanson, Steen Grüner; Johansen, Per Michael; Lynov, Jens-Peter; Skaarup, Bitten

Publication date:
2000

Document Version
Publisher's PDF, also known as Version of record

Link back to DTU Orbit

Citation (APA):
Hanson, S. G., Johansen, P. M., Lynov, J-P., & Skaarup, B. (2000). Optics and Fluid Dynamics Department annual progress report for 1999. (Denmark. Forskningscenter Risoe. Risoe-R; No. 1157(EN)).

DTU Library
Technical Information Center of Denmark

General rights
Copyright and moral rights for the publications made accessible in the public portal are retained by the authors and/or other copyright owners and it is a condition of accessing publications that users recognise and abide by the legal requirements associated with these rights.

- Users may download and print one copy of any publication from the public portal for the purpose of private study or research.
- You may not further distribute the material or use it for any profit-making activity or commercial gain
- You may freely distribute the URL identifying the publication in the public portal

If you believe that this document breaches copyright please contact us providing details, and we will remove access to the work immediately and investigate your claim.

Optics and Fluid Dynamics Department
Annual Progress Report for 1999

Risø-R-1157(EN)

**Edited by S.G. Hanson, P.M. Johansen,
J.P. Lynov and B. Skaarup**

**Risø National Laboratory, Roskilde, Denmark
May 2000**

Abstract The Optics and Fluid Dynamics Department performs basic and applied research within the three programmes: (1) optical materials, (2) optical diagnostics and information processing and (3) plasma and fluid dynamics. The department has core competences in: optical sensors, optical materials, biooptics, numerical modelling and information processing, non-linear dynamics and fusion plasma physics. The research is supported by several EU programmes, including EURATOM, by research councils and by industry. A summary of the activities in 1999 is presented.

ISBN 87-550-2650-8 (Internet)
ISSN 0106-2840
ISSN 0906-1797

Contents

1. Introduction

J. P. Lynov
E-mail: jens-peter.lynov@risoe.dk

The Optics and Fluid Dynamics Department performs basic and applied research in optical sensors and optical materials as well as in plasma and fluid dynamics. The research is conducted as a combination of science and technology with the following core competences:

- Optical sensors
  - Light propagation in complex systems
  - Diffractive optical components
  - Phase contrast methods
  - Laser-based sensors
- Optical materials
  - Polymers
  - Laser systems (diagnostics and information processing)
  - Laser ablation
  - Optical storage
- Biooptics
  - Light/tissue interaction
  - Biosensors, including microflows
  - IR spectroscopy
- Numerical modelling and information processing
  - Plasma and fluid dynamics, optics, ultrasound
  - Knowledge-based processing
  - Image processing ("data mining")
- Non-linear dynamics
  - Self-organisation
  - Turbulence
  - Vortex dynamics
  - Parametric processes
  - Photorefractive materials
- Fusion plasma physics
  - Theoretical plasma physics
  - Laser diagnostics

The output from the research activities is new knowledge and technology. The users are within industry, research communities and government, and the department is responsible for the Danish participation in EURATOM's fusion energy programme.

For the solution of many of the scientific and technological problems the department employs the following key technologies:

- Microtechnology for optical systems
  - Analogue and digital laser recording of holograms
  - Injection moulding of diffractive optical elements

- Optical characterisation and manipulation
    - Determination of material surfaces
    - Optical tweezers
- Temperature calibration and IR measurement techniques
    - Accredited temperature calibration
    - Fourier transform infrared (FTIR) measurements

During 1999 the department has strengthened its good contacts with Danish industry. Two new centre contracts under the strategic sensor initiative of the Danish Agency for Development of Trade and Industry were initiated. Both centre contracts run for three years and are called "Centre for miniaturisation of optical sensors - MINOS" and "Centre for on-line, non-contact control and regulation of industrial processes and systems - BIPS", respectively.

A formalised collaborative project between Risø, the Technical University of Denmark (DTU), two university hospitals and four companies was initiated in 1999 through the establishment of the "Centre for Biomedical Optics - BIOP". This collaboration has begun successfully with a new university course at DTU having fine attendance of both engineer students and medical doctors. Close collaboration has also been set up with the Medical Laser Centre in Lund, Sweden, where a PhD-student from the department is enrolled and where a master's student regularly participates in clinical experiments with various laser treatments in the associated hospital. At the end of 1999, the research area was granted support from the Danish Technical Research Council for a three-year talent project in biooptics.

The activities in scientific computing established the first close contacts with Danish industry in 1999. The two first industrial post doc projects in this field were initiated: with FORCE Institute in ultrasound and with IBSEN Micro Structures A/S in optics. Furthermore, the first commercial contract based on scientific computing was signed in the field of medico-technique. In this connection the first patent application in the research field was filed.

The collaboration with Danish universities was also extended during 1999. The department participated very actively in the Graduate School in Nonlinear Science together with DTU and the Niels Bohr Institute (NBI). In December 1999, Risø arranged the international Nonlinear Science Festival with participation of many internationally recognised scientists and many PhD-students. The department also has the full responsibility for two undergraduate courses: plasma physics at DTU and laser physics at NBI. As mentioned above, the department actively participates in the course in biomedical optics at DTU.

In the following sections, the scientific and technical achievements of the Optics and Fluid Dynamics Department during 1999 are described in more detail.

2. Optical materials

2.1 Introduction

P. M. Johansen
E-mail: per.michael.johansen@risoe.dk

The research programme on *optical materials* is primarily engaged in the areas of polymer optics, new laser systems, nonlinear optics, and functional materials.

The activities in polymer optics cover a wide span. A technological platform for close collaboration with industry has been established which enables us to master all the individual steps in the manufacturing of injection moulded diffractive optical elements. A refractive index sensor based on evanescent field coupling has been realised using a sol-gel Bragg waveguide produced in close collaboration with the Optical Science Center in Arizona, USA. Moreover, a novel method for producing, simultaneously, both a grating coupler and a waveguide has been made possible using a UV elastomer moulding technique. Experimental and numerical investigations of the performance of an optical waveguide with a grating coupler have been made. From these investigations the optical homogeneity of the surface as well as the influence of these structures on the incoupling peak has been examined. In the field of optical storage in azobenzene polymers we have performed extensive studies of the formation of a hologram with considerable diffraction efficiency after only one single shot of irradiation with a nanosecond laser pulse from a Q-switched YAG laser.

The efforts to prepare a high-power single-mode laser diode array with unique coherence properties have resulted in a system that displays single spatial and longitudinal modes, a coherence length of several centimeters, and an output wavelength tunable of many nanometers. We expect to develop the system into a commercial product together with a newly established Danish company.

The field of nonlinear optics encompasses various photorefractive phenomena such as parametric oscillation and amplification. Also the work on optical storage mentioned above is fundamentally nonlinear. In the field of optical storage in inorganic media two-step two-colour recording in $La_3Ga_5SiO_{14}$ has been demonstrated. Moreover, a novel effect of thermal fixing all the way down to room temperature has been revealed. Many of the fundamental nonlinear interactions underlying photorefractive parametric processes have been uncovered, and the corresponding space-charge wave theory has been utilised to explain the effect of quadratic recombination. The spectacular observation of an anomalously long decay time of resonantly excited space-charge waves has caused a vast amount of discussions among people working in the field. During the past year, however, this effect has been explained within existing theory in a joint collaborative effort between a Russian group and our group.

Functional materials activities on plasma properties have led to measuring the electron temperature in silver plasma produced by laser evaporation. Using the same technique, transparent conductive thin films with high transmission and low specific resistivity of aluminium-doped zinc oxide have been produced. Finally, a number of sputtering experiments on water ice have been performed in collaboration with a Polish group.

In the past year the change towards more technology-driven research and development has been further implemented. Under such dynamic and changing environmental conditions the results achieved both technologically and scientifically reflect a vital research programme with a highly committed staff.

2.2 Polymer optics

2.2.1 Injection moulded polymer surface relief holograms for new compact optical sensors

H. Pedersen, L. Lindvold, J. Stubager, C. Dam-Hansen (Kamstrup A/S)
E-mail: henrik.pedersen@risoe.dk

The purpose of the present project is to transfer the well-established CD technology to the production of diffractive optical surface relief elements. The individual steps in the production process are illustrated in Figure 1. At Risø the following parts of the process have been investigated:

- A computer program to calculate the position of the two recording beams that give the desired image beam at read-out has been developed.
- A stable and reliable recording set-up that gives a stable recording interference pattern for several minutes has been built.
- The qualities of surface structures in photoresist film, Ni master, and some injection moulded test elements have been assessed. These investigations are still ongoing, but one very positive result is that it has been possible to obtain complete filling of a sinusoidal structure with a period of 700 nm and a depth of approximately 250 nm with the polymer type ULTEM 1000, see Figure 2.
- The developed technology is currently being used in two industrial projects in connection with the production of low-cost sensor chips for water flow sensing (Kamstrup A/S) and water quality monitoring (Vir A/S).

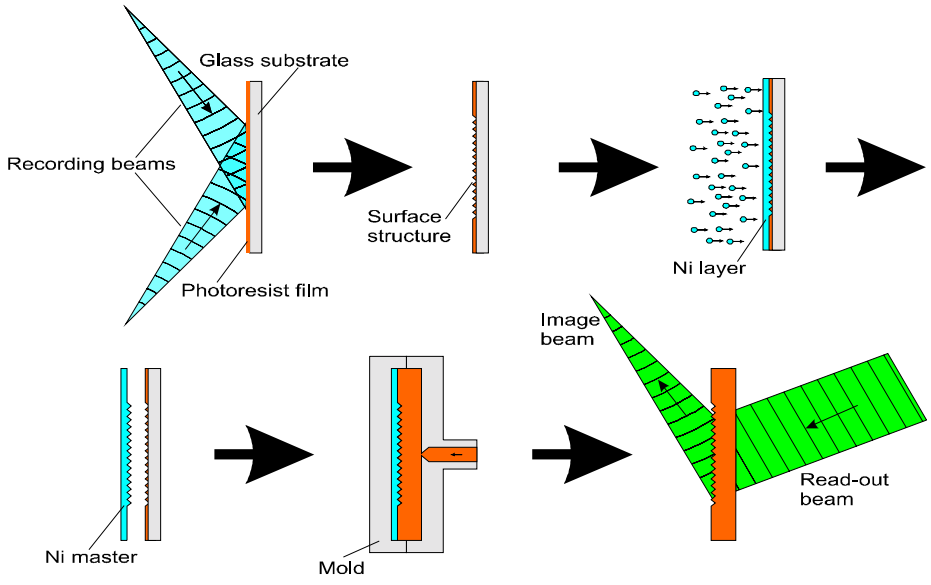

Figure 1. The individual steps in the manufacturing of injection moulded diffractive optical elements.

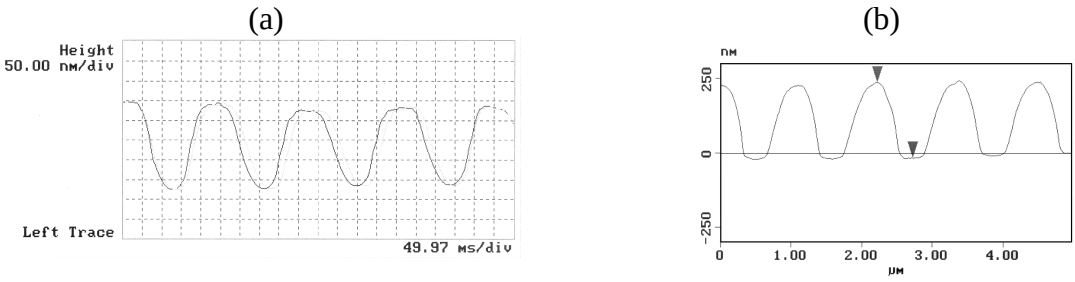

Figure 2. Atomic Force Microscope scans of (a) Ni master and (b) polymer chip (ULTEM 1000).

2.2.2 The coupled-cavity refractive index sensor (CRIS)

H. Imam, L.R. Lindvold and L. Lading
E-mail: lars.lindvold@risoe.dk

A new concept[1] for the detection of very small changes in the refractive index of a small sample of transparent material is given. The concept is based on measuring the frequency difference between two modes of a laser (possibly a twin-laser), where the evanescent field of one mode is affected by small refractive index changes. Intracavity sensing allows for orders of magnitude greater sensitivity than with external sensing. The frequency difference is obtained by light beating of the two modes. The concept has previously been demonstrated using HeNe-lasers. In order to take full advantage of the concept, a system based on evanescent sensing has been fabricated in collaboration with the Optical Science Centre in Arizona, USA.

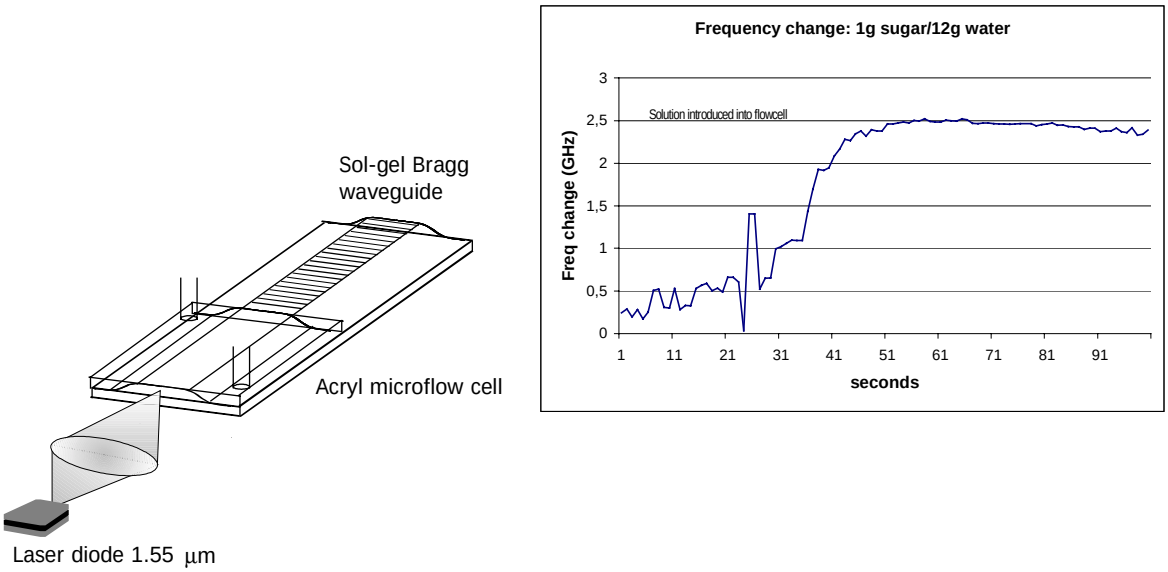

Figure 3. Outline of experiment with refractive index sensing. The sol-gel Bragg single-mode waveguide (chip size 2x3 cm) forms an extended resonator together with the laser diode. An aqueous sugar solution introduced through the microflow cell interacts with the evanescent field of the waveguide. Through this process the propagation constant changes and, hence, the laser frequency of the extended cavity.

The purpose of this experiment was to verify the concept of refractive index sensing in a microflow cell facilitated by a single-mode waveguide laser resonator. As it can be inferred from Figure 3, a frequency change could be detected by an optical spectrum analyser when a sugar solution was introduced into the flow cell. In order to demonstrate the concept of intracavity sensing by mode beating, two identical waveguide-laser systems will have to be coupled together.

1. WO9937996A1: Detection of a substance by refractive index change, published July 29 1999, L. Lading and L.R. Lindvold.

2.2.3 Fabrication of a waveguide grating coupler by UV replication

R. Horvath and L.R. Lindvold
E-mails: robert.horvath@risoe.dk, lars.lindvold@risoe.dk

A method capable of forming both a waveguide and a grating coupler simultaneously has been developed, see Figure 4. The method is based on the techniques that have been developed for microcontact printing (μCP). One of the key elements in this procedure is the fabrication of a mould made from an elastomer, poly(dimethylsiloxane) (PDMS). This moulding technique yields precision moulds with feature sizes down to 50 nm and aspect ratios from 1:0.5 to 1.2. This makes it very suitable for replicating surface relief diffracting structures. Due to the excellent release properties of the elastomer, direct copies from a photoresist master can be obtained without damaging the master. The elastomer copy can be utilised directly to make a polymer replica by sandwiching UV-curable resin between the elastomer mould and a substrate. Irradiating the UV-resin with UV-light hardens the resin in 10 sec.

If the UV-curable resin is spincoated onto a suitable substrate like glass in a thickness of approximately 1 micron, a planar waveguide will be formed concomitantly with the grating during the replication step.

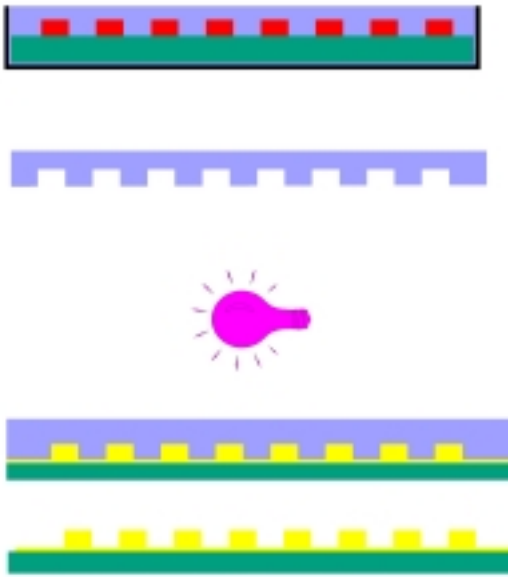

Figure 4. Steps in the UV replication process.

2.2.4 Effect of patterns and inhomogeneities on the surface of the waveguide in optical waveguide lightmode spectroscopy applications

R. Horvath, J. Voros (LSST, Switzerland) and L. Lindvold
E-mails: robert.horvath@risoe.dk, voros@surface.mat.ethz.ch, lars.lindvold@risoe.dk

The optical waveguide lightmode spectroscopy is a reliable, surface-sensitive experimental method. The main part of the instrument is an optical waveguide (optical chip), see Figure 5. The waveguide is a thin film with higher refractive index than the surrounding medium. On the top of the waveguide there is an optical grating (grating coupler). Light can be coupled into the waveguide by illuminating the grating with a laser beam at a certain angle (incoupling angle). The coupled light propagates in the film to the photodiode. These are the modes of the waveguide. With the photodiode we can measure the coupled light intensity (Figure 6).

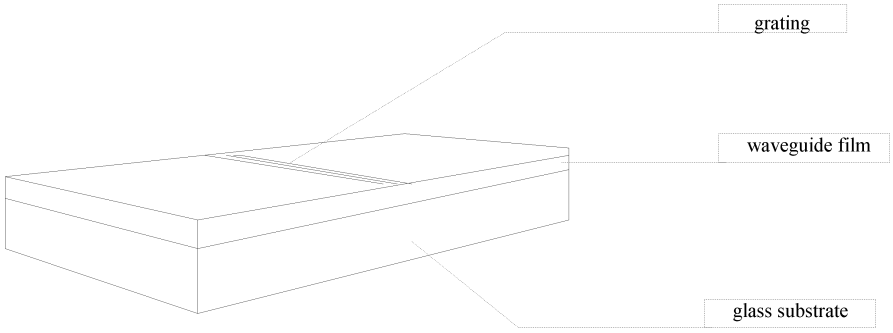

Figure 5. Optical waveguide with a grating coupler.

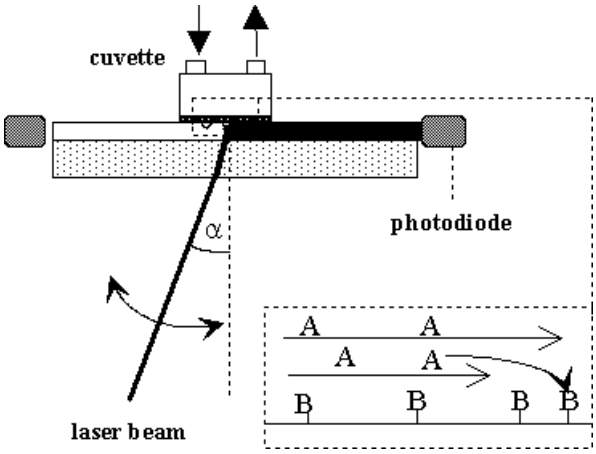

Figure 6. Cross section, experimental set-up, incoupling. Monitoring a molecule A – molecule B binding.

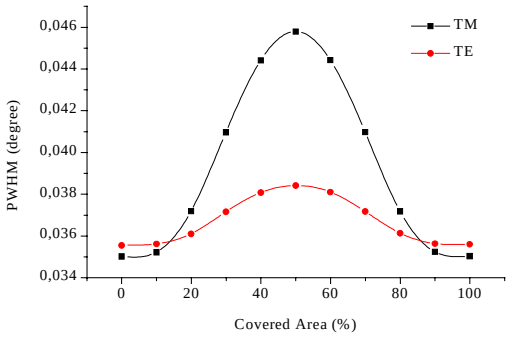

Figure 7. Calculated width at half maximum of the TM and TE polarisation peaks in the function of covered area.

Other authors have successfully used this technique to monitor protein adsorption, cell attachment and spreading of lipid bilayers. All of these works concentrated on measuring the incoupling peak position and from the position shift they concluded to the given surface process. With a numerical method we show that the incoupling peak half width contains valuable information about the optical homogeneity of the monitored surface (Figure 7). We also examine the effect of the surface structures on the incoupling peak (Figure 8).

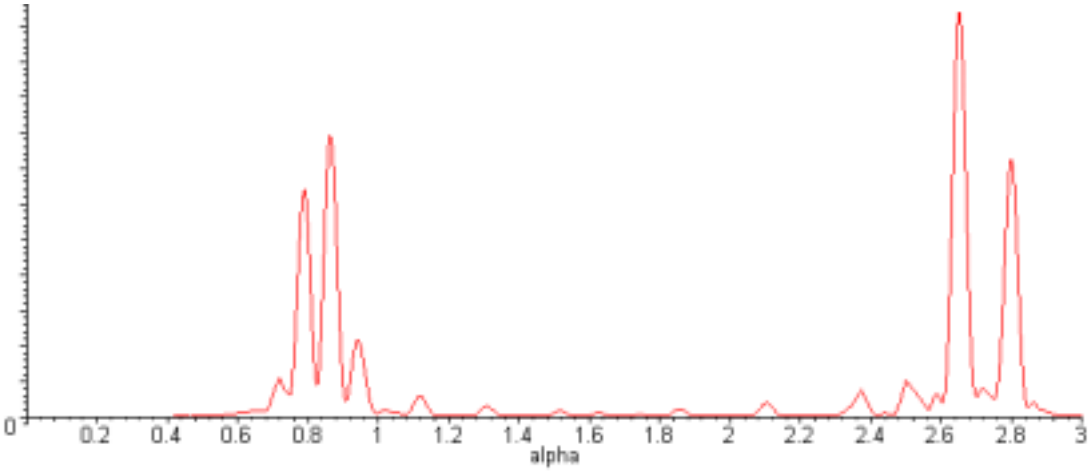

Figure 8. The calculated effect of the surface structures on the incoupling peak (degree - intensity).

2.2.5 **Explicit activities in optical storage**

P. S. Ramanujam and S. Hvilsted (Condensed Matter Physics and Chemistry Department)
E-mail: p.s.ramanujam@risoe.dk

Azobenzene-containing polymers have been under intensive investigation during the last decade as materials for digital and holographic storage. However, since storage in these polymers involves the physical reorientation of segments of long polymer chains, this process was thought to take place over several seconds, if not minutes. We have shown that holograms can be written in side-chain azobenzene polymers with a single pulse lasting 5 ns from a pulsed laser.[1,2]

The cyanoazobenzene side-chain polyester, P3aA, is prepared by transesterification of the cyanoazobenzene containing diol and diphenyl pththalate in the melt under vacuum. Approximately 3 mg of the polyester material is dissolved in 150 microlitres chloroform and cast onto a clean substrate. The film is dried in an oven at a temperature of 90 °C for ten minutes.

A polarisation holographic set-up is used to record holographic gratings. We use a commercially available small-frame frequency doubled YAG laser lasing at 532 nm as the source. This laser delivers Q-switched pulses of 5-7 s ns duration at 20 Hz, with a peak power output of 1.6 MW/pulse. The two beams overlap on the polyester film. An HeNe laser is used to read out the diffraction gratings. We find that just after one pulse from the laser, several orders of diffraction of the HeNe laser can be seen. The diffraction efficiency in the first order exceeds 4% at a spatial frequency of 160 lines/mm. An atomic force microscopic scan of the irradiated polyester shows considerable surface relief at the optical frequency (see Figure 9). A peak-to-valley value of approximately 90 nm was obtained at a spatial frequency of 900

lines/mm. In order to extend the scope of these investigations for practical holographic applications, the set-up was modified to fabricate Fraunhofer type holograms. The object beam was expanded to cover a transparency containing the word “Risø”. The size of the object was 12 mm. The resulting hologram was about 1 mm in diameter. The image was bright enough to be viewed on a screen. The appearance of the image is instantaneous.

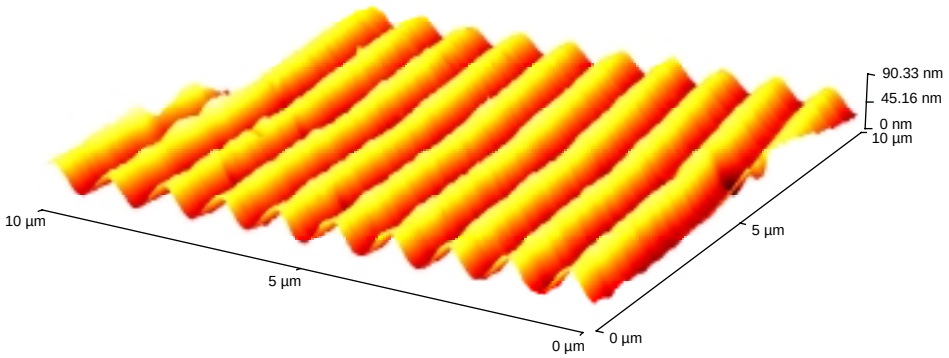

Figure 9. An atomic force microscopic scan of the irradiated area in P3aA.

In addition, the formation of holographic gratings in azobenzene side-chain polymethacrylates,[3] in peptides[4] and in Bis-DNO[5] have been investigated. The nature of the surface relief patterns when polarised light is used to irradiate azobenzene polymers has also beenstudied.[6] We have shown that large peaks or trenches result when the polymers are irradiated with polarised light through a transmission mask, depending on the architecture of the polymer. Combined main and side-chain azobenzene polyesters have also been synthesised and characterised for their potential for photoinduced nonlinear waveguides.[7]

1. P. S. Ramanujam, M. Pedersen and S. Hvilsted, Appl. Phys. Lett. 74, 3227 (1999).
2. P. S. Ramanujam and S. Hvilsted, SPIE International Technical Group Newsletter Holography, 10, 1 (1999).
3. L. Andruzzi, A. Altomare, F. Ciardelli and R. Solaro, Macromoleculels, 32, 448 (1999).
4. P. H. Rasmussen, P. S. Ramanujam, S. Hvilsted and R. H. Berg, J. Amer. Chem. Soc., 121, 4738 (1999).
5. P. H. Rasmussen, P. S. Ramanujam, S. Hvilsted and R. H. Berg, Tetrahedron Lett. 40, 5953 (1999).
6. N. C. R. Holme, L. Nikolova, S. Hvilsted, P. H. Rasmussen, R. H. Berg and P. S. Ramanujam, Appl. Phys. Lett. 74, 519 (1999).
7. F. Sahlén, T. Geisler, S. Hvilsted, N. C. R. Holme, P. S. Ramanujam and J. C. Petersen, Mat. Res. Soc. Symp.Proc. 561, 57 (1999).

2.3 New laser systems

2.3.1 High-power phase conjugate laser diode arrays

P. M. Petersen, S. J. Jensen and M. Løbel (Giga A/S)
E-mail: paul.michael.petersen@risoe.dk

A new high-power single-mode laser diode array with unique coherence properties has been invented enabling the use of GaAlAs semiconductor laser diodes for high-power applications.[1-3] The invented array configuration overcomes the usual diode array problem of a multimode non-diffraction limited output.

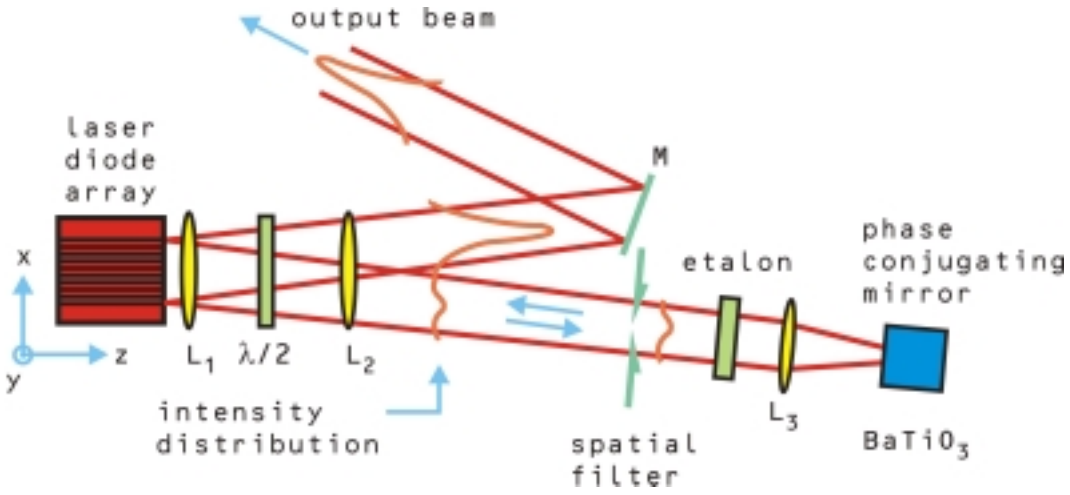

Figure 10. Experimental set-up. The radiation from a laser array is directed towards a photorefractive phase conjugate mirror. The phase conjugate feedback improves the coherence characteristics of the laser array. L1-4: lenses, WP: half-wave plate, BS: beamsplitter, SF: spatial filter, M: mirror, ET: etalon.

The experimental set-up is shown in Figure 10. A GaAlAs laser diode array is coupled to the phase conjugate feedback system that comprises a rhodium doped $BaTiO_3$ crystal, a Fabry-Perot etalon and a spatial filter. This feedback system forces the laser diode array to operate in a single spatial and a single longitudinal mode. If the etalon is replaced with a grating, the output wavelength is tunable.

We have demonstrated that, in comparison with the freely running laser diode array, the coherence length of the phase conjugate laser system has been increased by a factor of 70 and the output has become almost diffraction limited. The latter implies that the laser beam can be focused to a small spot at the size of a wavelength. More than 80% of the total energy provided by the freely running laser diode array can be extracted from this single-mode laser system. Furthermore, the frequency can be tuned continuously over a range of 6 nm around a centre wavelength of 812 nm.

The characteristics of the new laser system are:

- single longitudinal mode;
- single spatial mode (1.4 the diffraction limit);
- a coherence length of 7 cm;
- tunable output with a centre wavelength of 812 nm and a minimum tuning range of 6 nm.

The significantly enhanced coherence properties of the output from the laser diode array may lead to new applications of these lasers. Currently we are investigating the following applications:

- photodynamic therapy;
- material processing;
- coupling into single-mode fibres;
- new blue lasers based on frequency doubling.

Collaboration with a Danish company has been established with the purpose of developing a commercial product based on the new phase conjugate laser diode technology.

1. P. M. Petersen, S. J. Jensen and P. M. Johansen, "Phase locking of laser diode arrays using a photorefractive Rh:$BaTiO_3$ crystal", Invited paper, in *Laser Resonators II*, Editor Alexis V. Kudryashov, SPIE Proceedings **3611**, pp. 142-146, 1999.
2. M. Løbel, P. M.Petersen and P. M.Johansen, "Physical origin of laser frequency scanning induced by photorefractive phase conjugate feedback", J. Opt. Soc. Am. B. **16**, pp.219-227, 1999.
3. J. Limeres, M. Carrascosa, F. Agulló-Lopez, P. E. Andersen and P. M. Petersen, "Nonlinear grating interactions in multibeam photorefractive recording", J. Opt. Soc. Am. B 16, 414-419, 1999.

2.4 Nonlinear optics

2.4.1 Two-step two-colour recording and fixing in $La_3Ga_5SiO_{14}$ crystals

T. Nikolajsen and P. M. Johansen
E-mail: per.michael.johansen@risoe.dk

One of the most important demands for holographic data storage is that stored information can be read out without erasure. An attractive all-optical recording scheme has been suggested to meet the requirements of nonvolatile readout and reversibility. We have, for the first time, demonstrated this recording technique in a photorefractive $La_3Ga_5SiO_{14}$ crystal doped with praseodymium using cw laser radiation.[1] Using the 488 nm line from an AR-ion laser as the gating beam, gratings are written with a Ti:sapphire laser that operates in the range from 788 to 840 nm. The dependence of holographic recording on gating and writing intensity is investigated experimentally as well as theoretically. Also the saturation intensity and the threshold of photon energy are measured.

In the same material thermal fixing has been demonstrated all the way down to room temperature, see Figure 11.[2] From the temperature dependence of the characteristic time constant the thermal activation energy has been measured. Furthermore, the charge carrier density and the Debye screening length were measured.

1. T. Nikolajsen, P. M. Johansen, X. Yue, D. Kip, and E. Krätzig, Appl. Phys. Lett., **74**, 4037 (1999).
2. T. Nikolajsen and P. M. Johansen, Opt. Lett., **24**, 1419 (1999).

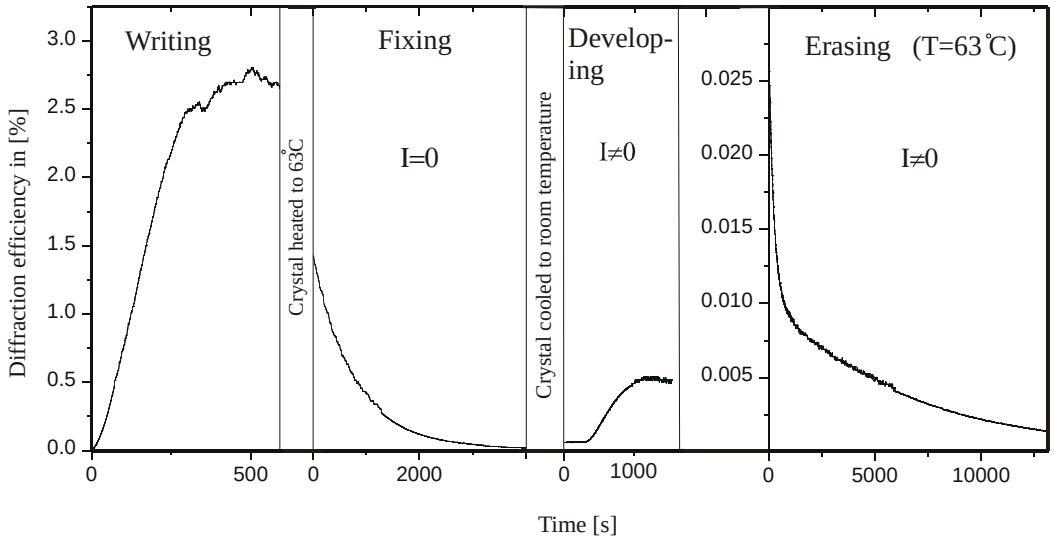

Figure 11. Dynamics of writing, fixing, development, and erasure of fixed holograms.

2.4.2 Nonlinear wave interactions in photorefractive media

P. M. Johansen, H. C. Pedersen, E. V. Podivilov and B. I. Sturman* (* Institute of Automation and Electrometry, Russian Academy of Sciences, Novosibirsk, Russia)*
E-mails: per.michael.johansen@risoe.dk, henrik.pedersen@risoe.dk

Parametrically generated waves in photorefractive media can be excited either by the running grating dc field technique or by the static grating ac field technique. The generation of such waves relies on nonlinear quadratic terms in the governing equations.

For the static grating ac square wave case we have analysed the simultaneous influence of higher-harmonic gratings and subharmonic gratings on the threshold for generating the subharmonic K/2 grating.[1] The presence of higher harmonic components causes feedback to the fundamental grating leading to a nonlinear correction in dissipation. Moreover, the threshold for subharmonic generation is substantially modified by the presence of higher order subharmonics.

In the running grating dc field case we have shown that the steady state solution for the space-charge field excited resonantly is stable against small perturbations for the values in the material parameters that are relevant to sillenite crystals.[2] The stability of the steady state fundamental component of the space-charge field is caused by higher harmonics. By using an alternative set-up for generating the parametric waves in which wave mixing between the recording beams is avoided, it has been possible to make a detailed comparison between theory and experiment.[3]

The so-called space-charge wave theory that has been developed to explain the above mentioned parametric processes theoretically can also be applied to analyse the influence of quadratic recombination, see Figure 12.[4] It is shown that the quadratic recombination alters the nonlinear properties of the space-charge waves. The influence of higher-harmonic components induces both a nonlinear frequency shift and a nonlinear shift in wave dissipation.

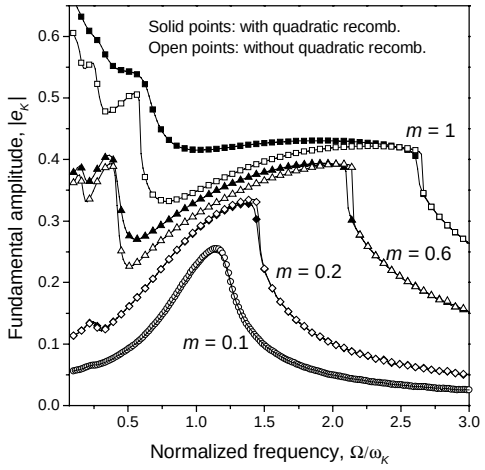

Figure 12. Amplitude of the fundamental space-charge field versus normalised frequency for four different values of contrast both with and without the effect of quadratic recombination.

The space-charge wave theory can also be utilised to explain the process of parametric amplification in which a strong running holographic grating pumps energy into a weak holographic grating.[5]

In the geometry in which the recording beams are allowed to exchange energy an anomalously long decay time of the resonantly excited space-charge wave has been reported. The interpretation of this long decay time was a very large quality factor that, in case it was correct, would call for a revision of the space-charge wave theory. However, by combining the space-charge wave theory with the equations that govern energy coupling we have shown that the anomalously long decay time is perfectly explained within the content of conventional theory.[6]

1. P. M. Johansen, H. C. Pedersen, E. V. Podivilov, and B. I. Sturman, J. Opt. Soc. Am. B, **16**, 103 (1999).
2. B. I. Sturman, E. V. Podivilov, K. H. Ringhofer, V. P. Kamenov, H. C. Pedersen, and P. M. Johansen, J. Opt. Soc. Am. B, **16**, 556 (1999).
3. H. C. Pedersen, P. M. Johansen, D. J. Webb, and E. V. Podivilov, Appl. Phys. B, **68**, 967 (1999).
4. P. M. Johansen, H. C. Pedersen, and E. V. Podivilov, J. Opt. Soc. Am. B, **16**, 1120 (1999).
5. H. C. Pedersen andf P. M. Johansen, J. Opt. Soc. Am. B, **16**, 1185 (1999).
6. B. I. Sturman, E. V. Podivilov, H. C. Pedersen, and P. M. Johansen, Opt. Lett., **24**, 1163 (1999).

2.5 Functional materials

2.5.1 Electron temperatures of a laser-induced silver plasma

B. Toftmann, J. Schou, T. N. Hansen and J. Lunney* (Trinity College, Dublin, Ireland)*
E-mails: j.schou@risoe.dk, bo.toftmann.christensen@risoe.dk

The plume of a laser-evaporated plasma from a metal surface is partly or fully ionised for laser intensities above 100 MW/cm^2. We have investigated the plasma properties at the intensities that are used for pulsed laser deposition of thin films. The current-voltage characteristics (I-V) of a laser-produced silver plasma have been recorded by a number of Langmuir probes positioned at different angles with respect to the target normal. From the plots an electron temperature T_e could be deduced on the basis of Langmuir theory.[1]

Figure 13 shows the electron temperature for an angle of 15^o with respect to the normal. The temperature increases up to about 0.3 eV and falls off slowly as a function of time. The time of the laser pulse impact on the silver surface is at t = 0. The maximum at 7 μs is close to the measured intensity maximum of the ion signal. The plasma is quasi-neutral with a small Debye length which means that the expanding plasma plumes of ions and electrons pass the probe simultaneously. This quasi-neutrality is based on the following argument: the magnitude of the density of arriving electrons derived from the electron temperature under the assumption that the electrons exhibit a Boltzmann distribution agrees well with that of the ion density measured directly with the probes.

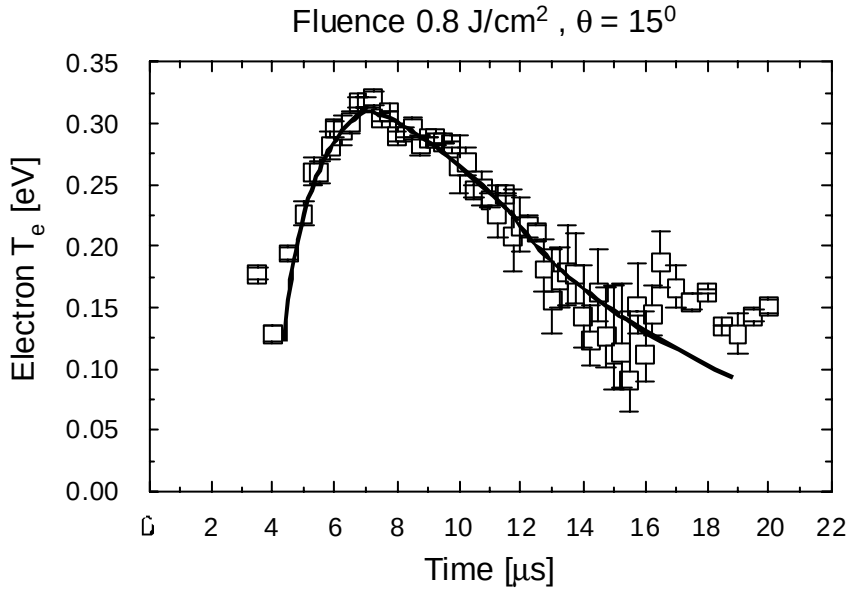

Figure 13. The electron temperature for a silver plasma as a function of time after the laser impact on the silver surface. Laser wavelength 355 nm, fluence 0.8 J/cm^2, angle 15^o with respect to the target normal. The thick solid line is merely a guide for the eye.

1. B. Toftmann, J. Schou, T.N. Hansen and J. Lunney, to be published.

2.5.2 Production of transparent conductive thin films by laser ablation

E. Holmelund, B. Thestrup, J. Schou, A. Nordskov, N. B. Larsen, M. M. Nielsen**
(Condensed Matter Physics and Chemistry Department)*
E-mails: j.schou@risoe.dk; birgitte.thestrup@risoe.dk

Thin films of transparent conductors are used in many technological applications, e.g. liquid crystal displays. We have produced films of the commonly used material ITO (indium tin oxide) by pulsed laser deposition, but have also recently fabricated films of AZO (aluminum-doped zinc oxide).[1,2] These materials have a transmission of 85-90 % for visible light and relatively low specific resistivity (down to about 1×10^{-3} Ωcm), see Figure 14. AZO is particularly interesting because aluminium and zinc are inexpensive, non-toxic metals.

The films have been produced at the set-up for pulsed laser deposition in the Optics and Fluid Dynamics Department. This method has the advantage that films of mixtures of different oxides may be produced directly from pressed powder targets of a certain chemical composition. Another important point is that the films can be produced in a reactive atmosphere, for example in an oxygen background gas.[1] For the transparent semiconductors, pulsed laser ablation is presently the only method by which conducting films can be fabricated on a substrate at room temperature.

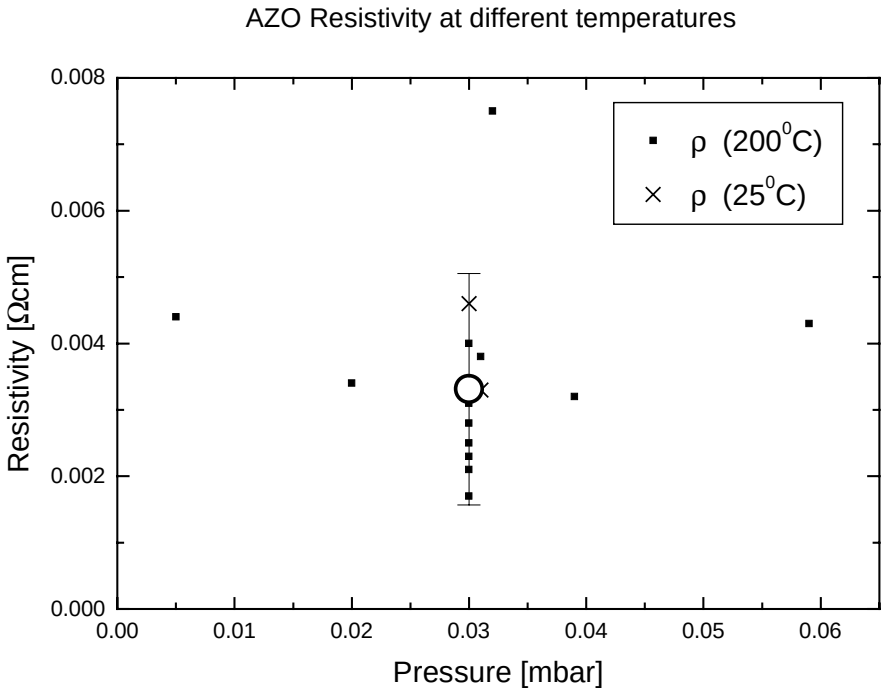

Figure 14. The specific resistivity ρ of AZO films deposited on a glass substrate at 25° C or 200° C as a function of the background oxygen pressure in the PLD-chamber. Laser wavelength 355 nm and fluence of 1.8 J/cm^2. The average value and the standard deviation are shown for the points at 0.03 mbar.

1) B. Thestrup and J. Schou, Appl. Phys. A (in press) (1999).
2) B. Thestrup and J. Schou, DOPS-nyt **4**, 17 (1999).

2.5.3 Sputtering of water ice

J. Schou, R. Pedrys, F. Krok*, P. Leskiewicz* (* Jagiellonian University, Krakow, Poland), U. Podschaske** and B. Cleff**(** University of Münster, Germany)*
E-mail: j.schou@risoe.dk

Water ice is one of the most important solids in planetary and interstellary physics. Since practically all data from the outermost part of the planetary system, i.e. planets, satellites or comet nuclei, have been obtained by spectroscopical methods, it means that the optical properties of the ice surface play an important role. A complicating feature is that the ice surfaces are eroded continuously by fast particles from the planetary magnetospheres. Therefore, it is important to study the rate and the underlying mechanism of erosion.

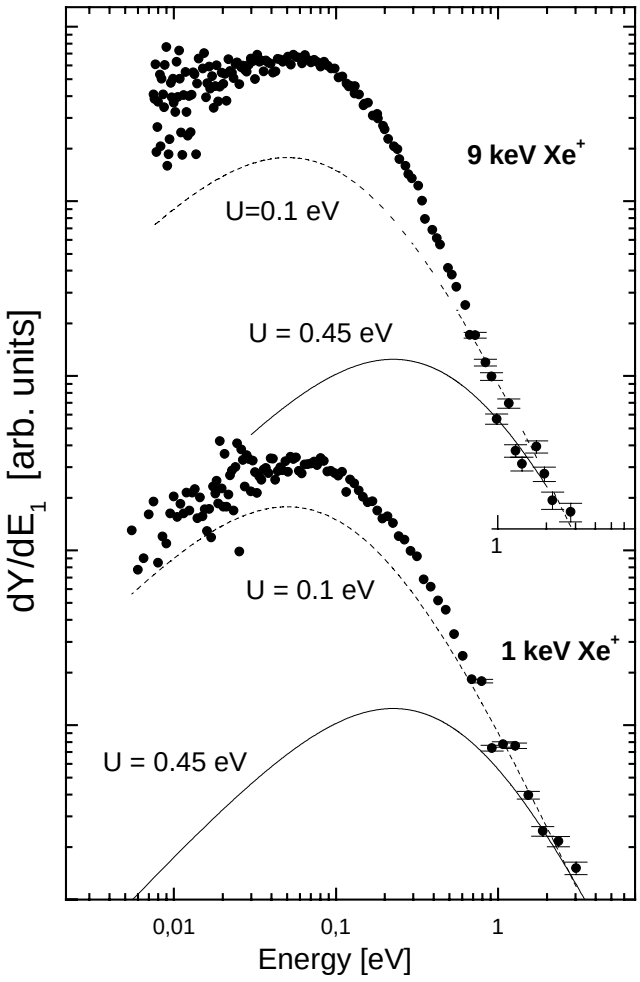

Figure 15. Energy distributions dY/dE_1 of D_2O molecules sputtered from frozen heavy water ice, D_2O, at 76 K by keV Xe ions as a function of ejection energy E_1.

We have performed a number of sputtering measurements in the set-up placed at the Institute of Physics in Krakow, see Figure 15. Water ice has been bombarded by 1-9 keV Xe ions. These ions are so heavy that collisional effects rather than electronic effects are responsible for sputtering. The energy distributions of the sputtered D_2O molecules have been plotted as a function of ejection energy E_1 for 9 and 1 keV Xe ion bombardment. Two typical predictions of linear collision cascade theory have been incorporated in the figure as well. The high-energy tail of the distribution follows the theoretical curve fairly well.[1] However, the origin of the low-energy peak is not yet clear.

1) R. Pedrys, F. Krok, P. Leskiewicz, J. Schou, U. Podschaske and B. Cleff, Nucl. Instr. Meth. B (in press).

3. Optical diagnostics and information processing

3.1 Introduction

S.G. Hanson
E-mail: steen.hanson@risoe.dk

The aims of the research undertaken in the Optical Diagnostics and Information Processing programme are both to convey new concepts to industry and to expand the scientific knowledge of "light" and accompanying technologies. Moreover, these themes are made available to postgraduate students.

A strong demand has been put onto the programme for a large industrial impact, which has resulted in an increase in the number of industrially related sensing and data acquisition projects. Five major themes are addressed in the programme: medical optics, infrared technology, phase contrast methods, optical measurement techniques and knowledge-based processing. Since 1978 a group within the programme has performed accredited temperature calibration; an activity that has now been extended to cover infrared thermometers. The main activities in the year 1999 are described below. Although the five themes may not seem directly connected, great emphasis is put into establishing large programmes - either industrially or purely scientifically related - where a collective effort enhances the chance of success. The field of medical optics will thus serve as a pivotal point for many future projects. Knowledge-based processing as well as infrared technology can be essential contributors to the field of medical optics, as is the use of miniaturised optical sensors.

In the field of infrared technology the main objective is the use of fast, but low-resolution Fourier transform infrared spectrometers (FTIRs) for the simultaneous determination of transmission and emission of spectra for infrared radiation through hot exhaust gases as a means of determining the content. These investigations have been conducted in a large European programme where we have experienced unprecedented results.

A key issue in knowledge-based processing with data-driven models is to control the trade-off between the model sensitivity and the model fit. This investigation has been successfully initiated in an industrial Ph.D. project at Intellix A/S, which is a Danish company specialising in the development of expert systems and decision support products founded on RAM-based neural networks (also denoted n-tuple neural nets). A collaborative effort has recently commenced to exploit two patents in this area.

General support of the work with medical optics has been given by the Danish company Torsana A/S and by a special contribution from Risø National Laboratory. A Ph.D. study granted by the Danish Technical Research Council addressing a non-invasive method for tomography in human tissue has been carried on, and a comprehensive theoretical description of the coherence properties of light reflected within turbid media has been presented. The Danish Technical Research Council has recently granted personal three-year financial support for future work in this field.

A project employing concepts developed and patented at the laboratory has been commercialised, and comprehensive theoretical descriptions of the dynamic behaviour of speckle patterns have been finished. A recently developed phase-coding method for obtaining lossless projection of light by using a generalisation of the well-known Zernike phase contrast has been demonstrated for decrypting and visualisation of phase encrypted information, and a

Ph.D. project will start in the beginning of 2000 to extend the same techniques for light projection to the field of optical tweezers.

The staff in the programme have successfully adjusted to the demands for industrial collaboration while at the same time maintaining the department's record as a centre for applied research.

3.2 Medical optics

3.2.1 Optical coherence tomography with ultrahigh resolution for non-invasive medical diagnostics

L. Thrane, P. E. Andersen, S. Grüner Hanson, H. T. Yura (Electronic Technology Center, The Aerospace Corporation, Los Angeles, CA, USA) and P. Bjerring (Department of Dermatology, Marselisborg Hospital, University of Aarhus, Aarhus, Denmark)
E-mail: lars.thrane@risoe.dk

The maximum probing depth is of considerable interest in the characterisation and optimisation of an optical coherence tomography (OCT) system when used for imaging in highly scattering tissue. Thus, we have developed a method for calculating the maximum obtainable probing depth based on the design variables of the OCT system, the detector characteristics and the optical properties of the tissue.[1]

The calculation is based on the minimum acceptable signal-to-noise ratio and a new analytical model[2] of the OCT technique which is valid in both the single and the multiple scattering regimes. The new model is based on the extended Huygens-Fresnel principle[3] and on the use of mutual coherence functions. The so-called shower curtain effect,[4] which manifests itself in standard OCT systems,[2] is an inherent property of this model.

We have demonstrated the utmost importance of including both multiple scattering and the shower curtain effect when calculating the maximum probing depth in tissue.[1] Furthermore, we have shown how the maximum probing depth depends on the design variables of the OCT system and the optical properties of the tissue.[1] As an example, in Figure 16 we have shown the maximum probing depth as a function of the tissue scattering coefficient and the reflection coefficient of the probed discontinuity for the case of shot-noise limited detection and a minimum acceptable signal-to-noise ratio of 4.

The present research project is supported by the Danish Technical Research Council under grant no. 9601565.

1. L. Thrane, H. T. Yura and P. E. Andersen, "Calculation of the maximum obtainable probing depth of optical coherence tomography in tissue," *to appear in* Proc. SPIE **3915** (2000).
2. L. Thrane, H. T. Yura and P. E. Andersen, "Analysis of optical coherence tomography systems based on the extended Huygens-Fresnel principle," J. Opt. Soc. Am. A **17**, 484-490 (2000).
3. R. F. Lutomirski and H. T. Yura, "Propagation of a finite optical beam in an inhomogeneous medium," Appl. Opt. **10**, 1652-1658 (1971).
4. I. Dror, A. Sandrov and N. S. Kopeika, "Experimental investigation of the influence of the relative position of the scattering layer on image quality: the shower curtain effect," Appl. Opt. **37**, 6495-6499 (1998).

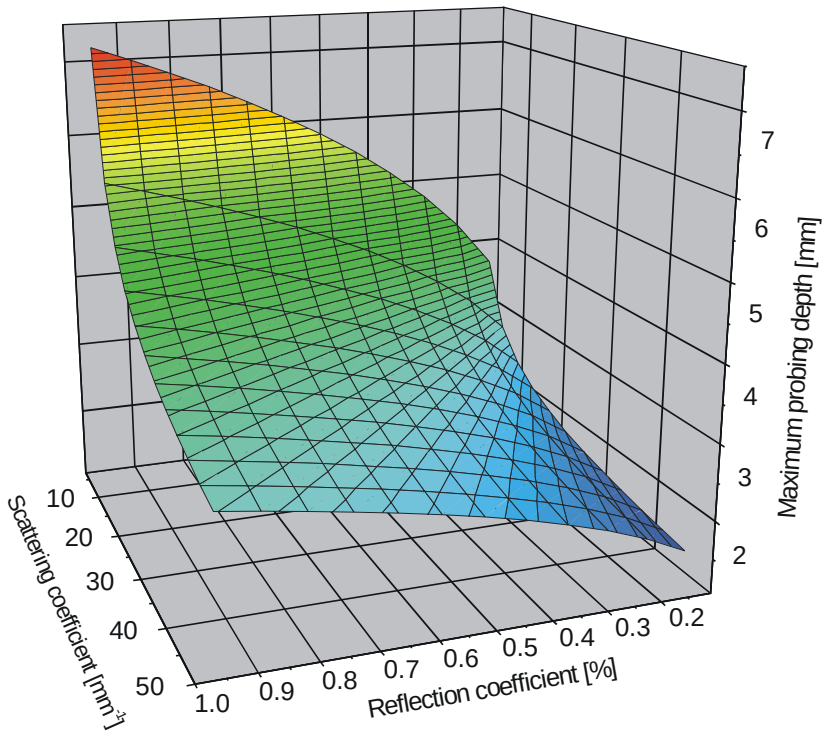

Figure 16. The maximum probing depth as a function of the scattering coefficient of the tissue and the reflection coefficient of the probed tissue discontinuity for the case of shot-noise limited detection (centre wavelength of the source 814 nm, focal length 10 mm, 1/*e* intensity radius of the reference and input sample beams in the lens plane 2 mm).

3.2.2 Determining the optical properties of scattering media using a single integrating sphere set-up and the inverse adding-doubling algorithm

P. E. Andersen, L. Thrane, L. Lindvold, S. W. Lindegaard and Henrik M. Jensen**
(DNP Denmark A/S, Skruegangen 2, DK-2690 Karlslunde, Denmark)*
E-mail: peter.andersen@risoe.dk

The optical properties, i.e. the asymmetry parameter g, the scattering coefficient μ_s, and the absorption coefficient μ_a, are to be determined for scattering and absorbing media assuming known values of sample thickness and refractive index. The main purpose of our work is to determine the optical properties of biological tissue samples. Furthermore, the technique described here can also be applied to solid or aqueous phantoms.

Assume that the sample under investigation is homogeneously scattering and absorbing and that the thickness and the refractive indices are known. The adding-doubling algorithm[1] provides the diffuse reflectance, the diffuse transmittance and the ballistic component by solving the transport equation for light propagation in random media given the optical parameters. The advantage of this method, over e.g. Monte Carlo simulations[1] (MCS), is that calculation of the diffuse reflectance, the diffuse transmittance and the ballistic component is fast. Vice versa, provided the parameters mentioned before are known, the adding-doubling method may be used to solve the inverse problem of finding the optical properties. Hence, the algorithm is called the inverse adding-doubling (IAD) method.[1]

The IAD algorithm is tested numerically by using MCS.[2] The slab used in the numerical test has a thickness of 1 mm with unity refractive index. In all MCS test runs 10^5 photon packages were used. Varying the optical parameters in the ranges 0.01 $mm^{-1} < \mu_a < 0.6$ mm^{-1},

$1\text{mm}^{-1} < \mu_s < 10\ \text{mm}^{-1}$ and $0.875 < g < 0.975$ resulted in typical relative errors δ_{abs}~2.5%, δ_{scat}~0.50% and δ_g~0.50%, respectively. Note that these errors are likely to decrease as the number of photons is increased. Therefore it is concluded that a single sphere configuration and a second set-up to measure the ballistic component in conjunction with the IAD algorithm are feasible means of determining the optical properties of random media.

Our experimental set-up consists of a single integrating sphere for measuring the reflected and transmitted diffusely scattered light, see Figure 17 (top). Both measurements are carried out using the substitution principle, which further has the advantage that the sphere parameters need not be known.[1] In a second set-up the collimated transmission, or ballistic component of the light, is measured, see Figure 17 (bottom). The light source in both set-ups is a 10 mW HeNe laser emitting at 633 nm.

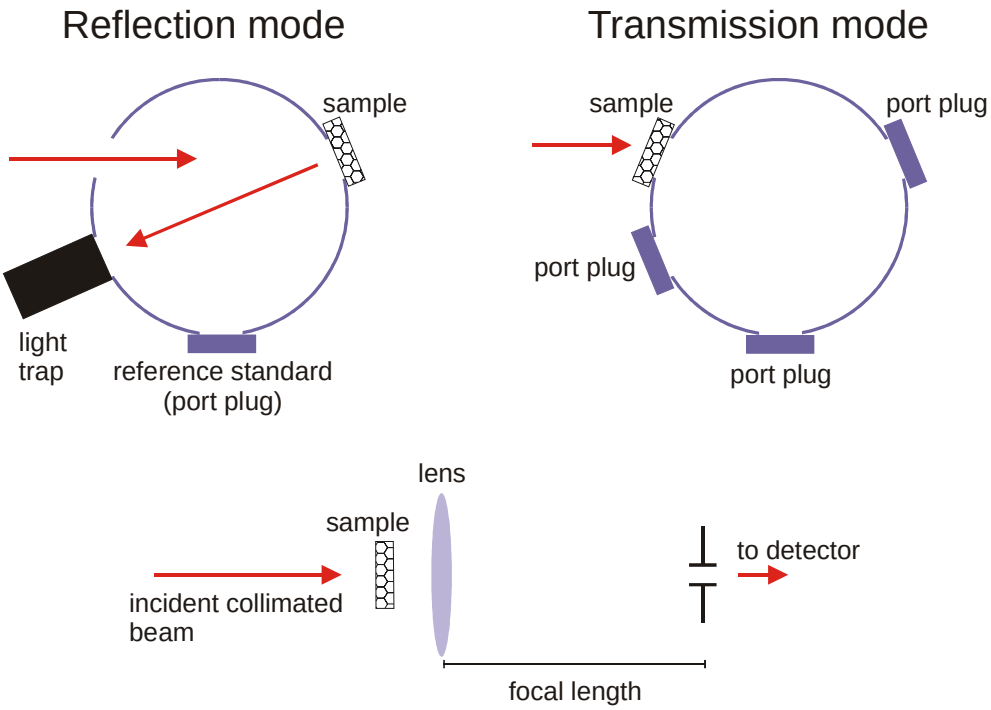

Figure 17. Top: The single integrating sphere set-up for reflection (top left) and transmission mode (top right). In reflection a light trap is inserted to exclude the specular reflection from the sample. In both cases a port plug was taken as reference standard. Bottom: Set-up for measuring the collimated part of the incident beam using a Fourier lens and matched pinhole.

Using the two set-ups mentioned above in conjunction with the IAD algorithm, eight solid scattering phantoms were examined. The refractive indices of the phantoms were 1.5, and the thicknesses ranged between 5.0 mm and 7.6 mm. Mie theory[3] was used to calculate the value of the asymmetry parameter, i.e. g=0.995 for refractive index of the scatterer of 1.55 and sphere diameter of 10 μm. The measured values of g matched the predicted values within 0.5%. In these phantoms the absorption coefficient was kept below 0.01 mm^{-1} with some characterised as non-absorbing, which was confirmed by the measurements. The measured scattering coefficients matched the predicted values satisfactorily and the values ranged from 0.9 mm^{-1} to 2.0 mm^{-1}.

However, to verify the measured values of the scattering coefficients, three non-absorbing samples were inserted in our optical coherence tomography system,[4] and the diffuse reflectance from one surface was measured through the scattering phantom using an identical experimental layout to that in Ref. 4. From the theoretical model[4] the so-called heterodyne effi-

ciency factor may be calculated as a function of the sample thickness using the asymmetry parameter and the scattering coefficients from the sphere measurements as parameters. The result is shown in Figure 18 demonstrating excellent agreement between theory shown as solid lines and the experimentally obtained values shown as squares. The scattering parameters are shown in the inset in Figure 18. Note that the asymmetry parameter has been used as fitting parameter in the calculations. However, the fitted value of *g* is within 0.2% of the experimentally determined value.

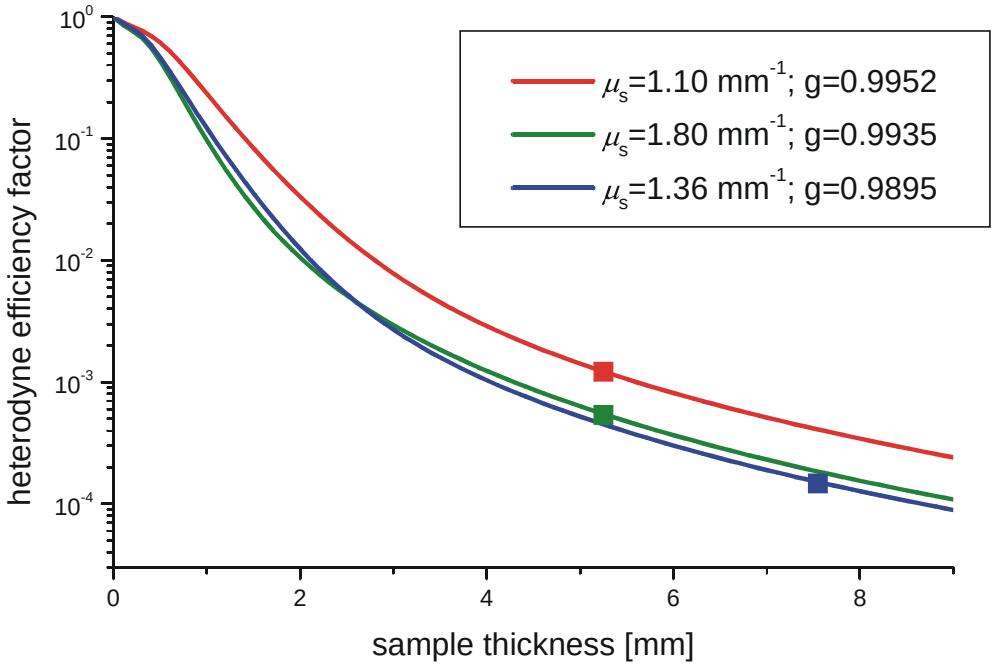

Figure 18. The heterodyne efficiency factor as a function of the thickness of the sample with the scattering properties as parameters.

In conclusion, the strength of the single integrating sphere set-up and the inverse adding-doubling algorithm has been demonstrated for determining the optical properties of random media. The integrating sphere measurements were verified using an optical coherence tomography set-up, and excellent agreement between the measured data sets was observed.

1. S. A. Prahl, “The adding-doubling method”, Chap. 5 in Optical-Thermal Response of Laser-Irradiated Tissue (eds. A. J. Welch and M. J. C. van Gemert), Plenum Press, New York, 1995.

2. S. L. Jacques and L. Wang, “Monte Carlo modeling of light transport in tissues”, Chap. 4 in Optical-Thermal Response of Laser-Irradiated Tissue (eds. A. J. Welch and M. J. C. van Gemert), Plenum Press, New York, 1995.

3. C. F. Bohren and D. R. Huffman, Absorption and scattering of light by small particles, J. Wiley & Sons, New York, 1983.

4. L. Thrane, H. T. Yura and P. E. Andersen, “Analysis of optical coherence tomography systems based on the extended Huygens-Fresnel principle”, J. Opt. Soc. Am A **17**, pp. 484-490 (2000).

3.2.3 Fourier Transform infrared spectroscopy of biological materials

P. S. Jensen, J. Bak, P. E. Andersen and S. Clausen
E-mail: peter.snoer.jensen@risoe.dk

The use of non-invasive diagnostic methods for monitoring the content of glucose in human blood has been the subject of intense studies around the world and is characterised by many claims of successful methods. Yet there does not exist a universally accepted robust analytical method for this purpose.

The complexity of the identification of a small concentration of glucose in a complex medium, such as the human body, necessitates advanced data processing involving chemometric methods and/or neural networks. The interference of various biological parameters and the influence of uncontrollable parameters in the attempts mentioned above to measure glucose are poorly understood. There is thus a need for more fundamental work to provide a basis for evaluating the claimed results and, thereby, determining the feasibility of the IR-spectroscopic methods.

At Risø National Laboratory, the FT-IR group and the biomedical optics group have initiated a study of a simple system that will lead to development of in-vivo measurements, namely the measurement of glucose in water using transmission FT-IR spectroscopy. Figure 19 presents the relevant signals for various glucose concentrations. The purpose of this study is to provide a foundation for evaluating the numerous claims of successful non-invasive glucose monitoring using IR and Raman spectroscopy. This should finally result in improved detection limits of trace organic compounds in aqueous systems and should have a broad range of applications.

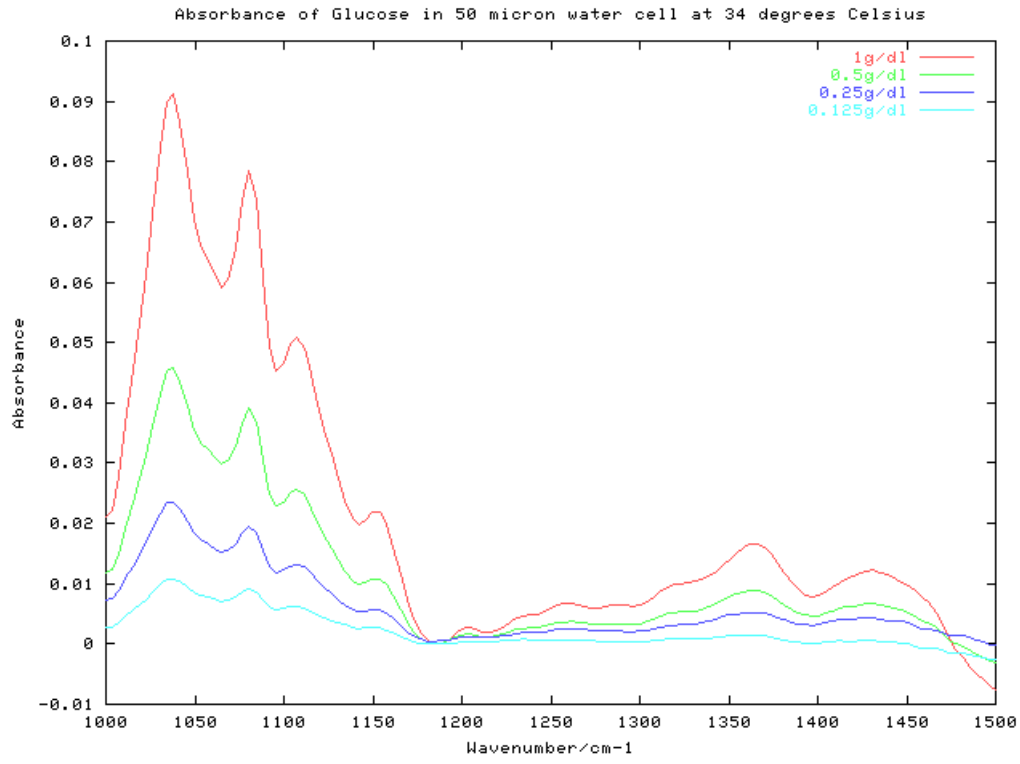

Figure 19. Absorbance of glucose in 50 µm water cell at 34 degrees Celsius for varying glucose concentrations.

3.2.4 The Wigner phase-space distribution for coherence tomography

L. Thrane, H. T. Yura (Electronic Technology Center, The Aerospace Corporation, Los Angeles, CA, USA) and P. E. Andersen
E-mail: lars.thrane@risoe.dk

It has recently[1] been suggested that new methods for medical imaging may be based on coherence tomography using measurements of Wigner phase-space distributions.[2] The Wigner phase-space distribution is particularly useful for medical imaging because the phase-space approach provides maximum information about the light being used. In order to further investigate these ideas in the context of the optical coherence tomography (OCT) technique, a theoretical analysis of the Wigner phase-space distribution has been carried out for the case of diffuse reflection and small-angle scattering in the OCT geometry shown in Figure 20.[3]

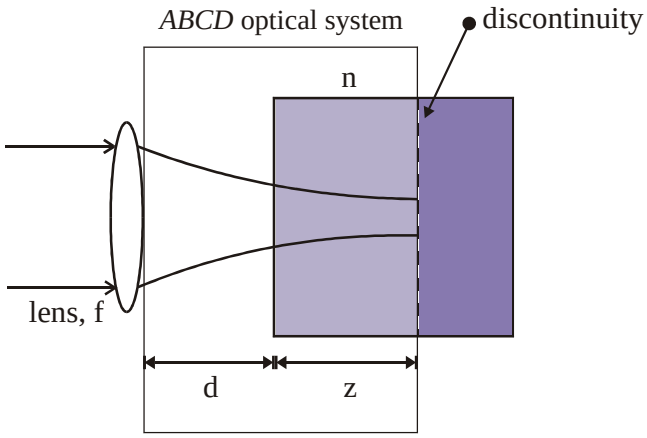

Figure 20. The OCT geometry showing the tissue discontinuity where the sample beam is reflected.

The theoretical analysis, which applies to highly scattering tissue, is based on the extended Huygens-Fresnel principle for the optical field,[4] and it is valid in both the single and the multiple scattering regimes. The results are general in that they apply to both an arbitrary scattering function and to arbitrary (real) *ABCD* optical systems.

On the basis of this theoretical analysis, a novel way of creating OCT images based on measurements of the momentum width of the Wigner phase-space distribution has been suggested, and the advantage over conventional OCT images has been specified.[3]

The present research project is supported financially by the Danish Technical Research Council under grant no. 9601565.

1. S. John, G. Pang and Y. Yang, “Optical coherence propagation and imaging in a multiple scattering medium,” J. Biomed. Opt. **1**, 180-191 (1996).
2. E. P. Wigner, “On the quantum correction for thermodynamic equilibrium,” Phys. Rev. **40**, 749-759 (1932).
3. H. T. Yura, L. Thrane and P. E. Andersen, “Closed form solution for the Wigner phase-space distribution function for diffuse reflection and small-angle scattering in a random medium,” accepted for publication in JOSA A.
4. R. F. Lutomirski and H. T. Yura, “Propagation of a finite optical beam in an inhomogeneous medium,” Appl. Opt. **10**, 1652-1658 (1971).

3.3 Infrared technology

3.3.1 Infrared temperature calibration

S. Clausen
E-mail: sonnik.clausen@risoe.dk

A reference laboratory for calibration of infrared instruments was established at Risø in 1996. Traceable calibration of pyrometers and infrared thermometers is made with blackbodies in the temperature range –50 °C to 1600 °C. The current work can be grouped in the following six main topics with the general aim of reducing uncertainties of non-contact temperature measurements:

- calibration service of infrared thermometers for customers;
- temperature measurements for customers;
- development of new and improved methods for infrared temperature measurements;
- measurement of spectral emissivity of samples and coatings;
- consultative service and information;
- international comparisons of standards and procedures.

In order to ensure the traceability and the comparability of the results, comparisons between the standards and laboratories must be carried out. Risø has participated in two international comparisons on radiation thermometry in 1999, i.e. the TRIRAT LT-scale and Th9 intercomparison covering the temperature ranges –50 °C – 300 °C and 600 °C – 1300 °C.

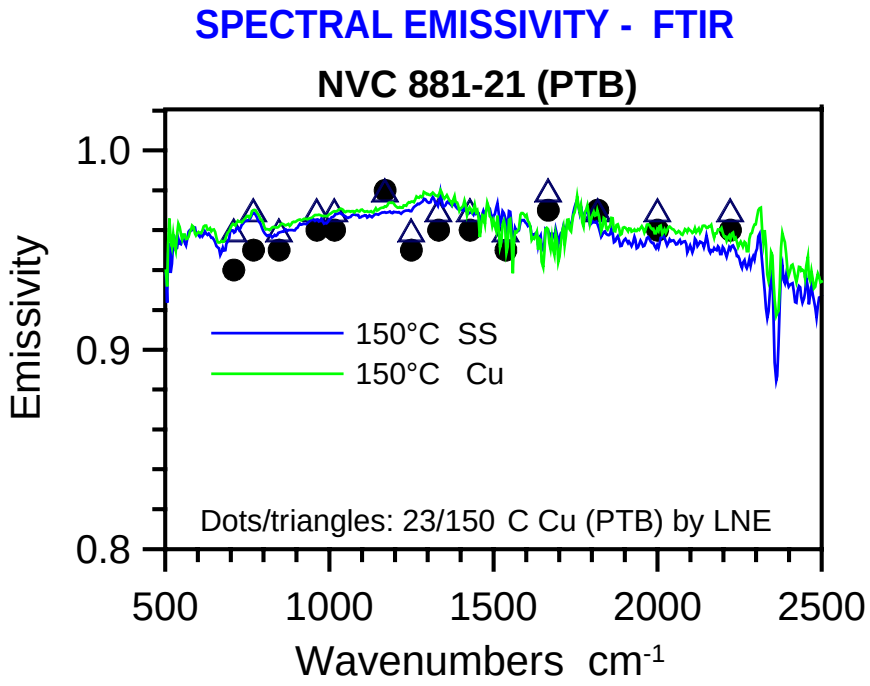

Figure 21. FTIR measurements of spectral emissivity of samples coated with Nextel Velvet Coating obtained using an FTIR spectrometer. Dots are measurements made by LNE on a similar Cu-sample. The measurements were performed on various samples and coatings in the EU-project TRIRAT.

Risø is involved in the EU project "TRIRAT" with participants from laboratories from most of Europe. The overall objective of the project is to provide improved, sub-Kelvin accuracy in infrared (IR) radiation thermometry at industrial levels in the range from –50 °C to 800 °C. The traceability is transferred from the highest metrological levels down to the industrial level. We work towards reaching sub-Kelvin accuracy of our calibration sources at temperatures in the range from –50 °C to 250 °C.

A high-precision water heat pipe blackbody (HP-BB) operating in the temperature range 50 – 250 °C was established and tested successfully in 1999 to be used for accurate calibration of infrared instruments, e.g. the heat pipe blackbody was used as a reference blackbody for calibration of FTIR spectrometers in the "Aeroprofile" project described below. With the combination of high-accuracy traceable blackbody sources and spectral measurements of infrared radiation with an FTIR spectrometer Risø has state-of-the-art calibration capabilities in the spectral range from 2 – 25 μm.

The Fourier Transform Infrared (FTIR) spectrometer is a powerful tool for measuring emissivity spectra with high signal-to-noise ratios and spectral resolution in the mid infrared spectral range from 2 to 25 μm, see Figure 21. Emissivity measurements using the two-point FTIR technique developed at Risø have been compared with two other techniques, see Ref. 1 for further details. Compared with the filter methods the high spectral resolution of the FTIR spectrometer is valuable especially for emissivity measurements of coated surfaces at low temperature where the emissivity might change significantly as a function of wavelength.

1. T M. Battuello (CNR-IMGC, Italy), S. Clausen (RISOE, Denmark), J. Hameury (LNE, France), P. Bloembergen (NMi-VSL, The Netherlands), The spectral emissivity of surface coatings, currently applied in blackbody radiators covering the spectral range from 0.9 to 20 μm an international comparison, (1999) TEMPMEKO.

3.3.2 Aeroprofile

J. Bak and S. Clausen
E-mail: sonnik.clausen@risoe.dk

Radiometric calibration

A three-temperature procedure is applied for calibration of the infrared spectrometer, i.e. three graphite or Nextel coated blackbodies are presently used in the project. Firstly, the blackbodies were calibrated during our visit to the German Aerospace Center (DLR) in June 1999 and were compared with Risø's water heat pipe blackbody (HP-BB). Secondly, a Nextel coated grooved blackbody was calibrated at Risø at 80 °C and 190 °C with the water HP-BB and Risø's FTIR spectrometer, and was included in the TRIRAT low-temperature intercomparison at Risø in November-December 1999. The emissivity of the Nextel coated blackbody was found to be approximately 0.985, which is close to the expected value for a grooved surface coated with the Nextel coating, see Figure 22.

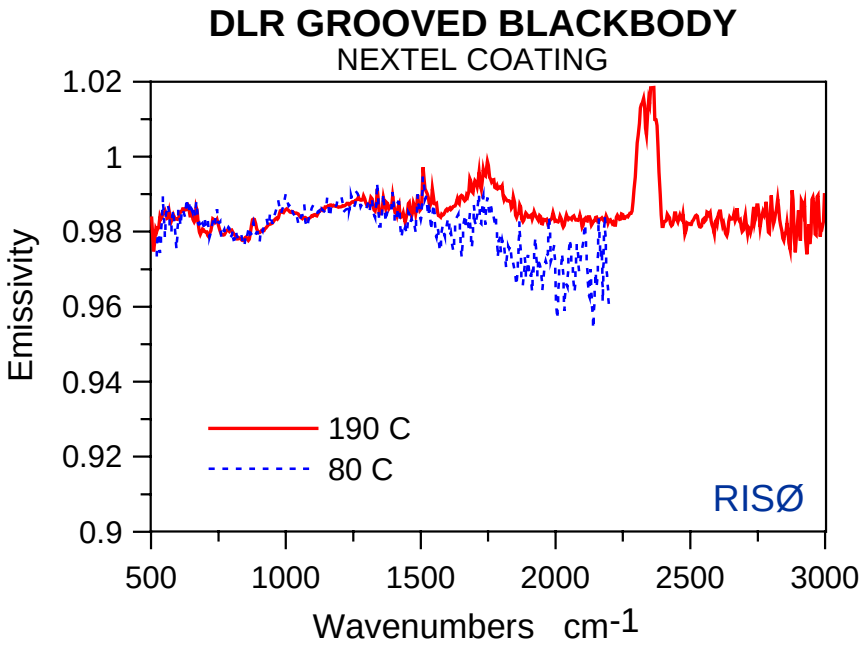

Figure 22. Measured emissivity of the Nextel coated grooved blackbody. The temperature of the blackbody was measured with a calibrated pt100 sensor and the emissivity measurement is compared with the water heat pipe blackbody (ε ~ 0.999).

The three-temperature calibration procedure used in the project could be simplified without loss of accuracy. A two-point calibration method in which the temperature of the two blackbodies is measured with two separately calibrated pt100 sensors would be a good alternative, see Table 1.

Table 1. Comparisons of advantages and disadvantages of different calibration methods.

Calibration Method	Advantages	Disadvantages
One-point	- Only one hot blackbody is required.	- Correction for radiation from FTIR, apertures, etc. is not possible. - Less accurate at low wave numbers and temperatures far from calibration point. - The blackbody temperature should be measured. - Temperature sensor should be calibrated periodically, e.g. once a year.
Two-point	- Calibration is off-set corrected for radiation from FTIR, apertures, etc. - The calibration can be made traceable. - The FTIR spectrometer can be calibrated with high accuracy with one hot high-quality blackbody and a simple blackbody at ambient temperature.	- The blackbody temperatures should be measured for both blackbodies. - Temperature sensors should be calibrated periodically, e.g. once a year.
Three-point	- Blackbody surface temperatures are found from the measured three-calibration spectra. - Spectra are off-set corrected for radiation from FTIR, apertures, etc.	- Three blackbodies are required. - Quality of calibration sensitive to noise, instrument drift and emissivity variations with temperature. - The calibration is not traceable.

High-temperature gas cell, FT-HOTGAS facility

The optical properties of hot gases must be determined in order to establish temperatures and chemical species in aircraft exhaust by non-intrusive FTIR measurements. Therefore, a new improved high-temperature gas cell was built at Risø in 1998 to be used for spectroscopic investigations of the transmissive and the emissive behaviour of exhaust gases in the

temperature range from ambient to 1000 K (upper limit 1273 K). The analytical procedures are described in refs. 4 and 6.

The FT-HOTGAS facility was taken from Risø to DLR in June 1999 for validation measurements with the MIROR spectrometer as planned. Risø brought three gas bottles (A, B, C) with three different gas mixtures. Information on the content of the gas bottles and the temperatures of the hot gas cell was not passed to DLR. Six complete data sets were obtained, i.e. emittance and transmittance measurements for each of the three gas bottles at two different temperatures, see examples in Figure 23. Further details about the instrumentation, experiments, data analysis and results will be described in a future paper.

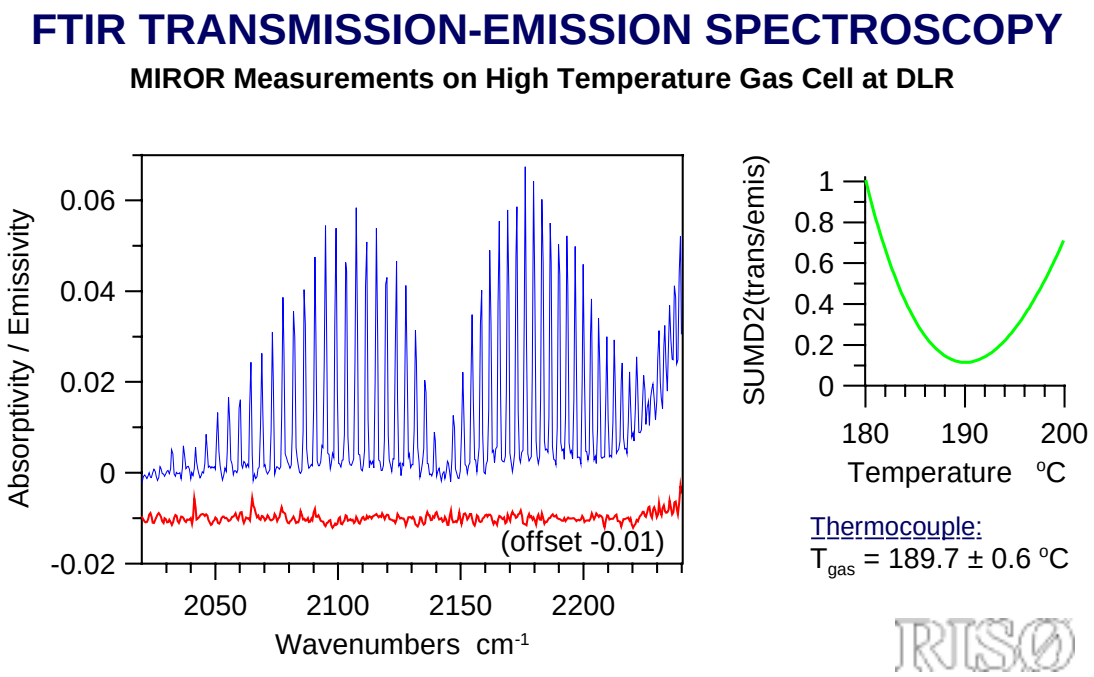

Figure 23. The gas temperature is determined to be 190 °C from the transmittance-emittance spectra of CO which is in good agreement with thermocouple measurements of the gas cell temperature (189.7 °C). The transmission-emission method (refs. 4 and 6) was applied to find the gas temperature. Measurements were performed with the MIROR FTIR spectrometer at DLR, Germany.

Low-resolution spectroscopy

A method based on chemometrics for rapid simulation of gas spectra has been developed.[1] The method is part of a new program which can be used to make quantitative predictions of measured gas spectra even if these spectra contain complex background signals. The program has been tested on measured 1 cm^{-1} CO spectra recorded at the Bomem MB100 interferometer. It has been shown that it is possible to make accurate predictions of CO based on spectra containing fluctuating baselines and interfering gaseous components. The method on which the program is based will be used to find the optimal set of parameters, i.e. CO/CO_2 concentrations and temperature of the test gas spectra measured at DLR, Munich, June 1999.

Thermovision camera

Risø's thermovision camera, Radiance PM, was installed at the wall of the test rig for monitoring thermal radiation from the hot exhaust gas. The camera was mounted with a special filter to enhance the structures of the gas temperature in the exhaust gas jet. Thermal pictures of the exhaust gas were stored digitally during all FTIR measurements; furthermore, about 32 selected pictures were stored on a flash card for image postprocessing.

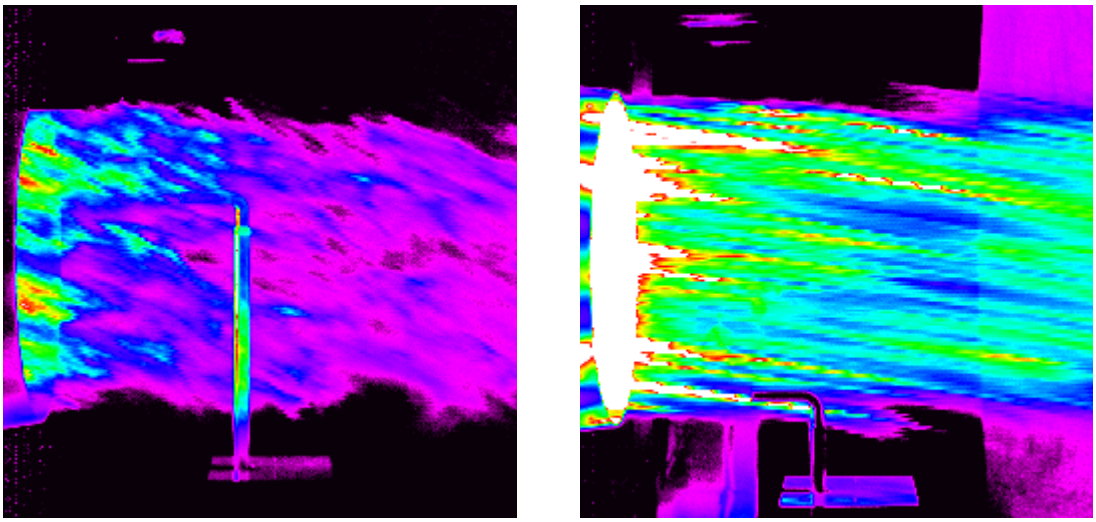

Figure 24. Thermal pictures of exhaust gas at idle (left) and take-off (right) recorded in the test rig at Fiat Avio, Naples, Italy.

The thermal pictures in Figure 24 show a relatively complex temperature distribution of the exhaust gas with hot spots in the outer region of the jet where combustion gas mixes with colder air.

Further details on the work and the results of the Aeroprofile project can be found in the references below.

1. Bak, J., Rapid method for simulating gas spectra using reversed PCR temperature calibration models based on Hitran data. *Appl. Spectrosc.* (1999) **53** , 1375-1381.

2. Clausen, S.; Bak, J., AEROPROFILE - Risø-målinger i München og Napoli. *Industriel IR-analyse. Nyhedsbrev* (1999) (no. December), 1-2.

3. Clausen, S.; Bak, J., Måling af forbrændingsgasser fra fly; Simulering af IR-gasspektre. *Industriel IR-analyse. Nyhedsbrev* (1999) (no. Marts), 1-2.

4. Bak, J.; Clausen, S., FTIR transmission-emission spectrometry of gases at high temperatures: Demonstration of Kirchhoff's law for a gas in an enclosure. *J. Quant. Spectrosc. Radiat. Transfer* (1999) **61** , 687-694.

5. Bak, J.; Clausen, S., Signal-to-noise ratio of FT-IR CO gas spectra. *Appl. Spectrosc.* (1999) **53** , 697-700.

6. Clausen, S.; Bak, J., FTIR transmission emission spectroscopy of gases at high temperatures: Experimental set-up and analytical procedures. *J. Quant. Spectrosc. Radiat. Transfer* (1999) **61** , 131-141.

3.3.3 Infrared combustion diagnostics

J. Bak and S. Clausen
E-mail: sonnik.clausen@risoe.dk

Optical measuring methods are useful for non-intrusive sensing in combustion and gasification systems, particularly in a sooty or aggressive environment and at high temperatures. Risø has developed methods for fast and precise measurement of gas temperature (300 – 2000 °C), e.g. with a fibre-optic infrared (IR) probe. The IR-probe is

suitable for collecting detailed measurements in small- and large-scale combustion facilities. The technique is mostly applied in situations where the quality of the process measurements is uncertain or more detailed process information is required. An example of simultaneous measurement of gas temperature, particle temperature and gas concentrations is shown in Figure 25. The work has been presented at the Pittcon conference[1].

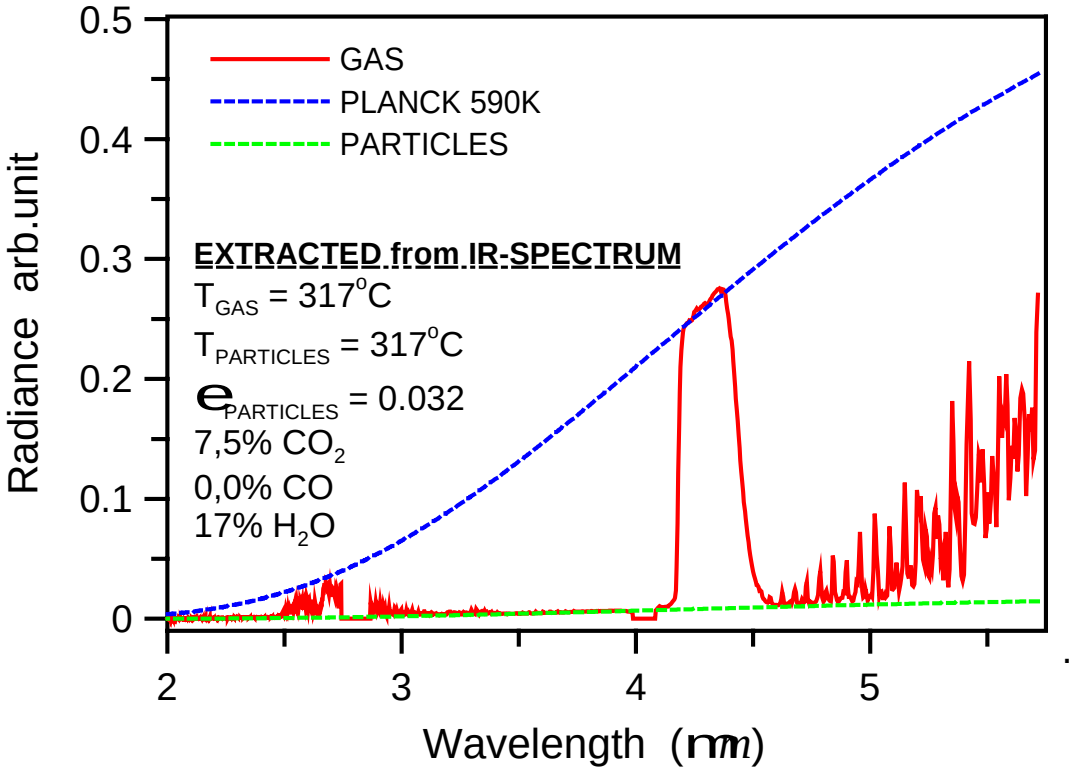

Figure 25 Results extracted from spectrum measured in a waste incinerator (Vestforbrænding I/S, Denmark) with Risø's IR-probe.

1. Bak, J.; Clausen, S., High temperature gas analysis in industrial environments. Pittcon '99, Orlando, FL (US), 7-12 Mar 1999. Unpublished.

3.3.4 FT-IR spectroscopic analysis of straw ashes

J. Bak
E-mail: jimmy.bak@risoe.dk

Diffuse reflectance infrared Fourier transform spectroscopy (DRIFTS) is a useful technique for measuring the ionic compounds present in ceramic powders quantitatively as well as qualitatively. In the BIOG project, sponsored by the Danish company ReaTech and the Danish Ministry of Environment and Energy, it has been demonstrated that DRIFTS can be used to determine the sort of ionic compounds in biomass materials such as straw ashes. Several kinds of straw ash samples were analysed. The following kinds of samples have been made and analysed:

- Determination of potassium hydrogen carbonate ($KHCO_3$) in barley ash samples. The content of potassium hydrogen carbonate in these samples was proved by the presence of spectral lines from this compound.

- Determination of hydrated potassium carbonate (K_2CO_3) in wheat ash samples. Two different samples gasified in water at different temperatures (wheat1: 850 °C and wheat4: 800 °C) were investigated. The IR analysis revealed that both samples contained a high amount of hydrated potassium carbonate. The content of the hydrated compound in these samples is verified by the observation that the spectral lines of the non-hydrated compound are split and shifted, see Figure 26.

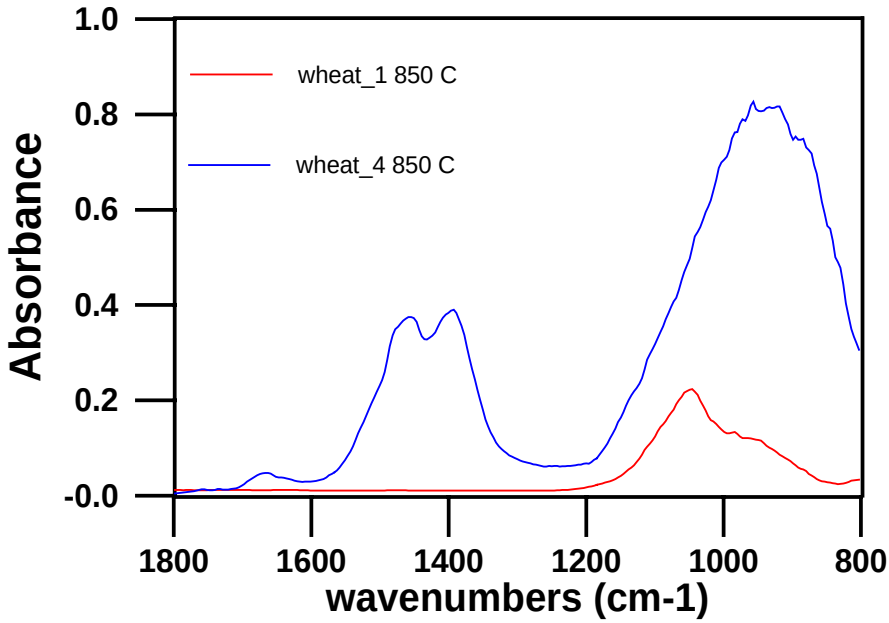

Figure 26. The double spectral peak at 1400-1500 cm^{-1} indicates the presence of hydrated potassium carbonate in wheat_4.

3.3.5 FT-IR measurements of biological materials

P. S. Jensen, J. Bak and S. Clausen
E-mail: peter.snoer.jensen@risoe.dk

The use of non-invasive diagnostic methods for monitoring the content of glucose in human blood has been the subject of intense studies around the world and is characterised by many claims of successful methods. However, there does not exist a universally accepted robust analytical method for this purpose. Determination of low concentrations of glucose in a complex medium, such as the human body, necessitates that sensitive detection systems and advanced software for data analysis are available. In order to measure small amounts of organic compounds in aqueous systems the influence of temperature variations and interferences should be investigated and well understood. There is thus a need for more fundamental work to be carried out in order to provide the necessary information and, thereby, determine the feasibility of the IR-spectroscopic methods. At Risø National Laboratory, the FT-IR group and the biomedical optics group have initiated a study of a simple to provide relevant information for future in-vivo measurements, namely the measurement of glucose in water using transmission FT-IR spectroscopy. The purpose of this study is to provide a foundation for evaluating the numerous claims of successful non-invasive glucose monitoring using IR and Raman spectroscopy which could result in new ideas of how to improve the detection limits of organic compounds in aqueous systems.

3.4 Phase contrast techniques

3.4.1 Optimising the common path interferometer: a theoretical framework

J. Glückstad and P. C. Mogensen
E-mails: jesper.gluckstad@risoe.dk and *paul.mogensen@risoe.dk*

We are developing a complete theoretical analysis for the general description and optimisation of the whole class of common path interferometers.[1-3] The aim is to treat all commonly used methods such as the Zernike and Henning phase-contrast techniques, the Smartt Interferometer and the generalised phase-contrast method. There is currently no definitive analytical method for such a treatment. The primary area of interest is the development of an approach for simultaneously optimising both the visibility (contrast) and the peak irradiance at the output of the optical system. At present this is often done by a largely trial and error basis. There are currently only a few specialist cases for which there exists some degree of successful analytical treatment.

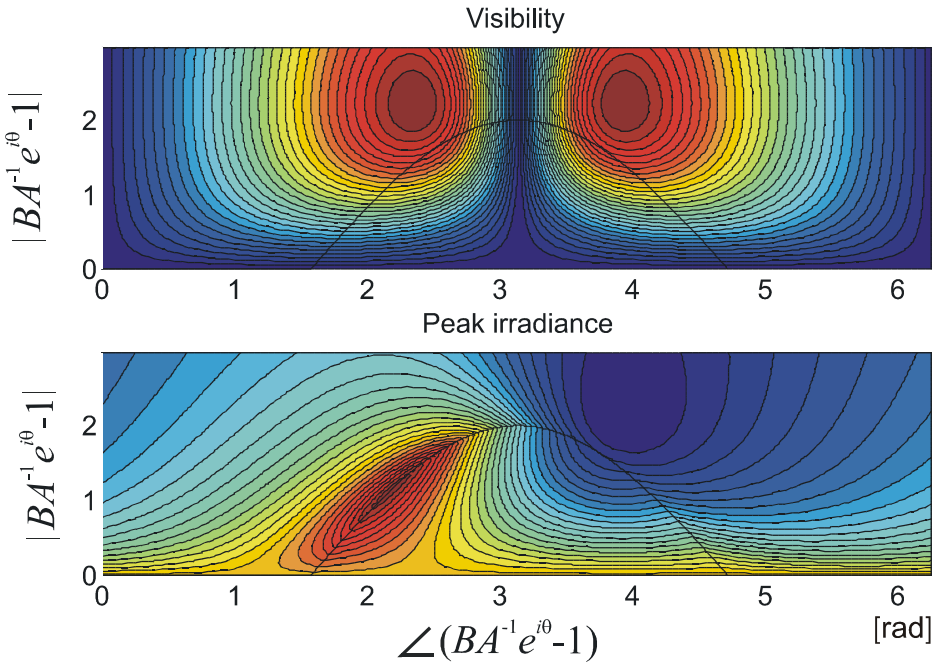

Figure 27. Contour plots of the visibility and peak irradiance for a common path interferometer as a function of the filter parameters *A*, *B* and θ in phase space. The maxima and minima of the contour plots are denoted by the red and blue regions, respectively. The curve shown on both plots indicates the regime of lossless operation in which there is no absorption in the filter (*A*=*B*=1).

In Figure 27 we show an example of a result from an analysis of a common path filtering system. There are actually a range of parameters that the filter can have which control the phase shift (θ) and attenuation in the filtering element (*A* and *B*) as well as the physical relationship between the size of the filtering element and the spatial frequency distribution in the filtering plane. Each of these parameters can be independently varied resulting in a large range of possible, though not necessarily useful, combinations. The aim behind our current work is to find an approach for optimisation of the filter parameters in a logical fashion. The plots in Figure 27 show how visibility and peak irradiance vary as a function of the modulus and angle of a vector describing the filter in phase space. The parameters *A*, *B* and θ relate to

the filter whilst the other parameters relate to properties of the input wavefront. It can be seen that there are a very small range of filter parameters for which either the visibility or the peak irradiance are maximised (the red regions in Figure 27). Changing the input phase values results in a modification of the choice of filtering parameters that one might wish to use to maximise the visibility.

1. J. Glückstad, "Phase contrast image synthesis", Opt. Comm. **130**, 225, 1996.
2. J. Glückstad, L. Lading, H. Toyoda and T. Hara, "Lossless light projection", Optics Letters **22**, 1373, 1997.
3. J. Glückstad, "Graphic method for analyzing common path interferometers", Appl. Opt. **37**, 34, 8151, 1998.

3.4.2 Phase-only optical encryption

J. Glückstad and P. C. Mogensen
E-mails: jesper.gluckstad@risoe.dk and *paul.mogensen@risoe.dk*

There is currently a high level of interest in the application of optical techniques to the fields of security and product authenticity verification. Optical encryption techniques offer a viable solution to these problems. The advantages inherent in an optical approach to encryption, such as a high space-bandwidth product, the difficulty of accessing, copying or falsification and the possibility of including biometrics are widely recognised.

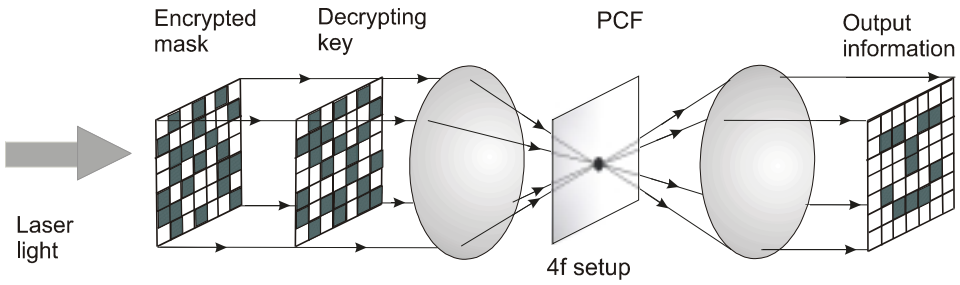

Figure 28. The generic optical encryption set-up. An encrypted phase mask is decrypted by the application of the correct phase key. The decrypted phase information is then visualised using the generalised phase contrast technique in which a phase contrast filter (PCF) placed in a 4f set-up is used to generate an intensity pattern containing the encoded information at the output of the optical system.

We have developed a phase-only optical encryption system in which the readout of phase information is by the application of the generalised phase contrast technique.[1] The generic encryption system is shown in Figure 28. Collimated laser light illuminates an encrypted mask, which consists of a random array of binary phase-shifting pixels. This phase-mask has been produced by electronically scrambling the binary information with a random binary pattern and using this to generate an encrypted mask. The decrypting key, implemented on a phase-only spatial light modulator (SLM) reverses the scrambling operation in the optical domain and decrypts the encrypted phase mask generating a wavefront in which the information of interest is encoded as a relative phase shift between different sections of the wavefront. This phase information is subsequently visualised using the generalised phase contrast technique with a phase contrast filter (PCF). Experimental results from a decryption of a fixed mask are shown in Figure 29, in this case the encoded information is a smiling face character which is seen as a decrypted image in Figure 29(a).

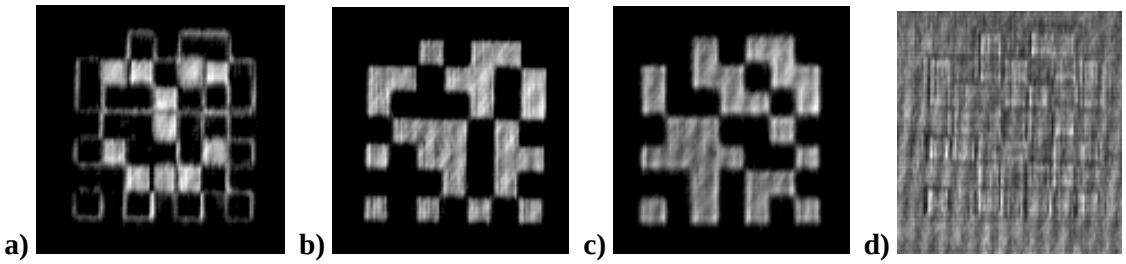

Figure 29. Decryption of a 7x7 pixel fixed mask with a 7x7 pixel dynamic key. (a) Shows a successful decryption, (b) shows an image of the fixed phase mask viewed with the PCF and (c) shows the corresponding image for the decrypting key. If the PCF is misplaced, then nothing relating to the encoded information is seen (d).

1. J. Glückstad, International Patent Application, PCT/DK99/0031, 03 July 1998.

3.4.3 Dynamic array generation for optical tweezers

J. Glückstad and P. C. Mogensen
E-mails: jesper.gluckstad@risoe.dk and *paul.mogensen@risoe.dk*

The use of optical tweezers for the trapping, study and manipulation of small dielectric particles is well established as a practical tool in a wide range of disciplines. Optical tweezers work by using the radiation pressure from a focussed laser beam to securely trap and hold small particles ranging in size from tens of nanometers to tens of microns.

It is often desirable to operate a number of optical tweezers simultaneously to control the relative movement or placement of molecules independently. We propose the use of a phase-only spatial light modulator to encode an image directly in the phase component of a laser beam. This phase-encoded information serves as the input for a phase-contrast system, in which a phase-contrast filter generates a high-contrast amplitude pattern that corresponds directly to the phase perturbation in the input wavefront. This amplitude pattern can then be focussed down using a microscope objective in order to produce a suitable wavefront for microscopic optical particle trapping.[1]

In Figure 30 we show the experimental arrangement that has been used to investigate the generalised phase contrast technique as an encoding approach for array generation in optical tweezers. A set of experimental results is shown in Figure 31. In this case we have chosen to generate and independently manipulate 16 individual light beams which have an annular profile. These so-called "doughnut" beams have applications in optical tweezers where their shape is well suited to the trapping of either high or low refractive index particles whilst also minimising the damage that can be inflicted on biological specimens.

1. J. Glückstad and P. C. Mogensen "Reconfigurable Ternary-phase array illuminator based on the generalised phase contrast method" Opt. Comm. **165**, pp. 169-175, 2000.

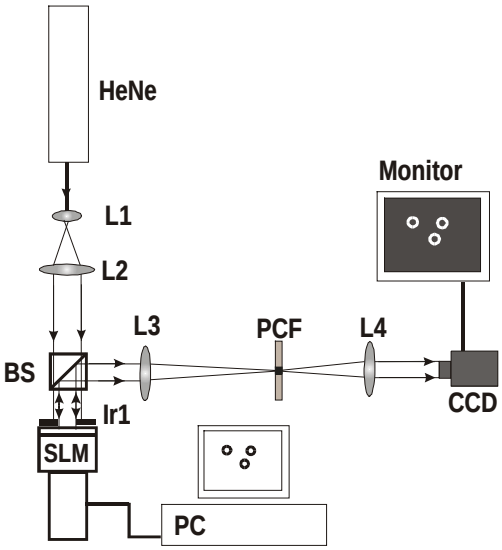

Figure 30. The experimental set-up. A HeNe laser beam (expanded with L1 and L2) is incident on the phase modulating SLM with an aperture defined by the iris (Ir1). A beamsplitter (BS) directs the modulated light into the 4-*f* system (formed by L3 and L4) containing the phase contrast filter (PCF).

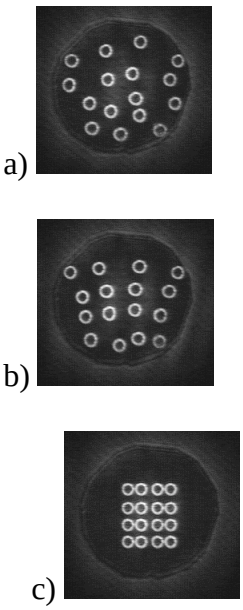

Figure 31. A set of high-contrast images showing the movement (a) and (b) of 16 "doughnut" beams to form a 4x4-array (c). The number, position and beam profiles can all be arbitrarily chosen to suit the desired application.

3.5 Optical measurement techniques

3.5.1 Three-dimensional speckles

R. Skov Hansen, H. T. Yura (Electronic Technology Center, The Aerospace Corporation, P.O. Box 92957, Los Angeles, California, 90009, USA), S. Grüner Hanson and B. Rose (IBSEN Micro Structures A/S, Gammelgaardsvej 65, DK-3520 Farum Denmark)
E-mail: rene.skov.hansen@risoe.dk

The space-time evolution of speckles in a plane has been extensively treated in literature, where many applications regarding measurements of surface roughness, object displacement and velocity have been made. Here we are concerned with the intrinsic 3D nature of speckles that are formed after propagation through an arbitrary optical system. For simplicity in notation, we consider only paraxial optical systems without limiting apertures as characterised by paraxial *ABCD* ray-matrix techniques (where the *ABCD*-system matrix is real valued). We discuss the space-time evolution of the 3D speckles that result from in-plane translation of a diffusely scattering object that is illuminated by a Gaussian shaped laser beam.

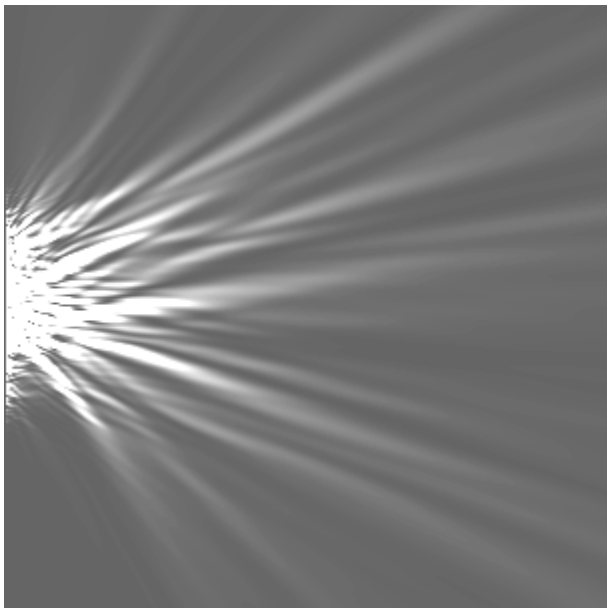

Figure 32. Simulation: Speckles emerging from an optically rough surface.

The most general description of the space-time evolution of a speckle pattern is given by the normalised spatio-temporal cross covariance of the optical intensities, $I(\mathbf{p}_1,t_1)$ and $I(\mathbf{p}_2,t_2)$, in the observation plane, $C_I(\mathbf{p}_1,\mathbf{p}_2;t_1,t_2)$. The vectors $\mathbf{p}_{1,2} = \{\vec{\rho}_{1,2} = \{x_{1,2}, y_{1,2}\},\ z_{1,2}\}$ denote the two spatial observation points of interest and $t_{1,2}$ are the corresponding observation times. If at a given time t_1 there is a bright speckle located at $\mathbf{p}_1$, then this speckle will, with a high degree of certainty, be located at $\mathbf{p}_2$ at time t_2 where the cross covariance has its maximum value. Thus, the cross covariance conveys information regarding the (average) motion of a speckle as an entity in space and time. Maximum values of the normalised cross covariance less than unity indicate a general decorrelation of the optical field at the position of the observer. On the other hand, quantitative estimates of the characteristic lateral and longitudinal speckle sizes and corresponding orientation can be obtained directly from the spatial distribution of the normalised autocorrelation function of the intensity, $C_I(\mathbf{p}_1,\mathbf{p}_2;0)$. In summary: $C_I(\mathbf{p}_1,\mathbf{p}_2;t_1,t_2)$ gives the mean movement of a speckle as a whole and $C_I(\mathbf{p}_1,\mathbf{p}_2;0)$ gives the size and orientation of the static speckle in each position in space.

The orientation of the speckles is (in mean) given by a straight line:

$$\Delta\vec{\rho} = \frac{D}{B}\vec{\rho}\Delta z, \tag{1}$$

where *D* and *B* are the matrix elements of the geometrical optical propagation matrix. A simulation of the 3D speckles can be seen in Figure 32.

When the object surface is moved in its own plane, the speckles will be moving in planes perpendicular to the optical axis:

$$\Delta\vec{\rho} = \tilde{A}\mathbf{v}\tau \text{ , and } \Delta z = 0. \tag{2}$$

where A and B are the matrix elements of the geometrical optical propagation matrix, $\tilde{A} \equiv A + B/R$, R is the radius of curvature of the illuminating beam, τ is the time difference, and $\boldsymbol{v}$ is the velocity of the object surface.

Some examples of the speckle orientation:

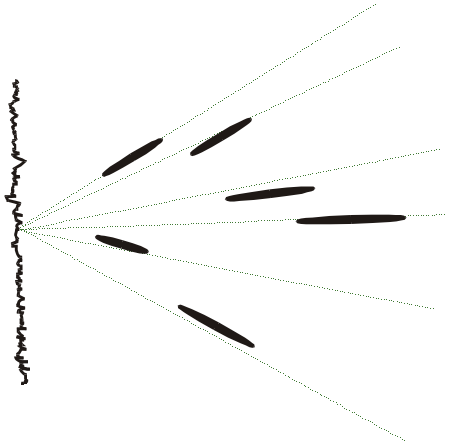

Free space configuration: A Gaussian laser beam illuminates a rough object surface. The speckles will be pointing towards the centre of the object illumination.

Imaging optical system: The speckles are pointing towards the optical axis at the image plane.

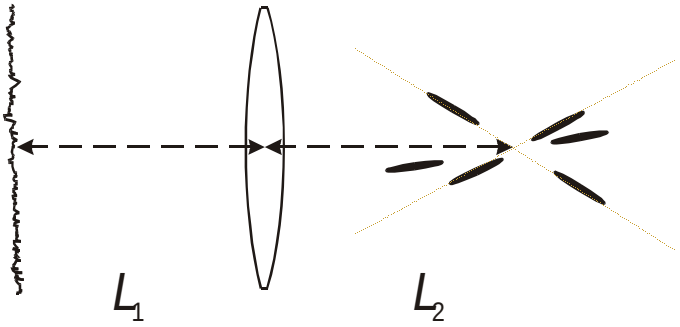

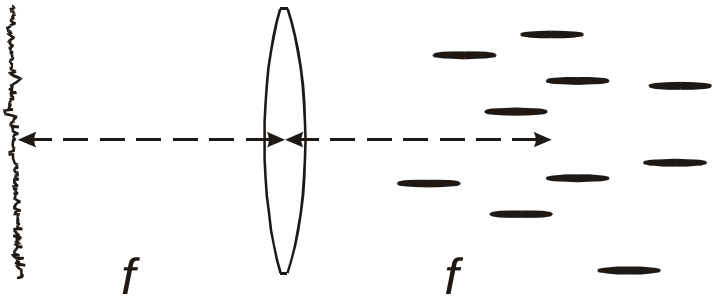

In the Fourier transforming optical system all the speckles are aligned in parallel with the optical axis.

Some examples of the speckle dynamics in the case of in-plane object translation:

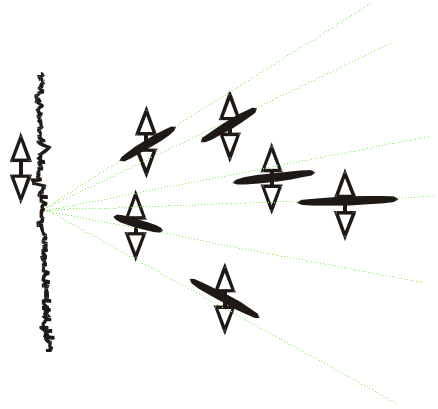

Free space configuration: The speckles will move in planes parallel with the object surface when the surface is moved in its own plane. The rate of the movement is proportional to the distance to the object surface. As can be seen, the speckles will always be pointing against the illumination centre. Therefore, as the speckles move, they will seem to rotate around the centre of the illumination spot.

In the imaging system the speckles will seem to be rotating around the intersection between the image plane and the optical axis.

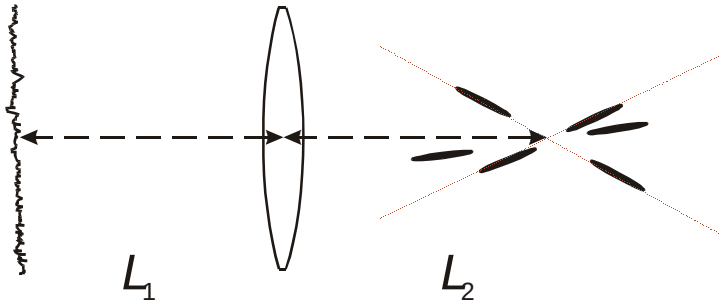

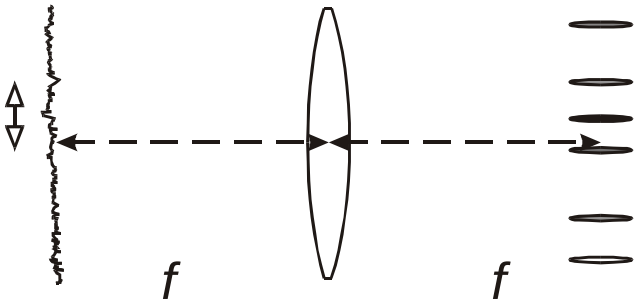

In the Fourier transforming system the speckles will not move at all. A decorrelation of the speckles will take place as new areas of the object surface enter the illumination spot.

1. Yura, H.T., Hanson, S.G., Hansen, R.S. and Rose, B., “Three-dimensional speckle dynamics in paraxial optical systems”. J. Opt. Soc. Am. A (1999) **16** , 1402-1412.
2. Hansen, R.S., Yura, H.T., Hanson, S.G. and Rose, B., “Three-dimensional speckles: static and dynamic properties”, in Fourth International Conference on Correlation Optics, Oleg V. Angelsky, Editor, Proceedings of SPIE Vol. 3904, 140-149.

3.5.2 Compact system for measuring rotational speed in two dimensions

S. G. Hanson, R. Skov Hansen and B. Hurup Hansen
E-mail: steen.hanson@risoe.dk

A simple system for detecting the rotation in two directions of a reflective ball has been developed. The primary goal for the set-up was to realise a simple and compact concept that has adequate precision to be used for PC-cursor control. A slightly diverging beam from a Vertical Cavity Surface Emitting Laser (VCSEL) mounted on a pcb-board with a diameter of 10 mm illuminates a reflective ball (Ø 4 mm) placed at a distance of 15 mm. Light scattered off the rotating ball produces a speckled field that sweeps across two pairs of elongated photodetectors arranged perpendicular to each other. The four photodetector signals are digitised and fed into an ASIC that determines the rotation of the ball in two directions including the sign of the rotation.

The principles previously put forward[1] have been followed in the design of this simple, inexpensive and compact optical measurement scheme. These virtues have been obtained while lessening the demand for accuracy. As shown in Figure 34 we use a slightly diverging beam from a commercially available multimode VCSEL with a wavelength of 850 nm and an output power of approximately 1.15 mW – modulated with a duty cycle of 30%. Light scattered off the surface of a partly reflective ball (diameter 4 mm) placed at a distance of 15 mm establishes a speckle pattern in the VCSEL plane where four elongated photodetectors are placed, in pairs, perpendicular to each other. Each pair of photodetectors (D_1, D_2, D_3 and D_4) determines the speckle pattern movement along the direction perpendicular to the major axes of the photodetectors.

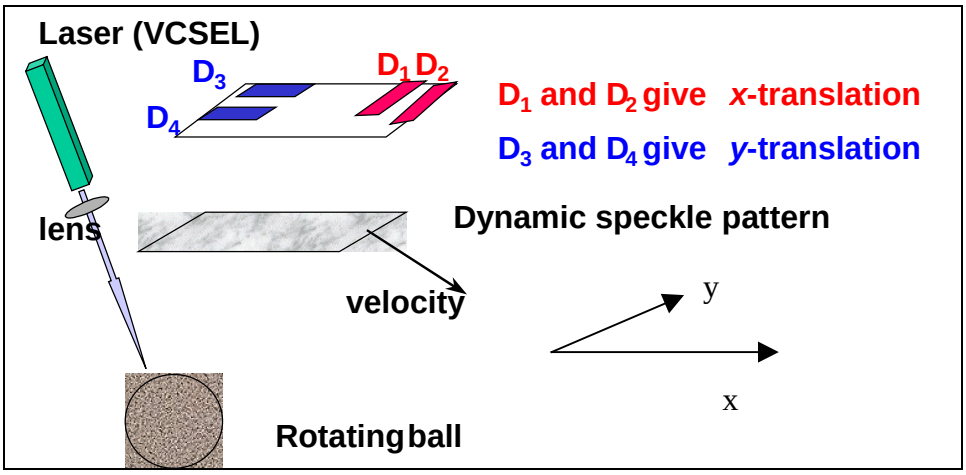

Figure 34. Temporally coherent light from a VCSEL is scattered by the reflecting ball and subsequently collected by the four photodetectors.

The requirement for the system was that it had to be small and rather inexpensive with only minor need for alignment.[2] Besides, its lifetime had to be high and the power consumption should be low. In contrast, the measurement accuracy for this application could be limited.

The optical layout is shown in Figure 35. The left-hand side shows the entire printed circuit board made as a flex print with the two ASICs of which the first processes the signals from the four photodetectors while the second ASIC transmits the cursor control signals to the PC.

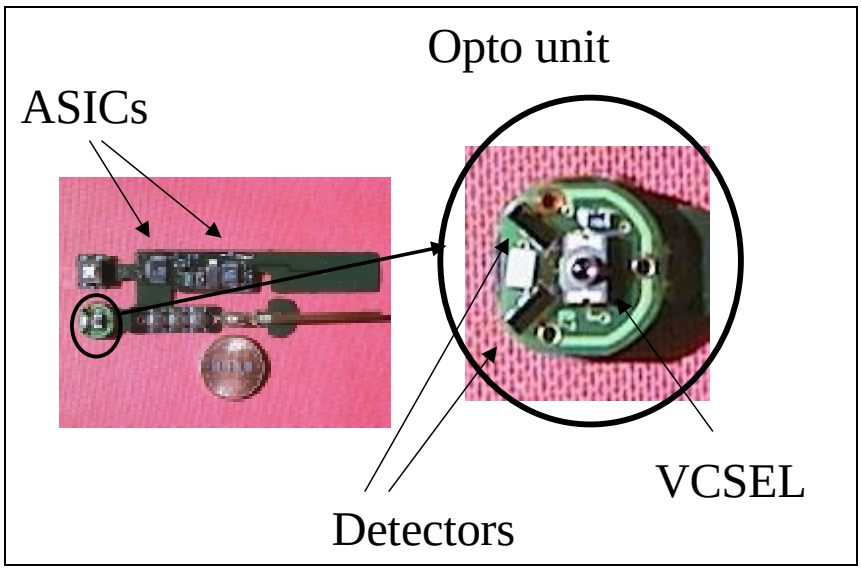

Figure 35. Flex board with expanded view of opto-unit.

The flex board, including the opto-unit, is inserted in a pen, shown in Figure 36, in which a Li-battery provides the necessary power. The radio signals are transmitted 40 times a second to a receiver inserted in the serial port of the computer. Besides the directional signals, the status of the pressure applied to the ball and the status of the three push buttons are also transmitted. Once driver software is installed in the PC, the pen can control cursor movement and perform the functions of a computer mouse. This project was performed for the Danish company Kanitech International A/S (www.freepen.dk).

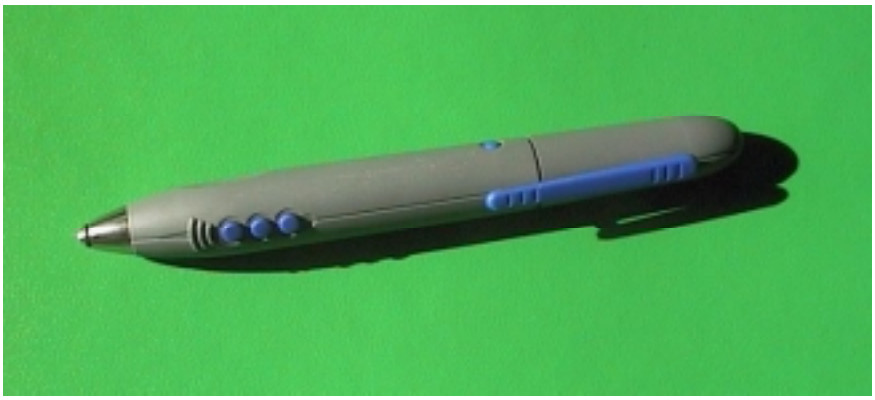

Figure 36. The complete pen unit with the ball in the pen tip. The opto-unit is mounted in the pen 15 mm from the ball and facilitates the probing of the angular deflection.

1. S. G. Hanson and B. H. Hansen, “Laser-based Measurement Scheme for Measurement of Specularly Reflective Shafts,” SPIE **2292** Fiber Optic and Laser Sensors XII (1994), pp. 143-153.
2. S.G. Hanson, R.S Hansen and B. H. Hansen, “Compact System for Measuring Rotational Speed in Two Dimensions”. In: Proceedings. Optical measurement systems for industrial inspection, Munich (DE), 16-17 Jun 1999. Kujawinska, M.; Osten, W. (eds.), (International Society for Optical Engineering, Bellingham, WA, 1999) (Proceedings of SPIE, v. 3824) pp. 115-123.

3.5.3 Angular encoder

S. G. Hanson, H. E. Larsen, S. Peo Pedersen and B. Rose (IBSEN Micro Structures A/S, Farum, Denmark)
E-mail: steen.hanson@risoe.dk

A technology for precise determination of angular displacement of a solid surface patented by the Danish company IBSEN Micro Structures A/S and Risø National Laboratory is currently being commercialised by the Danish company JJ-Measurement Technology. The idea is to develop an absolute encoder which will make it possible to position samples very accurately in scientific set-ups. This project is partly supported by VaekstFonden (Business Development Finance) and by CAT Science Park.

The basic idea has previously been reported[1,2] and relies on the fact that speckle translation observed in the Fourier plane of an optical system is related only to the angular displacement of the target, which is illuminated with a plane wave of coherent light. Any linear translation of the target will merely result in speckle decorrelation, but will not cause any collective speckle displacement.

The basic set-up is depicted in Figure 37 where a collimated laser beam illuminates the object, while the scattered light is detected by a linear array placed in the back focal plane of the lens, i.e. $z_2 = 0$.

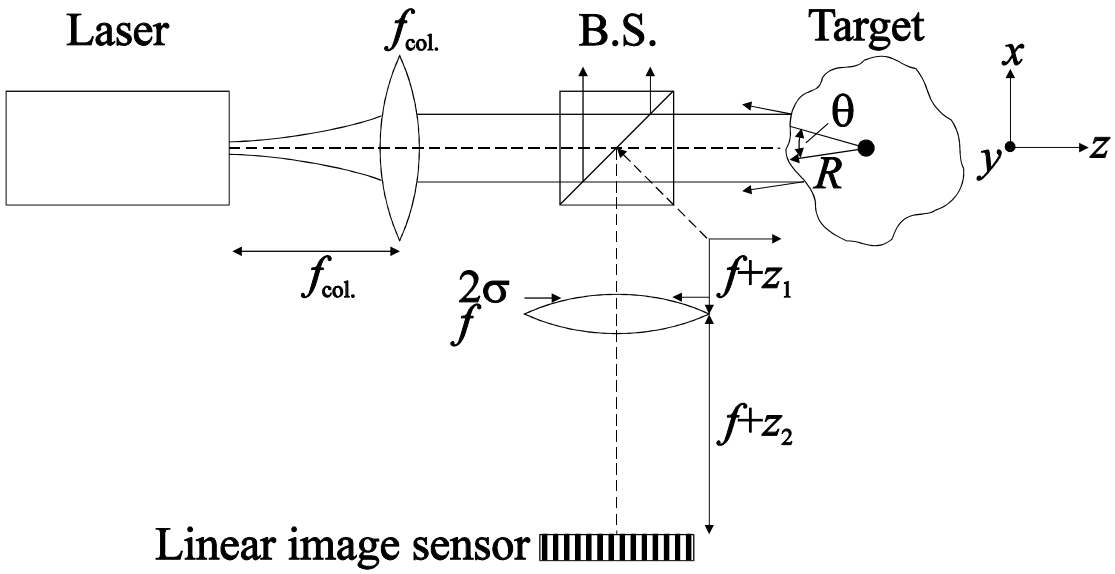

Figure 37. Optical diagram for the angular displacement sensor set-up.

It has here been shown that a small angular displacement, θ, will result in a linear displacement of the speckle pattern by an amount $2f\theta$ in the detector plane. Thus, the relation between applied angular and measured linear displacement does not depend on the wavelength of the light, the distance to the object and the axis about which the object is rotated.

The system will be used for determining the angular position of a rotary table. The speckle pattern is successively recorded around the entire circumference of the object, and the angular object displacement between adjacent speckle patterns is determined by calculating the displacement for obtaining maximum crosscorrelation between the two patterns. A large series of speckle patterns will be recorded, each being related to a certain angular position of the object. In this way a fingerprint of the entire surface has been recorded and high positional

accuracy can later be obtained as the table is rotated. A relative angular accuracy of 5 microradians may be achieved, while an absolute accuracy of 200 microradians will be feasible.

1. Rose, B.; Imam, H.; Hanson, S.G., Non-contact laser speckle sensor for measuring one- and two-dimensional angular displacement. J. Opt. (1998) v. 29 p. 115-120.
2. Rose, B.; Imam, H.; Hanson, S.G.; Yura, H.T.; Hansen, R.S., Laser-speckle angular-displacement sensor: Theoretical and experimental study. Appl. Opt. (1998) v. 37 p. 2119-2129.

3.5.4 Laser anemometry for control and performance testing of wind turbines

R. Skov Hansen
E-mail: rene.skov.hansen@risoe.dk

This research is funded in part by the European Commission in the framework of the Non-Nuclear Energy Programme JOULE III.

The general objective of the project is to improve the market position of wind power by reducing the costs of the energy produced and by enhancing its credibility with more accurate performance assessment.

The project, carried out in the Optics and Fluid Dynamics Department, deals with the construction of a flexible and portable instrument that remotely measures wind velocities in front of the wind turbine. These measurements would be attractive in order to optimise the energy production coming from wind power. A laser anemometer has been found to constitute the most flexible instrument for performing remote measurements of the wind speed.

The laser anemometer shall be mounted on top of the nacelle and focuses a single laser beam in front of the wind turbine. The velocity of the wind is determined by measuring the introduced Doppler shift of the laser light, scattered backwards from the aerosols in the beam waist. The measurement should be carried out as a sufficient distance from the turbine that the measured wind is unobstructed by the turbine and so that a 'feedforward' control that compensates for the response time of the turbine itself could be applied. These two requirements have led to a target measuring distance of 150 m. Based on the properties of available laser sources, the CO_2 laser with an optical wavelength of 10.6 μm has been selected. It seems unlikely that solid state lasers will be advantageous for this application within the foreseeable future.

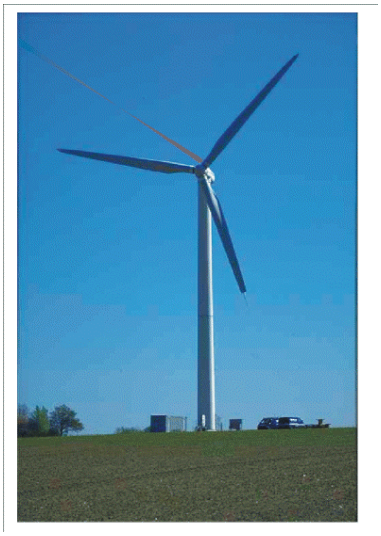

It is well known that feedback into a laser may perturb the power level. In fact, if the backscattered light is fed into the laser, the optical power of the laser will be modulated at the Doppler shift frequency. An autodyne detection system based on this concept would intrinsically be much simpler and more robust than a heterodyne system with external mixing. Additionally, the alignment of this set-up is much simpler than for the heterodyne system. Investigations as to whether such an autodyne system is suitable for the anemometer and the design criteria for the laser to be employed are under progress. In the autodyne scheme

considered here the light received from the measuring volume returns back through the same telescope as the transmitted beam and enters the laser whereby the laser is perturbed. The modulations on the laser power are measured by extracting approx. 80 mW of the power from the rear laser output to the detector.

The telescope, planned for the anemometer, consists of two off-axis parabolic mirrors, a small convex mirror in front of the laser and a large concave output mirror focusing the output beam, see Figure 38. Simulations predict that the system is capable of giving diffraction limited focusing of the output beam.

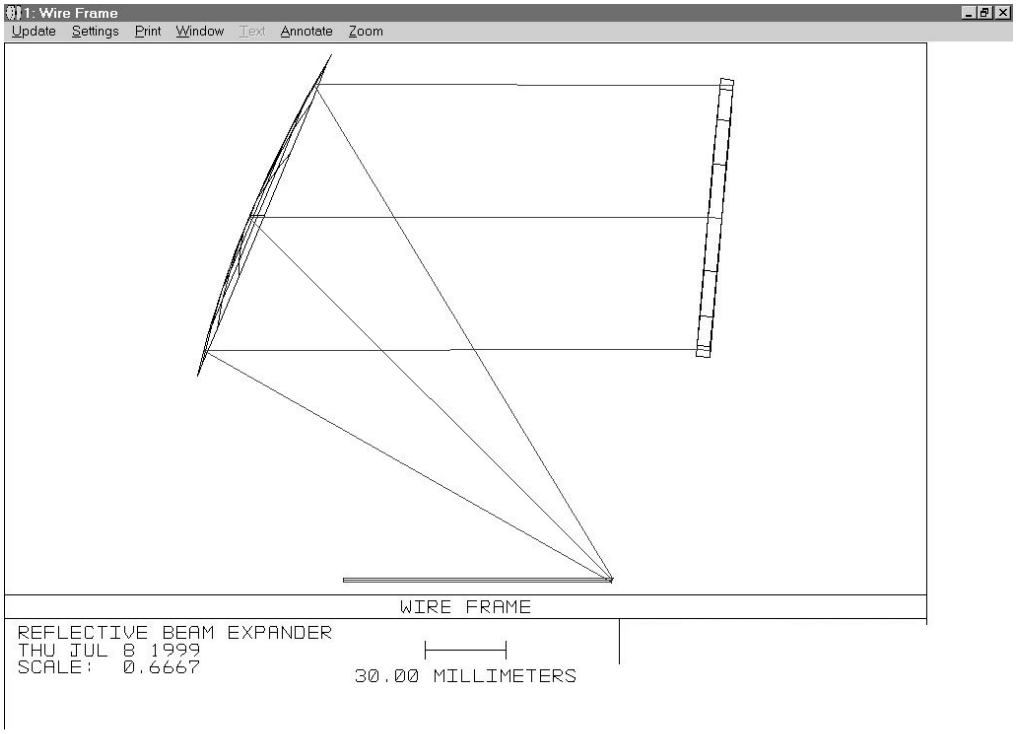

Figure 38. The telescope planned for the laser anemometer. The telescope consists of two off-axis parabolic mirrors. The output from the laser is incident on the small mirror at the bottom of the figure. The window at the output is for protecting the whole optical system.

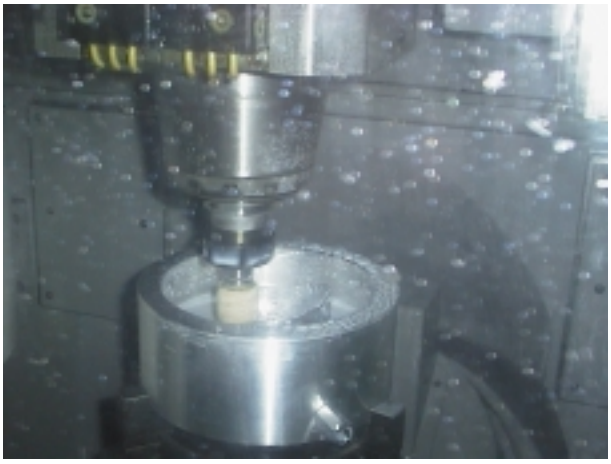

The overall tolerance of the mirror surfaces is given to be better than ±10 μm. It is possible to meet these tolerances on the surfaces by using a numerically controlled cutter. A set of mirrors is under production at the tool shop at Risø National Laboratory.

The cost price of the mechanics to fix the optical components is high, and especially the costs of turning of the mirrors in metal are extremely high. A method for obtaining a minimum price of the laser anemometer in volume production is to use a casting technique of especially the mirrors for the telescope and the mechanics for the fixing of the optical components. Comparing the elastic modulus of composite materials made of carbon fibres, $E \approx 9300$ N/mm^2, with most metals, these materials seem feasible for the production of both the mirror surfaces and the whole optical assembly. A further investigation of the usefulness of these materials is in progress. Building the mechanics for the laser anemometer in composite materials combined with the telescope configuration chosen enables a compact and low-weight construction of the laser anemometer.

3.6 Knowledge-based processing

3.6.1 Data mining and soft-modelling

T. M. Jørgensen and C. Linneberg
E-mail: thomas.martini@risoe.dk

The purpose of mathematical modelling is to describe relationships between observed variables within a given system. In hard-modelling one builds a model describing, e.g., the physical properties of a mechanical system using known physical laws. If they are not known in advance, the parameters in the hard model can then be estimated from multiple measurements on the system. Opposed to this is soft-modelling where nothing (or little) is known about the properties of the system in question. The main information available is several observations, each containing a number of coupled measurements on the system as well as the state of the system that we want to model.

A variety of techniques exist for soft-modelling and are mainly represented by the so-called machine learning algorithms and artificial neural networks. One such method is the n-tuple classifier which is a general learning-based method. It is appealing due to its simple design, the intrinsic possibility of performing so-called cross-validation of the obtained model and the fact that it is suited for both hardware and software implementation.

Even though the n-tuple based learning algorithm is around 40 years old, it has not previously been analysed in a proper statistical sense and, accordingly, it has not been clear when and whether the method could act as an approximate estimator to the theoretically optimal decision scheme. A theoretical framework has now been established which makes it possible to integrate and understand the n-tuple classifier (also denoted as a RAM-based neural network) from Bayesian probability theory.[1] The theoretical insight has in turn led to the development of essential improvements of the n-tuple architecture, accumulated in two patents[2,3] now held by Intellix A/S. The corresponding techniques have also been utilised in a commercial data mining project where the methods are used to detect patterns in a multidimensional data set that can be used to characterise a given class or behaviour.

1. Jørgensen, T.M.; Linneberg, C., Theoretical analysis and improved decision criteria for the n-tuple classifier. IEEE Transactions on Pattern Analysis and Machine Intelligence. (1999) 21, 336-347.
2. Linneberg, C.; Jørgensen, T.M., N-tuple or Ram based neural network classification system and method. DK patentansøgning PA 1998 00883; PCT patentansøgning WO DK/99/00340.
3. Jørgensen, T.M.; Linneberg, C., LUT netværk. DK patentansøgning PA 1998 00162.

3.6.2 Monte Carlo simulations of propagation of light in biological tissue

A. Tycho (Research Centre COM, Technical University of Denmark, Lyngby),
T. M. Jørgensen, L. Thrane and P. E. Andersen
E-mail: tycho@com.dtu.dk

Diffusely scattered light from tissue contains information about its underlying structures. By understanding how tissue parameters affect the scattered light it is possible to use optical methods for medical imaging. The optical techniques can then be used to monitor tissue parameters and to discriminate diseased tissue from healthy tissue.

An exact model of inhomogeneous and turbid tissue is not presently available. Generally, the tissue is instead represented as an absorbing bulk with scatterers randomly distributed over the volume. The so-called Monte Carlo simulation (MCS) technique may be used to simulate the light propagation. The MCS is based on the random walks that photons make as they travel through tissue. When the photons have been "injected", they are allowed to scatter or to be absorbed. The photons can then for instance be detected at the front or at a given depth of the medium in question. After propagating many photons, the net distribution of all the photon paths yields an accurate approximation to reality of the light propagation or distribution considered. Accordingly, MCS may be seen as an alternative to carrying out experiments which may otherwise be cumbersome to realise.

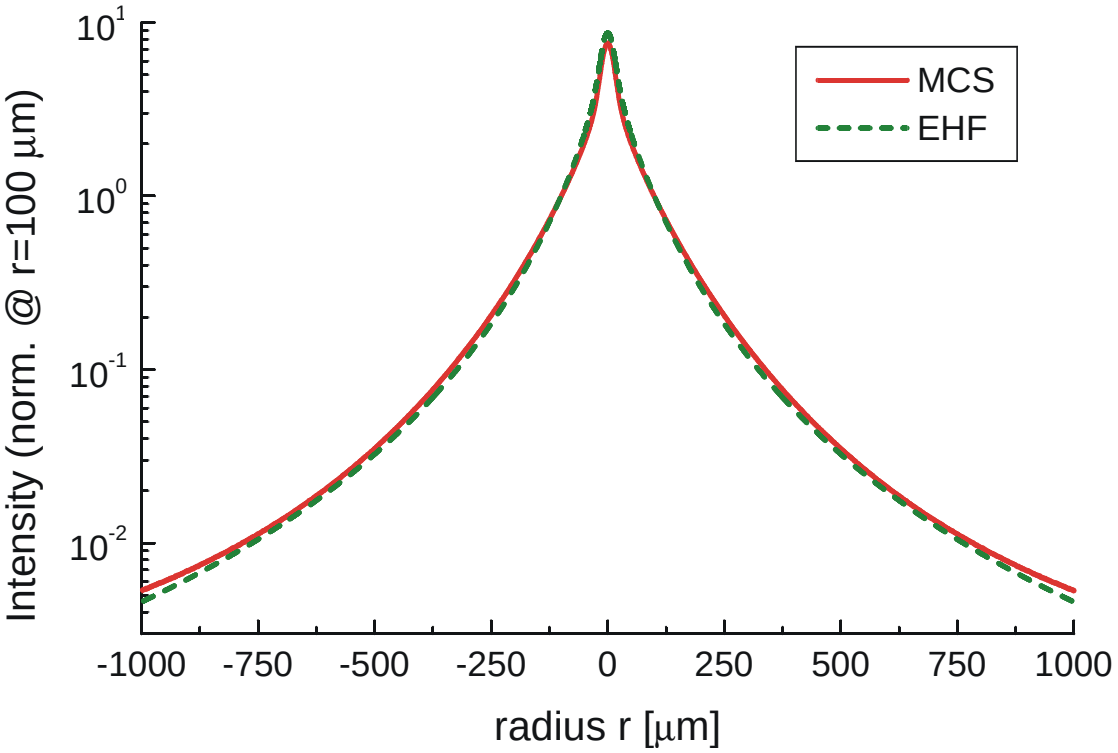

Figure 39. Comparison between the extended Huygens-Fresnel theory and the Monte Carlo simulation for propagation of light in tissue.

Within the BIOP centre one application of the Monte Carlo simulations is to test the applicability of using the extended Huygens-Fresnel (EHF) principle to a scattering medium characterised by the so-called Henyey-Greenstein scattering function.[1] This analytical model

has also been developed as a part of the BIOP centre. In Figure 39 the normalised intensity profiles obtained using an MCS and the EHF principle, respectively, are shown. These profiles are taken after propagating 0.7 mm into a tissue characterised by a scattering coefficient of 7 mm^{-1} and with the so-called asymmetry parameter equal to 0.9.

1. A. Tycho, T. M. Jørgensen and L. Thrane, “Investigating the focusing problem in OCT: Comparison of Monte Carlo simulations, the extended Huygens-Fresnel principle and experiments.” *To be published in* SPIE Proc. **3915** (2000).

4. Plasma and fluid dynamics

4.1 Introduction

J. P. Lynov
E-mail: jens-peter.lynov@risoe.dk

A unifying theme for the research performed in the Plasma and Fluid Dynamics programme is the dynamic behaviour of continuum systems. The continuum systems under investigation cover fluids, plasmas and optical media. Both linear and nonlinear problems are addressed in a combination of experimental, numerical and theoretical studies. Scientific computing in a broad sense plays a major part in these investigations and includes theoretical modelling of the physical phenomena, development of accurate and efficient numerical algorithms, visualisation and animation of the computed results and last, but not least, validation of the numerical results by detailed comparisons with carefully conducted experiments.

Due to the broad approach to the problems, the various projects are scientifically overlapping, not only inside the programme, but to a large extent also with projects in the rest of the department as well as in other departments at Risø. This overlap is considered a strength since it gives rise to considerable synergy between different parts of the laboratory.

The goals of the scientific studies are two-fold: on the one hand the investigations aim at achieving a deeper understanding of the fundamental behaviour of complex physical and technical systems; on the other hand the acquired knowledge is sought utilised in the definition and design of solutions to specific technological problems. In the following three subsections, descriptions of the scientific projects carried out during 1999 are collected under the headings: *fusion plasma physics*, *fluid dynamics* and *optics*.

4.2 Fusion plasma physics

4.2.1 Localised measurements of density fluctuations in the W7-AS stellarator

N.P. Basse, M. Saffman (Department of Physics, University of Wisconsin, USA), S. Zoletnik (CAT-Science, Budapest, Hungary), W. Svendsen (Niels Bohr Institute, Ørsted Laboratory, Copenhagen, Denmark), G. Kocsis (KFKI-RMKI, Budapest, Hungary), M. Endler (Max-Planck-Institut für Plasmaphysik, Teilinstitut Greifswald, Germany), B.O. Sass, J.C. Thorsen and H.E. Larsen
E-mail: nils.basse@risoe.dk

Since 1996 electron density fluctuations have been measured in W7-AS plasmas using collective CO_2 laser scattering.[1] The major challenge with this type of small-angle scattering diagnostic is how to achieve localised measurements. The poloidal wave number measured depends on the scattering angle θ_s of the two beams that define the measurement volumes according to $k_{pol} \upsilon k_{laser}\theta_s$. To maintain an acceptable S/N ratio (fluctuations decrease at least as k_{pol}^{-3}) we have to measure rather small k_{pol} – that is, θ_s is required to be quite small. A

consequence of this limitation is that the detected signals are line integrated along the vertical measurement volumes.

The CO_2 group at the TORE SUPRA tokamak[2] has demonstrated that volume localisation of broad beams can be obtained using the pitch angle variation of the magnetic field lines along a vertical measurement volume. In 1999 we verified this approach in W7-AS.

Using a novel two-point correlation technique we crosscorrelate two spatially separated narrow measurement volumes in order to obtain localised measurements.[3] Figure 40a) shows a top view of the two measurement volumes. Their relative positions are defined by the angle θ_R which is computer-controlled. We assume that the fluctuations are stretched along the field lines ($k_\varepsilon \pi k_{\rho\rho}$) and that the cross-field correlation length is of the order of 1 cm. The normalised crosscorrelation of the signals from the two volumes

$$P^n{}_{12}(\omega) = F_1^*(\omega)F_2(\omega) / \sqrt{\left[F_1(\omega)F_1^*(\omega)F_2(\omega)F_2^*(\omega)\right]}$$

displays the correlated fluctuations from the position along the vertical measurement volumes where the magnetic field pitch angle is parallel to θ_R. $F_i(\omega)$ is the Fourier transform of detector signal i. Figure 40b) shows the amplitude of $P^n{}_{12}(\omega)$ for three identical plasma discharges where θ_R has been changed in steps. The 0 Hz peaks stem from instrumental effects. It is observed that as θ_R is varied, the correlated maximum peak in frequency changes sign (i.e. direction with respect to the major radius *R*; see, e.g., Figure 35 in Risø-R-1100(EN)). This is interpreted as poloidally moving structures in the vicinity of the plasma edge. These low frequency peaks are travelling in the ion d.d. (**d**iamagnetic **d**rift) direction and are thought to be connected to the small positive radial electric field measured at or slightly beyond the LCFS (**l**ast **c**losed **f**lux **s**urface).[4] We have made complementary experiments using the TORE SUPRA method to verify our findings. These experiments support our conclusion that we do indeed observe low-frequency ion d.d. fluctuations; furthermore, high-frequency counterpropagating fluctuations inside the LCFS in the electron d.d. direction have been observed, which is consistent with the sign change of the radial electric field.

Another conclusion from Figure 40b) is that the core density fluctuations are several times smaller than the edge fluctuations.

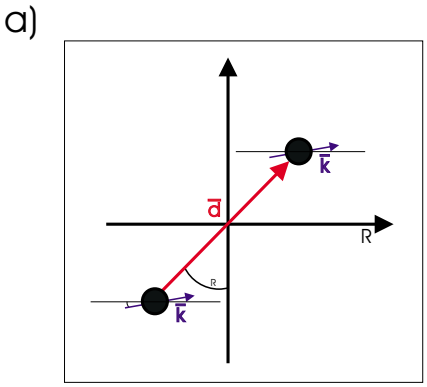

Figure 40 a): The narrow volume set-up at W7-AS. The measured k_{pol} have a small angle α with respect to the major radius *R*.

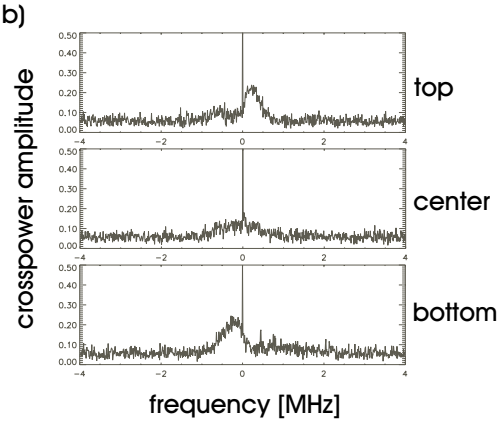

Figure 1 b): Amplitude of crosspower spectra for three angles, k_{pol} = 20 cm^{-1}. The text on the right-hand side indicates the vertical position of the observed signal.

In summary, we state that we can effectively select a vertical portion of the plasma where the detected signal originates by changing θ_R. This method will be further pursued in late 2000 when W7-AS is operating as a divertor machine.

1. S. Zoletnik et al., 26th EPS, Maastricht, **ECA 23J** 1493-96 (1999).
2. A. Truc et al., Rev. Sci. Instrum. **63** (7) 3716-24 (1992).
3. N.P. Basse, S. Zoletnik et al., 12th Int'l Stellarator Workshop, Madison (1999).
4. J.Baldzuhn et al., Plasma Phys. Control. Fusion **40** 967-86 (1998).

4.2.2 Reynolds stress and shear flow generation

S. B. Korsholm, V. Naulin, J. Juul Rasmussen, P. K. Michelsen and L. Garcia (Universidad Carlos III, Madrid, Spain)
E-mail: soeren.korsholm@risoe.dk

One of the major challenges in the research towards a fusion power plant is the understanding and control of the plasma turbulence leading to anomalous transport of particles and energy. In various turbulence models it has been observed that shear flows suppress turbulence and, thereby, the associated transport. Poloidal flows might, indeed, be responsible for the so-called H-modes (High confinement modes), which are projected to be the standard for fusion reactors. These flows are generated and affected by several effects and the full mechanisms are not yet fully understood. In this numerical work we investigate the relation between the so-called Reynolds stress[1] and the poloidal flow generation.

The model used in the numerical investigations is the three-dimensional drift wave Hasegawa-Wakatani model.[2] The simulations are performed in a slab geometry periodic in y and z (corresponding to the poloidal and the toroidal directions, respectively) while we use non-permeable walls in the radial direction, i.e. Dirichlet boundaries in x, ϕ (x=0)= ϕ(x=L_x)=0 and n(x=0)=n(x=L_x)=0, where ϕ is the electrostatic potential fluctuations, n is the density fluctuations and L_x is the domain length. The simulations are performed using pseudo-spectral methods in the periodic directions and finite difference methods in the bounded direction.

The Reynolds stress is a measure of the anisotropy of the turbulent velocity fluctuations that produce a stress on the mean flow. This may cause acceleration of the flow in the plasma, which could e.g. be a poloidal flow (y-direction).

To determine the Reynolds stress defined as:

$$\mathrm{Re}_\phi = -\langle v_x v_y \rangle = \left\langle \frac{\partial \phi}{\partial y} \frac{\partial \phi}{\partial x} \right\rangle,$$

one needs the value of the fluctuations in the potential. Since accurate measurements of the potential perturbations are quite difficult, especially in large plasma devices, a pseudo-Reynolds stress based on much easier obtainable density measurements has been proposed. The pseudo-Reynolds stress is defined as:

$$\mathrm{Re}_n = \left\langle \frac{\partial n}{\partial y} \frac{\partial n}{\partial x} \right\rangle.$$

We find that the Reynolds stress Re_ϕ and the pseudo-Reynolds stress Re_n are strongly correlated with a correlation of 0.8. The reason for the strong correlation between Re_n and Re_ϕ is that the density and the potential fluctuations are strongly correlated for drift waves.

The conclusion of this is that the pseudo-Reynolds stress gives a good estimate of the real Reynolds stress and it may thus be possible to predict flow generation by measuring density fluctuations. In Figure 41 we compare the poloidal flow with the flow predicted by the pseudo-Reynolds stress. The observed behaviour may, however, be specific to this particular turbulence model and more models have to be investigated.

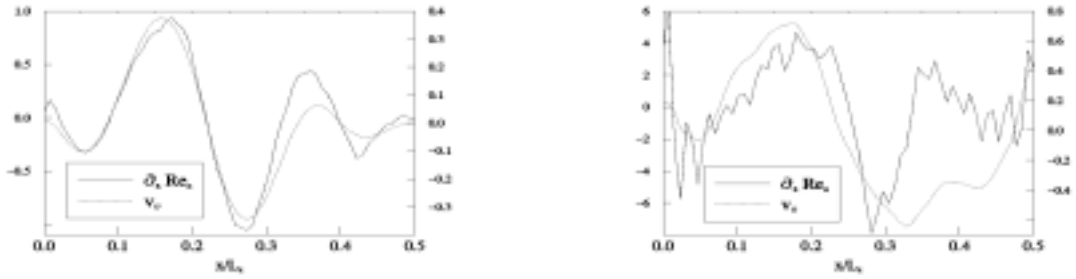

(a) (b)

Figure 41. The poloidal flow compared with the flow predicted by the drift wave pseudo-Reynolds stress at two instants in time a) t=75 and b) t=100.

1. D. J. Triton, *Physical Fluid Dynamics*, Clarendon Press, Oxford, 2nd ed., 1988, Chapter 19.
2. A. Hasegawa and M. Wakatani, Phys. Rev. Lett. **50** (1983) 682-686.

4.2.3 Three-dimensional flux driven drift wave simulations

S. B. Korsholm, V. Naulin, J. Juul Rasmussen and P. K. Michelsen
E-mail: soeren.korsholm@risoe.dk

The understanding of turbulence and transport of plasma is crucial in the development of fusion energy. Several turbulence models have been developed and implemented at Risø with the aim of obtaining a better understanding of edge region plasma turbulence.

In the models it has most often been assumed that the plasma density gradient is constant, i.e. it is not perturbed by the turbulence. Another assumption that might be more realistic is to assume that the flux of density from the core of the plasma into the edge region is constant. Such flux driven systems are being implemented and preliminary results indicate that the turbulence is saturated due to a flattening of the gradients. Furthermore, the saturation level of the turbulence is significantly lower than for the gradient driven case.

4.2.4 Identification and tracking of vortices in turbulent flows

T. Jessen and P.K. Michelsen
E-mail: thomas.jessen@risoe.dk

Coherent vortices are a prominent feature of two-dimensional turbulence and have been observed in, e.g., atmospheric flows and fusion plasmas. We have developed a new method for detecting and tracking vortices in turbulence simulations in order to quantify vortex properties and assess their importance. Two related algorithms have been developed: (1) identification of vortices from a frozen snapsnot (a “still”) of the flow field, and (2) tracking of individual vortices from a sequence of stills.

In free 2D turbulence the vorticity field, i.e. the curl of the velocity field, tends to be concentrated in small regions of extreme values that form the vortex centres around which the fluid rotates. Often vorticity can be considered concentrated in points rather than being smeared out continuously, which results in a point vortex model. This model, however,

becomes inappropriate when vortices of the same circulation approach each another. In this case the typical outcome is a vortex merger, an example of which is shown in Figure 42.

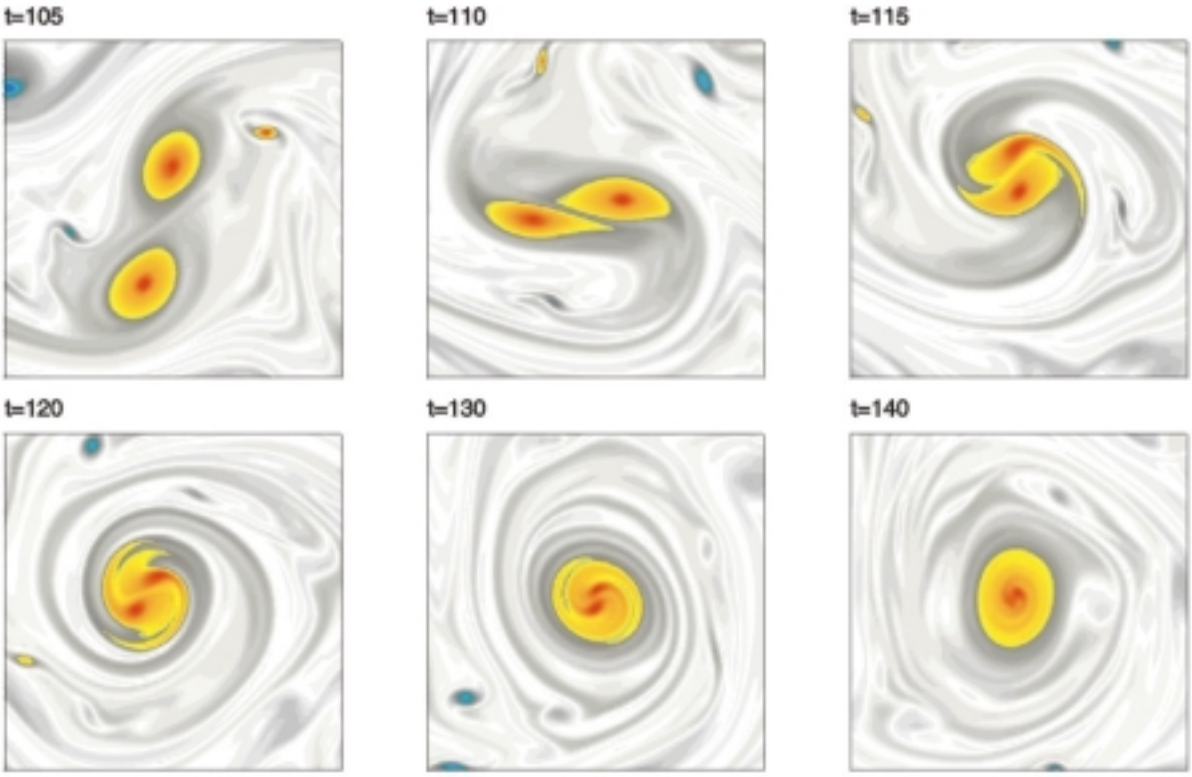

Figure 42. A vortex merger in a plasma turbulence simulation. A colour-coded vorticity (charge density) map is shown. Two positively charged vortices, of counterclockwise rotation, merge to form a single supervortex.

Vortex mergers tend to organise the flow into fewer, but larger, vortices and hence to transfer energy towards the large scales of motion. On the other hand, they also strain and filmentate fluid elements, thereby transferring enstrophy (vorticity squared) towards the smaller scales. Thus, they are intimately connected with the dual cascade of energy and enstrophy, which is characteristic of 2D turbulence.

Hitherto, quantitative analysis of coherent vortices has been restricted by the need for a human observer. Vortex behaviour has qualitatively been described on the basis of naked eye inspection of flow field plots. This is a time consuming and subjective procedure, and quantitative results are likely to be based on poor and biased statistics. In contrast, an automated procedure allows analysis of large data and yields representative statistics based on objective criteria.

A vortex identification algorithm has been developed. It is primarily based on the Weiss criterion, and essentially designates regions where rotation rate exceeds rate of strain as vortex candidates. An example is shown in Figure 43. The left-hand figure shows the instantaneous stream lines of a turbulent plasma flow. The right-hand figure shows the associated Weiss field, colour coded with vortex candidates coloured blue. Vortex candidates are marked with crosses and are seen to coincide with regions of closed streamlines.

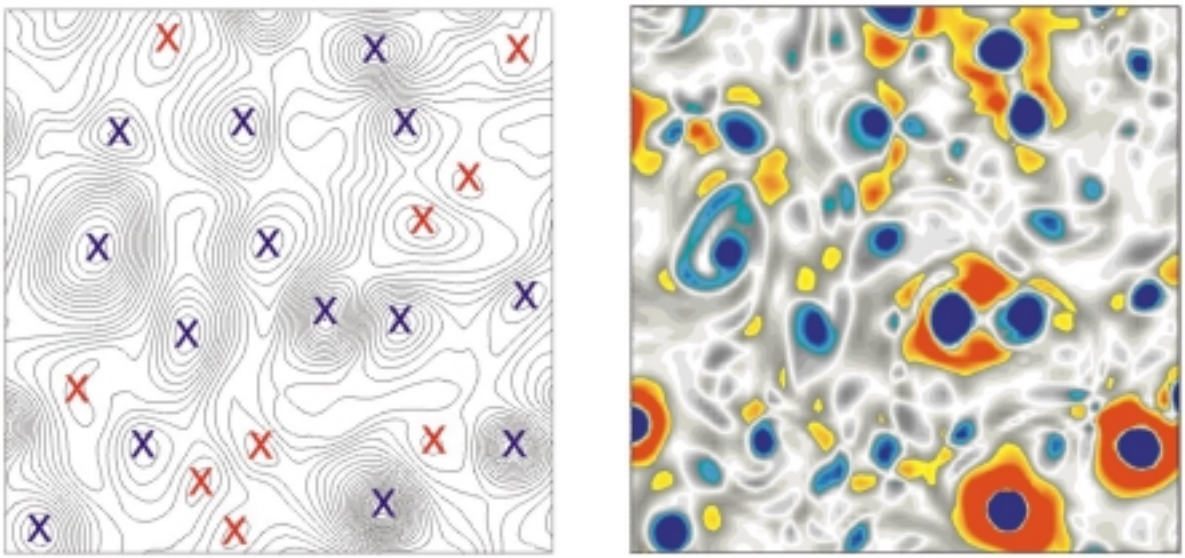

Figure 43. Left: Streamlines of a turbulent plasma flow. Vortical structures are indicated by crosses. Coherent structures are marked by blue crosses. Right: The associated Weiss field. Rotation dominated regions are blue, strain dominated regions are red.

A newly developed vortex tracking algorithm is capable of recording the fate of individual vortices and, hence, of calculating vortex lifetimes and diffusivities. This allows us to distinguish between incoherent temporary vortices, due to random fluctuations of the turbulent field, and persistent coherent vortices. In Figure 43 incoherent vortices have been marked with red crosses. Vortices existing for more than one full rotation period are said to be coherent and have been marked with blue crosses.

The automated vortex identification and tracking algorithms are now as a routine used to sample vortex statistics in turbulence simulations. Distributions of vortex size, mass, charge, lifetime, etc. are calculated and offer new insight into vortex dynamics.

4.2.5 Transport barriers in pressure driven flute mode turbulence

V. Naulin, J. Nycander (FOA, Stockholm, Sweden) and J. Juul Rasmussen
E-mail: volker.naulin@risoe.dk

We investigate the evolution of turbulence and the associated formation of transport barriers in a model system for 2D electrostatic pressure driven flute modes. The fluctuations are flux driven and are generated via a Rayleigh-Taylor instability setting in where the pressure gradient exceeds the magnetic field strength gradient. This pressure gradient is forced by a constant temperature difference between the two sidewalls of the computational domain. The temperature difference sustains a thermal flux.

Turbulent equipartition predicts the background profiles and gradients resulting from the homogenisation of the Lagrangian invariants due to the strong mixing by the turbulence. This is clearly revealed for large aspect ratios, $L_y/L_x > 2.2$, where x is in the direction of the gradients (“radial direction”) and y is perpendicular to the gradients (“poloidal direction”) (the confining magnetic field is in the z-direction). These profiles, which correspond to the marginal profiles, are flatter than the profiles that will result from classical viscous diffusion in the absence of the turbulence. For small aspect ratios, however, the numerical simulations show a strong tendency for the evolution of a poloidal shear flow that quenches the effective turbulent mixing and the transport changes from being anomalous, i.e. fluctuation driven, to

being diffusive. Thus, a much steeper gradient evolves on a diffusive timescale. Subsequently, the resulting steep gradient is prone to the Rayleigh-Taylor instability again, and short burst-like destabilisations which flatten out the profiles occur locally. The transport associated with these burst-like events propagates down the background gradient and has properties of avalanche-like event. In Figure 44 we show the evolution of the heat flux for different aspect ratios.

The mechanisms for the shear flow generation and the influence of the shear flow on the turbulence are presently under investigation.

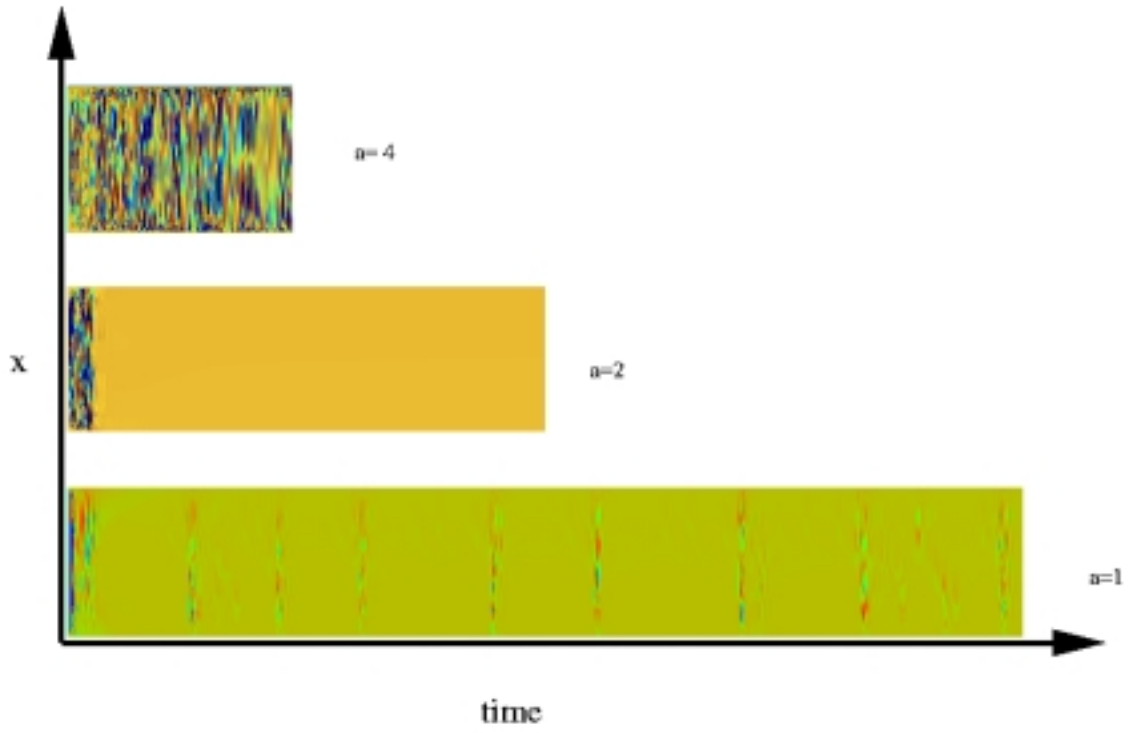

Figure 44. Time evolution of the poloidally averaged radial heat flux for three values of the aspect ratio: a = Ly/Lx. The system is heated from the left. For a = 1 the bursts occur at random intervals, with a characteristic time interval determined by the diffusive timescale.

4.2.6 Dispersion of ideal particles in developed 2D and 3D turbulence

V. Naulin, A.H. Nielsen and J. Juul Rasmussen
E-mail: volker.naulin@risoe.dk

The dispersion properties of particles in inhomogeneous turbulence are still not well understood. Covering a variety of important areas from the diffusion of pollutants to the behaviour of heavy ions in fusion devices this area connects basic research with applications. In the past, idealised maps of the turbulence were used to elaborate on the diffusion of particles as turbulence simulations were not available for the long time series needed. Making use of Risø's 2D and 3D plasma turbulence codes, we are able to track a larger number of particles for rather long time compared with the fundamental frequencies of the considered system. Of special importance is the influence of coherent structures on the particle dispersion. Due to the appearance of travelling waves in the turbulence, the interaction between structures and waves is important as it changes the probability distribution of the

velocity fluctuations. Then the variance of these fluctuations might not be well defined and sub- or super-diffusive (Levy Flights) behaviour is observed. The diffusion is anisotropic with respect to the background density gradient or the propagation direction of the travelling waves.[1]

1. Naulin, V., Nielsen, A.H. and Rasmussen, J.J. Phys. Plasmas, **4,** pp. 4575-4585, 1999.

4.2.7 Comparison of simulations with simple plasma experiments

V. Naulin, D. Block, F. Greiner*, U. Grulke*, S. Niedner*, A. Piel* and U. Stroth**
*(*Christian-Albrechts-Universität, Kiel, Germany)*
E-mail: volker.naulin@risoe.dk

Small-sized plasma experiments with a simple geometry are an ideal playground to test various hypotheses concerning, e.g., statistics of plasma turbulence, plasma transport and the appearance of coherent structures in these nearly 2D systems. Well-developed diagnostics and good control of the experiments make it possible to verify numerical codes with these experiments. Their relatively low plasma temperatures put the relevant spatial sizes in a range where today's numerical resolution is sufficient to simulate the whole plasma cross section. At Kiel University probe measurements of the linear experiment KIWI and the simple magnetised torus TEDDI will be compared with results from Risø's 2D and 3D codes. If successful, information about coherent structures, turbulent transport and statistical properties of the plasma turbulence will be obtained. Unique and essential properties of theory and modelling will be matched with experimental results. Advanced methods for time series analysis will be used as well as visualisation of the turbulent fields. As a second step we plan to perform a comparison of the numerical results with measurements from the geometrical much more complex TJ-K. A goal will be to isolate the most important and persistent ingredients to the turbulence as the turbulence often shares similar behaviour between experiments of different sizes and geometries.

4.2.8 Stellarator geometry for a 3D code of drift Alfven turbulence

V. Naulin, S.B. Korsholm, P.K. Michelsen and J.J. Rasmussen
E-mail: volker.naulin@risoe.dk

Plasmas relevant to thermonuclear fusion are characterised by a complicated structure of the confining magnetic field. While the poloidal component of the magnetic field in a tokamak is created via a toroidal current in the plasma, a so-called stellarator creates the magnetic field structure through complicated outer coils alone. This goes along with a loss in rotational symmetry. Magnetic field aligned coordinates thus vary in all three spatial dimensions. A numerical code reflecting this geometry therefore needs 3D information on the MHD equilibrium for which the stellarator has been optimised.

In collaboration with the IPP in Greifswald and CIEMAT in Madrid relevant stellarator geometries will be prepared for numerical drift Alfven simulations. In fusion plasmas the local change of the magnetic field due to the density fluctuations should be considered even for a small plasma beta. The existing TYR-code (See Risø-R-1100(EN) 1999, sec. 4.2.6) was therefore extended from an electrostatic three-field model to a five-field electromagnetic model where the parallel Alfven dynamics are considered.

4.3 Fluid dynamics

4.3.1 Three-dimensional aspects of a forced anticyclone in a rotating paraboloid

B. Stenum and J. Juul Rasmussen
E-mail: bjarne.stenum@risoe.dk

It is well known that a flow pumped into a rotating fluid produces an anticyclone and that the azimuthal velocity of the anticyclone is proportional to F/r, where F is the flow rate and r is the distance from the inlet. The three-dimensionality of such an anticyclone has been studied in the paraboloid rotating at the velocity at which the free surface of the water in the tank matches the shape of the paraboloid. The inlet of the circulated flow takes place in the middle of the tank and the water is drained away at the outer periphery of the tank. A vertical cross section of the flow inside the anticyclone is visualised by adding some fluorescent dye to the inlet, illuminating with a vertical light sheet and using a close-up video camera view (Figure 45). As can be seen in the figure, inside a well-defined distance R the fluorescent dye is distributed in a three-dimensional flow structure. Outside R the flow takes place in the thin Ekman layer at the bottom (the water above the Ekman layer has not been dyed and cannot be seen). The explanation for this remarkable flow structure is that close to R the azimuthal velocity of the anticyclone becomes so large that the fluid is not rotating in the laboratory system and, hence, the two-dimensionality of the flow breaks down inside R. Outside R the flow is rotating in the laboratory system and the two-dimensionality of the flow is maintained as predicted by the Taylor-Proudman theorem. In this way such a simple experiment is a clear demonstration of the two-dimensionality of rotating fluids.

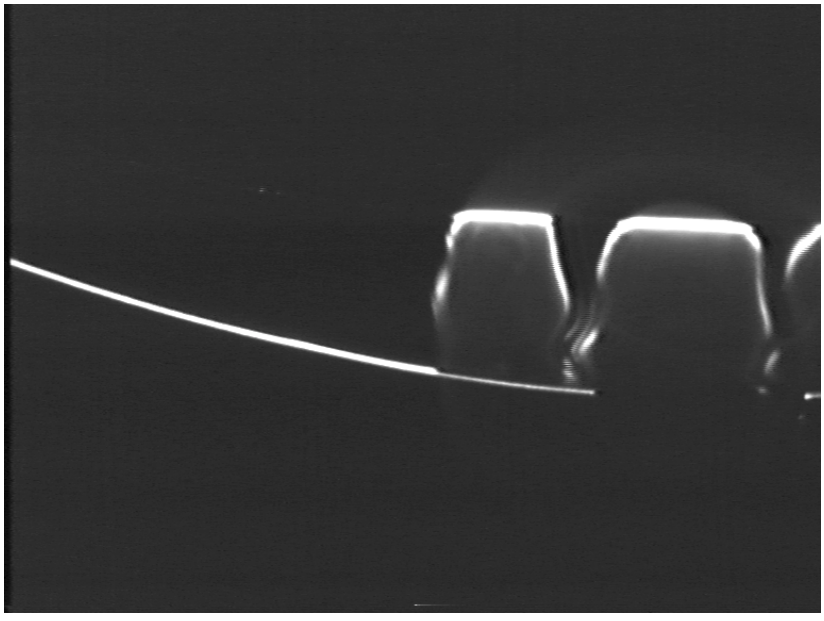

Figure 45. Vertical cross section of the flow inside a forced anticyclone visualised with fluorescent dye.

4.3.2 Homogenisation of potential vorticity and formation of large-scale flows

J. van de Konijnenberg, V. Naulin, J. Juul Rasmussen and B. Stenum
E-mail: jens.juul.rasmussen@risoe.dk

We have performed a laboratory experiment in a rotating fluid with sloping bottom to investigate the formation of large-scale flows by mixing and homogenisation of the potential vorticity. Specifically we consider a rotating tank with radially symmetric bottom topography and a rigid lid. The bottom has a constant slope in the radial direction; the slope may be either negative (the shallowest part is at the centre) or positive (the deepest part is at the centre). As is well known, this topography is equivalent to the varying Coriolis parameter for flows on a rotating planet, and the shallower part corresponds to the pole on the planet. For this system the so-called potential vorticity $PV = \omega + \beta r$ is a Lagrangian conserved quantity. Here ω is the relative vorticity and β is proportional to the slope of the bottom. Thus, it is readily seen that for $\beta < 0$ an effective mixing that homogenises PV will lead to replacing the high PV near the centre with low PV from the outside, and this will appear as an anticyclonic vortex over the centre, "the pole", where ω will to be lower than near the wall. For $\beta > 0$, on the other hand, a cyclonic vortex will appear. This is in qualitative agreement with our experimental observations, where the mixing is brought about by locally injecting and rejecting fluid periodically near the outer boundary of the tank at two azimuthal positions opposite to each other.

We have modelled the set-up numerically by solving the quasi-geostrophic vorticity equation in the β-plane approximation on a disk. Using the parameters of the experiment we find satisfactory agreement. Recalling the analogy between Rossby wave dynamics on the β-plane and drift-wave dynamics in a magnetised plasma with a density gradient perpendicular to the magnetic field, a similar mechanism may apply for the formation of azimuthal flows in a cylindrical plasma. The density is here maximum in the centre and the analogous "fluid"-model will have $\beta > 0$; thus, we expect the formation of a cyclonic rotation around the plasma column, resulting from the homogenisation of the PV, which is clearly revealed by the numerical investigations of drift-wave turbulence in a cylindrical plasma. The homogenisation of generalised PV is therefore an effective mechanism of forming sheared azimuthal plasma flows. These flows appear to be of outmost importance to the plasma confinement.

4.3.3 Interaction of a vortex ring with the free surface of ideal fluid

V.P. Ruban (Landau Institute for Theoretical Physics, 2 Kosygin str., 117334 Moscow, Russia)
E-mail: jens.juul.rasmussen@risoe.dk

The interaction of a small vortex ring with the free surface of a perfect fluid is considered in the framework of the Hamiltonian description of ideal incompressible fluids. In the point ring approximation the asymptotic expression for the Fourier components of radiated surface waves is obtained in the case where the vortex ring comes from infinity and has both horizontal and vertical components of the velocity. The non-conservative corrections, due to Cherenkov radiation of surface waves, to the equations of motion of the ring are derived, and the implied effects on the motion of the vortex ring are considered.

4.3.4 Periodically driven flows

F. Okkels, B. Stenum and J. Juul Rasmussen
E-mail: fridolin.okkels@risoe.dk

In the rotating parabolic tank we study a periodically forced circular shear flow produced by a periodic motion of the inner part of the tank relative to the outer part. Due to the periodic forcing, vortices are created and destroyed at a higher rate than in the traditional set-up where constant angular velocity difference is used. Since the velocity difference has zero mean, the state of the forcing is only given by the frequency and the amplitude of the velocity difference.

By gradually increasing the frequency and the amplitude the state of the flow changes from a stationary radially symmetric flow to a time-periodic regular flow which then becomes unstable.

During the regular state the forcing produces a strong unstable shear layer during each half period. This layer breaks up into a series of small eddies which interact mutually before they are destroyed by the next half period of vortices that have opposite sign.

The entire flow field is measured either by particle tracking or by measuring the variations in the water height by the change in light absorption and then assuming the flow to be geostrophic.

The transitions between the different regions have been measured thoroughly giving a detailed picture of the parameter space with the different kinds of behaviour of the system.

One quantitative characterisation of the states in the non-stationary regions is the number of vortices in the flow which change as a function of frequency and amplitude. By associating this number to the largest wave number possible in the flow, the number of vortices can theoretically be estimated to be in very good agreement with the observed number of vortices.

4.3.5 Turbulent shell models

F. Okkels and M. H. Jensen (CATS, Niels Bohr Institute, University of Copenhagen)
E-mail: fridolin.okkels@risoe.dk

The biggest problem in direct numerical simulation of 3D turbulence is the rapid growth in free variables and calculations as the turbulence intensity is increased. This problem can be overcome by creating reduced models of turbulence, and some of the most successful reduced models are the shell models that have been given their name because they are defined in wave number space which is divided into spherical shells. The present work is based on the GOY shell model named after its creators Gletzner, Ohitani and Yamada.

The state of each shell is given by a complex amplitude, and the dynamics of the model comes from a set of ordinary differential equations each consisting of a forcing term that injects energy into the model, a coupling term to the neighbouring shells that redistributes the energy among the shells, and a viscous term that dissipates the energy away. Even though this model only simulates the flow of energy in turbulence and has no spatial resolution, the equations of the GOY model have the same conserved quantities, invariants and shape as the wave number representation of the Navier Stokes equations which are the main equations governing fluid motion.

Despite the simplicity of the model its statistical properties match those of experimentally measured turbulence surprisingly well.

We try to explain this success by analysing the temporal structures seen in the time-evolution of the model.

4.3.6 Experimental studies of particle-wall interactions in flow channels

B. Stenum and S. Lomholt
E-mail: bjarne.stenum@risoe.dk

The dynamics of rising particles has been studied experimentally in vertical and inclined flow channels in order to validate the results of the numerical studies (see section 4.3.7). The experiments are carried out in a rectangular flow channel with a cross section of 100 mm × 10 mm and a flow channel with a square cross section of 10 mm × 10 mm, both with a length of 150 mm. The 2 mm polymer particles are released from below into a resting mixture of water and glycerol. The positions of the particles are determined with subpixel accuracy by digital image processing.

In the vertical rectangular channel a particle at the axis of symmetry is rising at a constant velocity, but due to the wall effects the rising velocity is reduced relative to that in an infinite geometry. In the inclined (9.3 degrees) rectangular channel both the velocity component along the flow channel and that across the flow channel are found to be reduced when the particle is approaching the wall (Figure 46). In the rectangular flow channel the observed wall effects are in agreement with the analytical results for a channel defined by two parallel infinite walls.[1] The effects close to the walls are not captured with the numerical code without including the dipole term (see section 4.3.7).

In the squarely shaped channel the velocities of the rising particle are additionally reduced due to the effects of the two additional walls close to the particle. In the inclined channel the velocity profiles across the channel of the two velocity components are found to be more flat around the axis of symmetry which shows that an exact reproduction of the geometry is important for numerical modelling. For this geometry no analytical solutions exist.

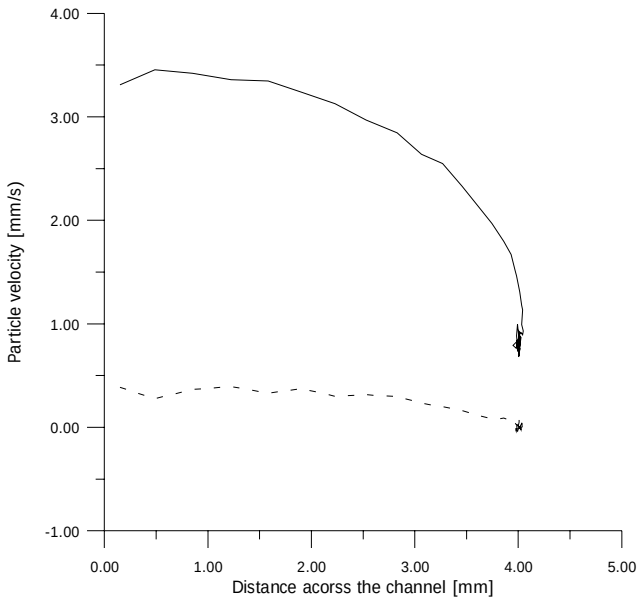

Figure 46. Velocity profiles in the inclined rectangular flow channel. Solid line: velocity component along the channel. Dashed line: velocity component across the channel

1. J. Happel and H. Brenner: Low Reynolds Number Hydrodynamics, Prentice-Hall, London 1965.

4.3.7 Force coupling method for computing particle dynamics in microflows

S. Lomholt, B. Stenum and M. Maxey (Department of Applied Mathematics, Brown University, Providence, USA)
E-mail: sune.lomholt@risoe.dk

The motion of rigid particles in a fluid flow is determined by solving the Navier-Stokes equations

$$\frac{\partial u_i}{\partial x_i} = 0 \tag{1}$$

$$\frac{Du_i}{Dt} = -\frac{\nabla p}{\rho} + \nu\nabla^2 u_i \tag{2}$$

subject to the no-slip boundary condition at the particle surfaces

$$u_i = v_i + \varepsilon_{ijk}\Omega_j\left(x_k - Y_k\right) \ , \tag{3}$$

where v_i, Ω_i and Y_i are the velocity, the angular velocity and the position of the particle. Furthermore, the boundary conditions for the bounding geometry must be satisfied. The straightforward method is a direct simulation with the flow around the particles fully resolved. This requires a new mesh for each time step, and for a particle close to a wall or another particle a very fine mesh is needed in order to resolve the flow. Therefore direct simulations are extremely computationally expensive and the number of particles will be limited.

An alternative method is force coupling, where the no-slip boundary condition on the particles is approximated by specifying a force in the flow at the position of the particle. The momentum equation (2) becomes

$$\frac{Du_i}{Dt} = -\frac{\nabla p}{\rho} + \nu\nabla^2 u_i + \sum_{n=1}^{N} F_i^n \Delta\left(\mathbf{x} - \mathbf{Y}^n\right), \tag{4}$$

where $\mathbf{F}^n$ is the force exerted by particle n on the fluid due to the no-slip boundary condition, and $\Delta\left(\mathbf{x} - \mathbf{Y}^n\right) = \left(2\pi\sigma^2\right)^{-3/2} \exp\left(-\left(\mathbf{x} - \mathbf{Y}^n\right)^2 \Big/ 2\ \sigma^2\right)$ is a Gaussian localising the effect of the force. This first-order approximation only includes the force from the particle on the fluid due to translation. Higher order approximations can be obtained by adding the forces due to rotation, interaction, etc. The length scale σ is a parameter related to the particle radius and thus reflects the finite size of the particle.

While equation (4) yields reasonably good results for particles moving parallel to bounding walls, comparisons with experiments for particles moving toward walls show that equation (4) does not capture the effect of the wall. This is due to deformation of the fictitious particle. The rate of strain in the fluid occupying the domain of the particle is not zero and the rigid particle consequently deforms. This is obviously not physical for a rigid particle. Therefore the model in equation (4) must be extended to include a dipole term, i.e.

$$\frac{Du_i}{Dt} = -\frac{\nabla p}{\rho} + \nu\nabla^2 u_i + \sum_{n=1}^{N} F_i^n \Delta\left(\mathbf{x}-\mathbf{Y}^n\right) + F_{ij}^n \frac{\partial \Theta(\mathbf{x}-\mathbf{Y}^n)}{\partial x_j}, \qquad (5)$$

where $\Theta\left(\mathbf{x}-\mathbf{Y}^n\right) = \left(2\pi\sigma_\Theta^2\right)^{-3/2} \exp\left(-\left(\mathbf{x}-\mathbf{Y}^n\right)^2 / 2\sigma_\Theta^2\right)$ and σ_Θ is a length scale different from σ. The dipole term ensures that the rate of strain in the fluid that occupies the domain of the rigid spheres is zero in an average sense. The dipole term may be interpreted as a resistance to deformation, which then acts on the fluid as a force.

Figure 47 shows the particle trajectory for a sphere of radius a moving perpendicular to a plane wall. The analytic solution is from Brenner,[1] while the two other trajectories have been computed with equations (4) and (5). Clearly, introducing the dipole term in the model yields a better approximation of the wall effect although it is not perfect. One reason for the discrepancy between the analytic and the dipole model is that the average strain rate for the spheres is not low enough, i.e. the spheres do still deform. Hence the approximation may be improved by ensuring that the average strain rate becomes sufficiently small.

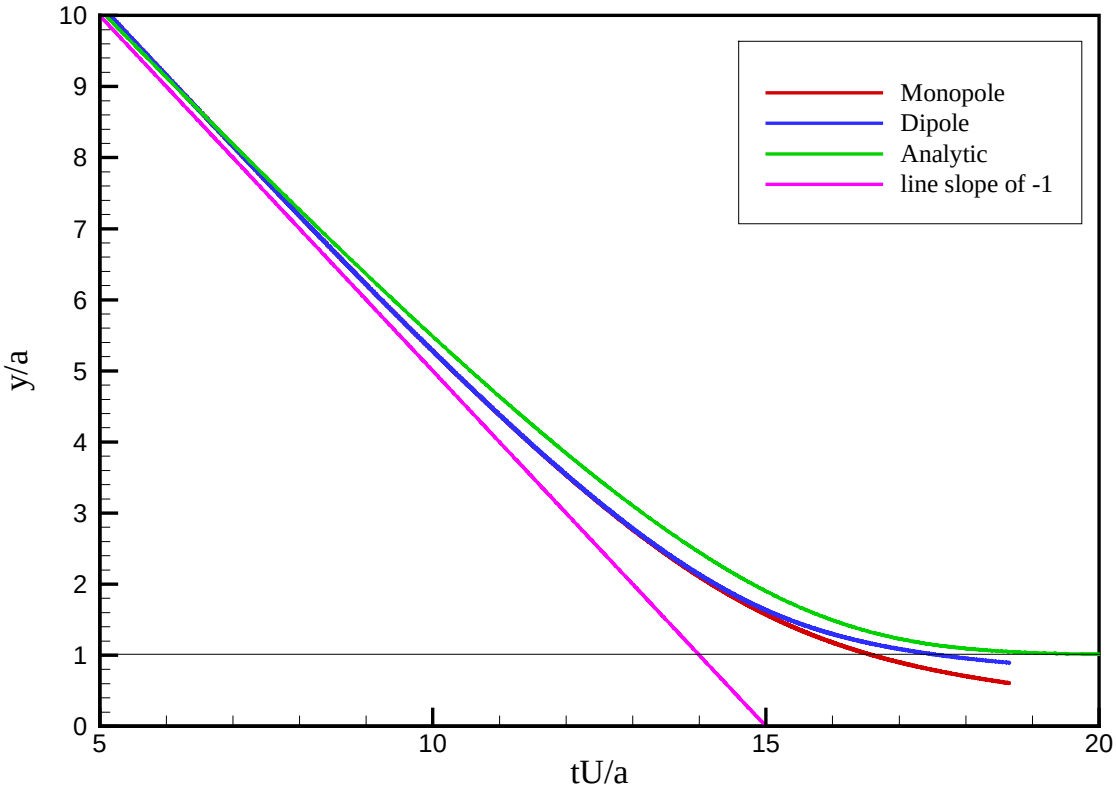

Figure 47. Particle trajectory for a sphere moving perpendicular to a wall. y/a is the reduced distance from the wall divided by the particle radius and tU/a is the reduced time.

1. H. Brenner, The slow motion of a sphere through a viscous fluid towards a plane surface, Chem. Eng. Sci., Vol. 16, pp. 242-251, 1961.

4.3.8 Two-dimensional turbulence in bounded flows

A. H. Nielsen, J. J. Rasmussen, D. J. Torres (Physics Dept. and Geophysical Research Center, New Mexico Tech, USA), H. J. H. Clercx (University of Technology, Eindhoven, The Netherlands) and E. A. Coutsias (University of New Mexico, Albuerqueque, USA)
E-mail: anders.h.nielsen@risoe.dk

Two-dimensional turbulence in unbounded or double periodic domains in neutral fluids as well as in plasmas has been investigated intensively during the last decades by means of numerical simulations. These flows exhibit an inverse cascade of energy, and coherent structures comparable with the size of the domain will eventually emerge. Thus, the presence of boundaries and the conditions imposed on them will play a significant role in the evolution of the turbulence and the coherent structures.

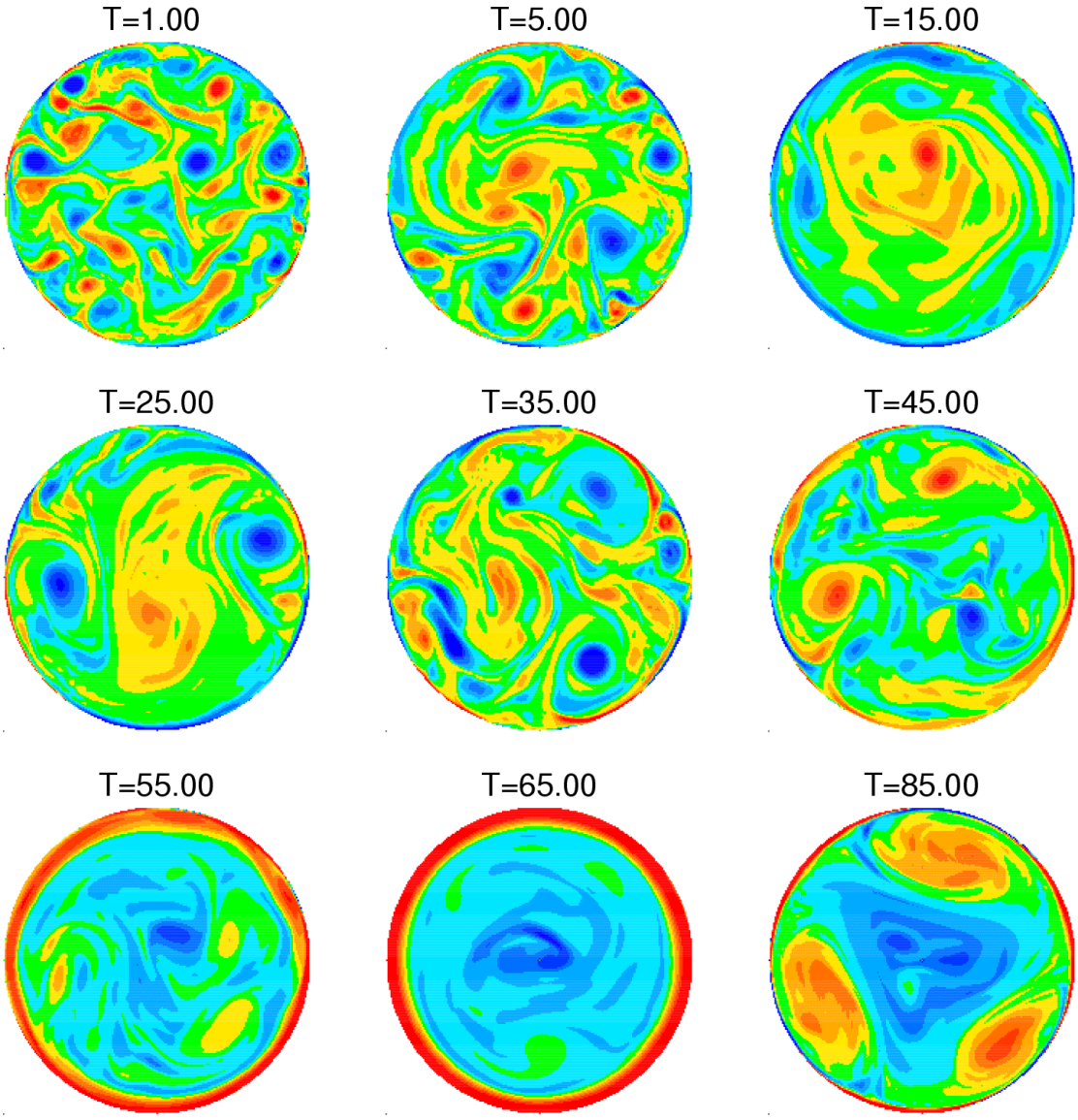

Figure 48. The vorticity field of a flow field using no-slip boundary condition. Red colours correspond to positive values, whereas blue colours correspond to negative values. Spectral evolution M = 1024 (radially), N = 512 (azimuthally). The Reynolds number increases from Re=2150 for T=1.0 to Re=8730 for T=85.0.

In this project we numerically investigate forced (and decaying) turbulence on circularly or squarely bounded domains and compare with results obtained from double periodic geometries. The model equations are the Navier-Stokes equations that are solved using a pseudospectral method. Using low-level noise as initial condition we force the flow by injecting energy and enstrophy at a specific length scale. An example of such an evolution is shown in Figure 48. For small times, T<5.0, the evolution is quite similar to the unbounded case where the flow, thus vortex merging, organises into larger and larger structures. As structures comparable with the size of the domain are formed, they will interact strongly with the boundary. This will stop the inverse cascade as small-scale structures are injected into the interior of the domain, see e.g. T=35. For large time the flow enters a semistationary state, T=50-80, with a single structure in the middle surrounded by a high boundary layer. This state eventually breaks down into a quadruple structure where the three satellites are made up by wall-generated vorticity.

4.4 Optics

4.4.1 Rigorous 2- and 3D analysis of diffractive optical elements

P. G. Dinesen, J. S. Hesthaven (Brown University, Rhode Island, USA) and J. P. Lynov
E-mail: palle.dinesen@risoe.dk

The time-domain spectral collocation method in 2D for the analysis of grating couplers has already been proved to be competitive in terms of accuracy, geometrical flexibility and computer resource requirements in comparison with other numerical methods. The major drawback of the spectral collocation scheme is the relatively long time it takes to reach the steady state solution for wave propagation in a grating coupler. We have therefore successfully implemented Prony's method which can speed up the computation of the steady-state solution significantly. In Prony's method a time series of values is fitted to a number of periodic and exponentially decaying functions, and from the non-decaying functions the steady state solution can then be extrapolated. The method has proved to be very efficient for our analysis of focusing grating couplers and typically reduces the computation time by a factor of 3 to 4.

Using the spectral collocation scheme in 2D, a high number of simulations of focusing grating couplers have been performed. The outcome of these simulations has led to the surprising conclusion that the depth of the surface relief grating used in these couplers not only influences the amount of energy coupled into free space, but also has a very strong influence on the focal distance as well as on the intensity profile of the outcoupled light. This is in contrast to a geometrical optical analysis by which the amplitude of the surface relief has no influence on these quantities. These surprising results have been confirmed in a comparative study performed in colloboration with the Technical University of Denmark. In this study the spectral collocation was compared with the Finite-Difference Time-Domain method, and good agreement was achieved.

A 3D general version of the spectral collocation method used for the analysis of diffractive optical elements has also been developed. Focusing grating couplers as shown in Figure 49 have been analysed. These computations require extensive use of parallel supercomputers, and typically 32 processors are needed for 24 hours to compute steady state solutions.

Figure 49 also shows a first example of a focused out-coupling from a grating coupler. The surface relief is essentially the 2D relief that is then rotated so that the grating maximas form

concentric circles as indicated in the figure. The near-field plot shows that focusing does indeed occur at a distance of 40 wavelengths above the surface relief. The expected focal distance is 100 wavelengths and we attribute this deviation to the way the origin of the rotation of the surface relief is chosen. Further analysis is in progress.

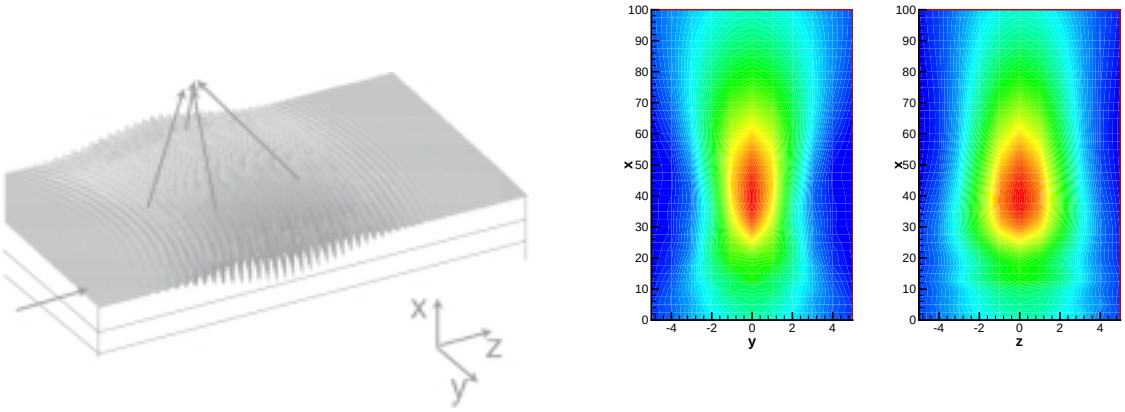

Figure 49. 3D surface relief grating and near-field integration contours. Focusing occurs at a distance of 40 wavelenghts from the surface relief.

4.4.2 Grating coupler analysis using a boundary variation method

P. G. Dinesen and J. S. Hesthaven (Brown University, Rhode Island, USA)
E-mail: palle.dinesen@risoe.dk

This project is aimed at introducing a fast, approximate method for the analysis of focusing grating couplers. While the spectral collocation method that we have used hitherto is extremely accurate, it is also time- and memory consuming and typically requires several hours on four or eight parallel processors to compute a steady state solution to a problem of realistic size. Such a computation time prohibits the use of this method when the task is to optimise a grating coupler geometry to meet given design specifications, typically requiring several tenths or even hundreds of computations of the wave propagation problem.

The boundary variation method was introduced seven years ago for the analysis of diffraction on a periodically modulated boundary between two dielectric layers. The basis for the method is that the solution to a problem of diffraction on a corrugated boundary can be found by analytic continuation of the known solution to the problem of refraction on the uncorrugated (even) boundary. Based on this result, a method has been developed where the diffracted field, E_{diff}, is expanded in a Rayleigh series

$$E_{diff} = \sum_{r=-\infty}^{\infty} B_r(\delta)\exp(i\alpha_r x + i\beta_r z),$$

where the Rayleigh coefficients are then found in a power series expansion of the perturbation, δ, from the uncorrogated boundary. The coefficients in this expansion are found using a recursive formula derived from the nature of the incident field, whose analytic expression must be known, and the Fourier series of the boundary corrugation.

In the present work we have altered the boundary variation method by changing the incident field from a plane wave to the analytic solution of a guided wave in a thin film waveguide. In this way the boundary variation may be used for analysing grating couplers rather than transmission gratings.

To demonstrate the stunning results from using this fast and *approximate* method we have performed a number of comparisons with the highly accurate spectral collocation method. An example is seen in Figure 50, which shows the far-field radiation pattern of a focusing grating coupler computed with both these methods. For the specific problem, the boundary variation used five minutes on a single processor, while the spectral collocation required four hours on four parallel processors!

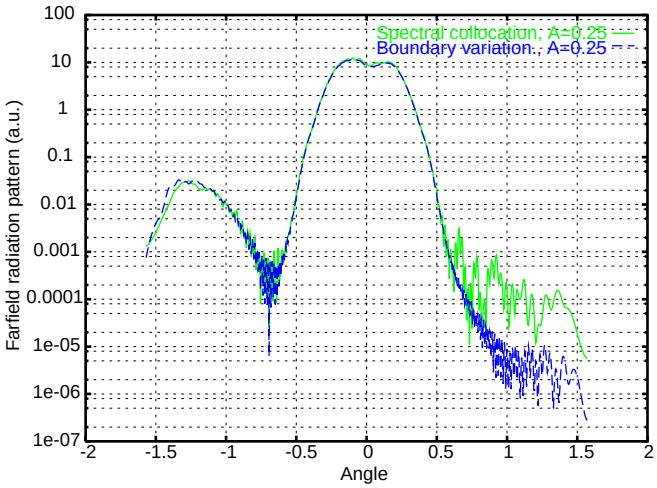

Figure 50. Comparison of far-field radiation pattern from a focusing grating coupler computed using the spectral collocation and boundary variation methods, respectively. A is the ampitude of the grating in units of the wavelength.

4.4.3 Instabilities and pattern formation in optical second-harmonic generation in the presence of competing parametric oscillations

P. Lodahl, M. Bache and M. Saffman (University of Wisconsin, Madison, USA)
E-mail: peter.lodahl@risoe.dk

Cavity enhanced $\chi^{(2)}$ nonlinear processes have recently drawn much attention on the generation of pattern forming instabilities. These structures appear as modulated intensity patterns in the plane perpendicular to the propagation direction of the light beam. Compared with many alternative materials a major advantage of $\chi^{(2)}$ nonlinearities is the very fast time response that leads to new effects and is a prerequisite for future applications in information processing.

We perform experimental and theoretical investigations on pattern formation in the process of optical second-harmonic generation both in singly resonant[1] and doubly resonant[2] configurations. It turns out to be important to consider the possibility of the generated second-harmonic field to decay through a nondegenerate parametric process, and this competing parametric process can modify the pattern formation dynamics decisively. The combined system of second-harmonic generation and competing parametric oscillations contains a rich scenario of instabilities that lead to the formation of localised structures as well as stationary and dynamic transverse structures.

A combination of analytical and numerical analysis can be used to investigate the pattern formation dynamics. In the most simple situation it is possible to obtain analytical solutions above threshold for the instability that can be used to test the numerics. Figure 51 (left) shows a comparison between the numerics and the analytical solutions and very good agreement is obtained. For more complicated patterns the numerics is tested by performing a weakly nonlinear analysis in order to derive approximate equations that are more easily solvable. Very

complicated structures are also found as, e.g., the spiral pattern shown in Figure 51 (right). This pattern appears from a secondary instability in the system.

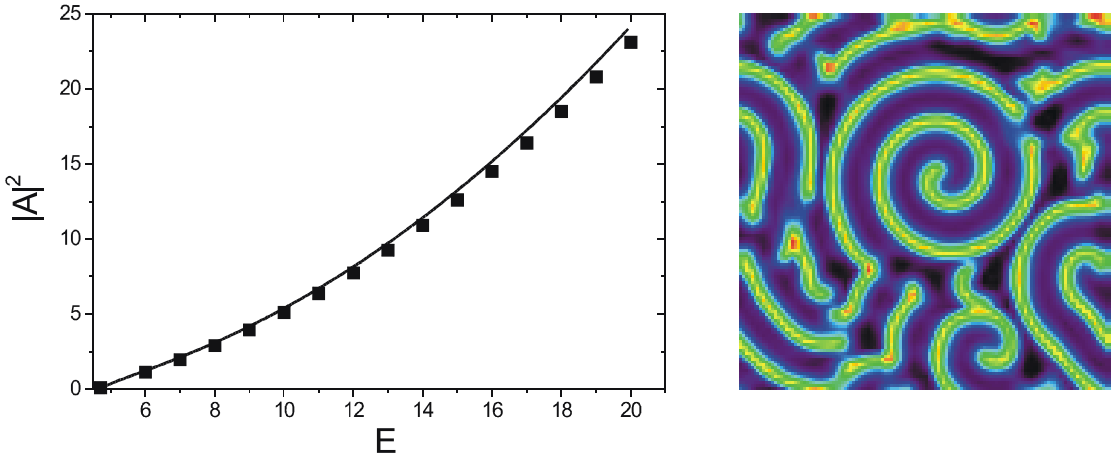

Figure 51. Left: Comparison between numerics (squares) and analytical solutions (full curve) for a simple "tilted-wave" transverse instability. The intensity of the parametric fields $|A|^2$ has been plotted as a function of the cavity pump field E. Right: Numerical simulation showing spiral wave instability in the situation where the "tilted-wave" becomes unstable. The plot shows the parametric intensity distribution in the transverse plane.

1. P. Lodahl and M. Saffman, "Pattern formation in singly resonant second-harmonic generation with competing parametric oscillation", Phys. Rev. A **60**, 3251 (1999).
2. P. Lodahl, M. Bache, and M. Saffman, "Modification of pattern formation in doubly resonant second harmonic generation by competing parametric oscillation", submitted (1999).

4.4.4 Studies of spatial quantum structures in optical second-harmonic generation

P. Lodahl, M. Bache and M. Saffman (University of Wisconsin, Madison, USA)
E-mail: peter.lodahl@risoe.dk

During the last decade $\chi^{(2)}$ nonlinear processes have proved to be the most efficient candidates for generation of light with non-classical properties. So far, most attention has been paid to light with temporal quantum fluctuations that can be useful for spectroscopic measurements with better signal-to-noise ratio than is obtainable with classical light. Recently the existence of spatial quantum correlations in the spatial structures originating from pattern formation has been proposed. Thus, by studying the quantum correlation functions more elaborate information about the complex pattern formation dynamics is obtained than is otherwise revealed from a classical analysis. Furthermore, in principle these multimode quantum patterns allow measurements of very small displacements with better precision than with classical single-mode light.

The current project has been initiated in order to study spatial quantum correlations in second-harmonic generation (SHG) analytically and numerically. Until now all work has been concerned with the optical parametric oscillator, but the success of SHG in generating interesting spatial structures in addition to strong quantum correlations makes it a promising new candidate for studies of quantum patterns. We have derived a set of Langevin equations that describe quantum fluctuations in SHG. The equations are linearised under the assumption that the stochastic terms are small compared with the coherent field amplitudes, which is a good approximation for SHG. The quantum origin of the fluctuations is included through an input/output formalism where the input fluctuations obey certain statistical relations that originate from the quantisation of the electromagnetic field. Strong squeezing is found in the

system, and current work is about evaluating also the spatial correlation functions and numerical implementation.

4.4.5 Splitting, bunches and snakes in the 3D non-linear Schrödinger equation with anisotropic dispersion

R. Grauer, K. Germashewski* (* University of Düsseldorf, Germany), L. Bergé (CEA/Bruyéres-le-Châtel, B.P. 1,2 Bruyéres-le-Châtel, France), V. K. Mezentsev (Institute for Automation and Electrometry, Novosibirsk, Russia) and J. Juul Rasmussen*
E-mail: jens.juul.rasmussen@risoe.dk

We have employed a newly developed numerical scheme with very high spatial resolution to resolve the detailed dynamics of the solution to the 3D cubic Schrödinger equation (CSE) of the form:

$$i\frac{\partial\psi}{\partial t}+\nabla_\perp^2\psi+s\frac{\partial^2\psi}{\partial z^2}+p|\psi|^2\psi=0\ ,\ \text{where}\ \nabla_\perp^2\psi\equiv\frac{\partial^2\psi}{\partial x^2}+\frac{\partial^2\psi}{\partial y^2}$$

This equation is a generic model for the non-linear evolution of the slowly varying amplitude field of electromagnetic waves in media where the refractive index depends linearly on the field intensity, i.e. Kerr-type media. These include various non-linear optical materials, plasmas and gases. Here ψ is the complex envelope field and z is the direction of propagation. The second term models the diffraction in the transverse plane; the third term models the dispersion along the axis of propagation ($s > 0$ yields anomalous dispersion; $s < 0$ yields normal dispersion). The last term on the left-hand side models the Kerr effect, where $p > 0$ corresponds to focusing, and $p < 0$ corresponds to defocusing. Here we only considered $p > 0$, and the investigations were mainly concerned with the propagation of wave beams in media with anisotropic/normal dispersion ($s < 0$). We clearly confirmed the theoretical predictions:[1] light beams (light bullets) will not collapse to a singularity (as for the case of $s > 0$), but the "bullets" split into two or more individual "bullets" along the z-axis. Furthermore, the number of resulting "bullets" in the asymptotic stage was below the maximum number predicted. We emphasise that the very high resolution in the numerical calculations obtained by using adaptive mesh refinement is essential for resolving the initial narrowing of the wave beam prior to the splitting events and, therefore, also for revealing the details of the splitting process.

We also considered stationary beam solutions to the CSE in the form of radial symmetric waveguides that are perturbed in the z-direction. We have investigated both sausage- and snake-like perturbations. The initial evolution is in accordance with the linear stability analysis:[2,1] unstable bunches emerge from a sausage-like perturbation of a cylindrically-symmetric waveguide both for $s > 0$ and $s < 0$, while the snake-like perturbations are stable for $s > 0$ and unstable for $s < 0$.

1. L. Bergé, and J. Juul Rasmussen, Phys. Plasmas v. 3, 824 843 (1996).

2. V.E. Zakharov and A.M. Rubenchik, Zh. Eksp. Teor. Fiz. V. 65 997 (1973) [Sov. Phys. JETP v. 38, 494 (1974)].

4.4.6 Self-guiding light in layered non-linear media

V. K. Mezentsev (Institute for Automation and Electrometry, Novosibirsk, Russia), L. Bergé (CEA/Bruyéres-le-Châtel, B.P. 1,2 Bruyéres-le-Châtel, France), P. L. Christiansen (IMM, Technical University of Denmark, Lyngby), Yu. B. Gaididei (Institute for Theoretical Physics, Kiev, Ukraine) and J. Juul Rasmussen
E-mail: jens.juul.rasmussen@risoe.dk

Self-trapping and self-focusing of intense optical beams that propagate in a bulk (two transverse dimensions) diffractive, non-linear Kerr medium may result in catastrophic collapse for beam intensities above a critical value. This will have damaging effects on the medium. For intensities below this critical value the beam will simply diffract and spread out. We have demonstrated that it is possible to avoid the collapse and to form a stable beam in media with periodically varying non-linear refractive index by exploiting the ideas for obtaining so-called dispersion managed solitons[1] in non-linear optical fibres. By means of analytical estimates based on a variational approach we have obtained the conditions for obtaining "stable" beams with constant radius and intensity averaged over the period of the variation of the non-linear refractive index. This result is confirmed by numerical solutions of the 2D cubic non-linear Schrödinger equation with varying non-linear coefficient. Thus, beams with appropriate shapes, having a power close to the self-focusing threshold, are shown to propagate over long distances as quasi-stationary waveguides, see Figure 52.

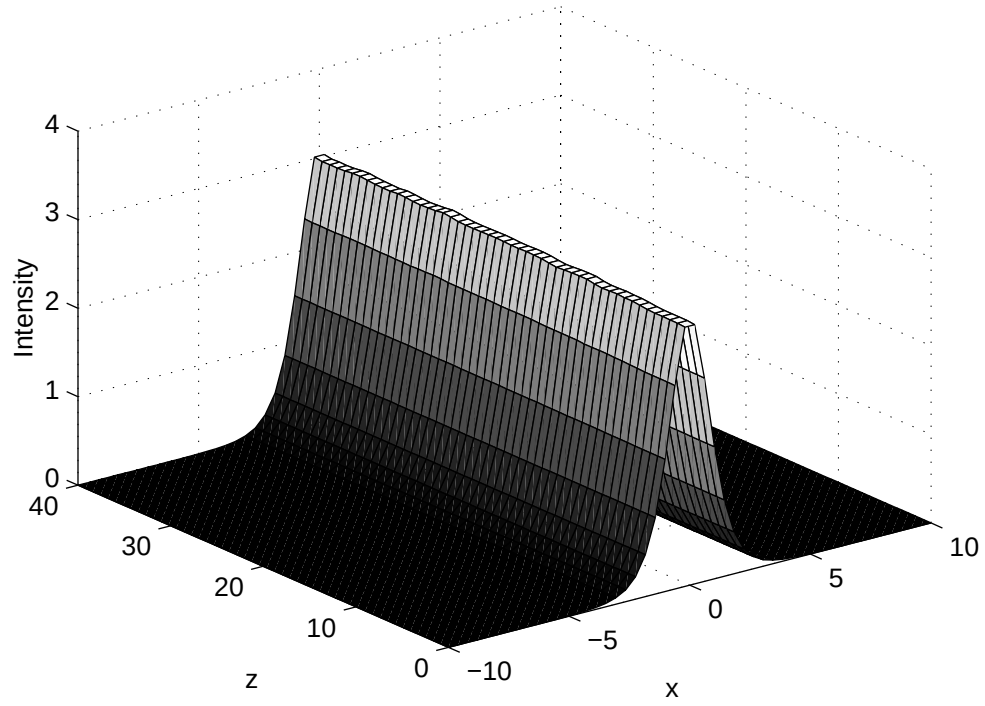

Figure 52. Intensity versus the transverse coordinate x and the propagation coordinate z of the quasi-periodic beam propagating in a layered non-linear medium.

1. S.K. Turitsyn, V.K. Mezentsev and E.G. Shapiro, Optical Fiber Technology **4**, 384–452 (1998).

4.4.7 Dynamics of solitons in higher order non-linear Schrödinger equations

V.I. Karpman (Racah Institute of Physics, Hebrew University, Jerusalem, Israel), A. Shagalov (Institute for Metal Physics, Ekaterinburg, Russia) and J. Juul Rasmussen
E-mail: jens.juul.rasmussen@risoe.dk

The evolution of localised soliton solutions to the generalised non-linear Schrödinger (G-NLS) equation is investigated analytically and numerically. The G-NLS equation describes, e.g., the evolution of ultrashort pulses in optical waveguides. Using suitable normalisations the equation reads:

$$iu_t + \tfrac{1}{2}u_{\xi\xi} + |u|^2 u = -i\alpha u_{\xi\xi\xi} + i\beta |u|^2 u_\xi + i\gamma \left(|u|^2\right)_\xi u,$$

where the coefficients α, β, and γ are real. In particular, we have focused our attention on the case of $\gamma = 0$, where the G-NLS has a Hamiltonian structure. For that case it is well-known that for a specific choice of the parameters, i.e., $\alpha = \beta/6$, the equation is integrable and has a stationary localised soliton solution. We have investigated the dynamics of this solution when the parameters α, β are in the neighbourhood of the specific values. The third-order dispersion, with the coefficient α, is found to give rise to radiation from the localised pulse, and this effect will hinder the formation of a completely stationary solution for $\alpha \# \beta/6$. However, a quasi-steady pulse with a weak tail of radiation is found numerically to evolve from initial conditions corresponding to the soliton solution for the specific parameters.

5. Publications and educational activities

5.1 Optical materials

5.1.1 International publications

Andersen, P.E.; Johansen, P.M.; Pedersen, H.C.; Petersen, P.M.; Saffman, M. (eds.), Advances in photorefractive materials, effects, and devices. 7. Topical meeting on photorefractive materials, effects and devices (PR'99), Elsinore (DK), 27-30 Jun 1999. (Optical Society of America, Washington, DC, 1999) (OSA trends in optics and photonics series, v. 27) 675 p.

Andruzzi, L.; Altomare, A.; Ciardelli, F.; Solaro, R.; Hvilsted, S.; Ramanujam, P.S., Holographic gratings in azobenzene side-chain polymethacrylates. Macromolecules (1999) v. 32 p. 448-454.

Hansen, T.N.; Schou, J.; Lunney, J.G., Ion time-of-flight study of laser ablation of silver in low pressure gases. Appl. Surf. Sci. (1999) v. 139 p. 184-187.

Holme, N.C.R.; Nikolova, L.; Hvilsted, S.; Rasmussen, P.H.; Berg, R.H.; Ramanujam, P.S., Optically induced surface relief phenomena in azobenzene polymers. Appl. Phys. Lett. (1999) v. 74 p. 519-521.

Holme, N.C.R.; Nikolova, L.; Norris, T.B.; Hvilsted, S.; Pedersen, M.; Berg, R.H.; Rasmussen, P.H.; Ramanujam, P.S., Physical processes in azobenzene polymers on irradiation with polarized light. Macromol. Symp. (1999) v. 137 p. 83-103.

Johansen, P.M.; Pedersen, H.C.; Podivilov, E.V.; Sturman, B.I., Ac square-wave field-induced subharmonics in photorefractive sillenite: Threshold for excitation by inclusion of higher harmonics. J. Opt. Soc. Am. B (1999) v. 16 p. 103-110.

Johansen, P.M.; Pedersen, H.C.; Podivilov, E.V., Influence of quadratic recombination on grating recording in photorefractive crystals. J. Opt. Soc. Am. B (1999) v. 16 p. 1120-1126.

Limeres, J.; Carrascosa, M.; Agullo-Lopez, F.; Andersen, P.E.; Petersen, P.M., Nonlinear grating interactions in multibeam photoreactive recording: Theoretical investigation. J. Opt. Soc. Am. B (1999) v. 16 p. 414-419.

Løbel, M.; Petersen, P.M.; Johansen, P.M., Physical origin of laser frequency scanning induced by photorefractive phase-conjugate feedback. J. Opt. Soc. Am. B (1999) v. 16 p. 219-227.

Naydenova, I.; Nikolova, L.; Ramanujam, P.S.; Hvilsted, S., Light-induced circular birefringence in cyanoazobenzene side-chain liquid-crystalline polyester films. J. Opt. A (1999) v. 1 p. 438-441.

Nikolajsen, T.; Johansen, P.M.; Yue, X.; Kip, D.; Kratzig, E., Two-step two-color recording in a photorefractive praseodymium-doped $La_3Ga_5SiO_{14}$ crystal. Appl. Phys. Lett. (1999) v. 74 p. 4037-4039.

Nikolajsen, T.; Johansen, P.M., Low-temperature thermal fixing of holograms in photorefractive $La_3Ga_5SiO_{14}:Pr^{3+}$ crystal. Opt. Lett. (1999) v. 24 p. 1419-1421.

Pedersen, H.C.; Johansen, P.M.; Webb, D.J.; Podivilov, E.V., Longitudinal parametric oscillation in photorefractive sillenites: Comparison between theory and experiment. Appl. Phys. B (1999) v. 68 p. 967-970.

Pedersen, H.C.; Johansen, P.M., Space-charge wave theory of photorefractive parametric amplification. J. Opt. Soc. Am. B (1999) v. 16 p. 1185-1188.

Pedersen, M.; Hvilsted, S.; Holme, N.C.R.; Ramanujam, P.S., Influence of the substituent on azobenzene side-chain polyester optical storage materials. Macromol. Symp. (1999) v. 137 p. 115-127.

Pedrys, R.; Warczak, B.; Leskiewicz, P.; Schou, J.; Ellegaard, O., Sputtering by excitonic and elastic processes from solid neon by He ion bombardment. Nucl. Instrum. Methods Phys. Res. B (1999) v. 157 p. 121-125.

Ramanujam, P.S.; Hvilsted, S., Instant holography. Holography Newslett. (1999) v. 10 (no.2) p. 1,5.

Ramanujam, P.S.; Pedersen, M.; Hvilsted, S., Instant holography. Appl. Phys. Lett. (1999) v. 74 p. 3227-3229.

Rasmussen, P.H.; Ramanujam, P.S.; Hvilsted, S.; Berg, R.H., A remarkably efficient azobenzene peptide for holographic information storage. J. Am. Chem. Soc. (1999) v. 121 p. 4738-4743.

Rasmussen, P.H.; Ramanujam, P.S.; Hvilsted, S.; Berg, R.H., Accelerated optical holographic recording using bis-DNO. Tetrahedron Lett. (1999) v. 40 p. 5953-5956.

Sturman, B.I.; Podivilov, E.V.; Chernykh, A.I.; Ringhofer, K.H.; Kamenov, V.P.; Pedersen, H.C.; Johansen, P.M., Instability of the resonance excitation of space-charge waves in sillenite crystals. J. Opt. Soc. Am. B (1999) v. 16 p. 556-564.

Sturman, B.I.; Podivilov, E.V.; Pedersen, H.C.; Johansen, P.M., Critical slowing down of space-charge field relaxation in photorefractive sillenites. Opt. Lett. (1999) v. 24 p. 1163-1165.

Thestrup, B.; Schou, J.; Nordskov, A.; Larsen, N.B., Electrical and optical properties of thin indium tin oxide films produced by pulsed laser ablation in oxygen or rare gas atmospheres. Appl. Surf. Sci. (1999) v. 142 p. 248-252.

Yue, X.F.; Mendricks, S.; Nikolajsen, T.; Hesse, H.; Kip, D.; Kratzig, E., Transient enhancement of photorefractive gratings in lead germanate by homogeneous pyroelectric fields. J. Opt. Soc. Am. B (1999) v. 16 p. 389-394.

5.1.2 Danish publications

Juul Jensen, S., Spatial structures and temporal dynamics in photorefractive nonlinear systems. Risø-R-1142(EN) (1999) 114 p. (ph.d. thesis).

Petersen, P.M. (ed.), Optics in Denmark 1999: DOPS white book. (Dansk Optisk Selskab, Roskilde, 1999) (DOPS-nyt, v. 14:3, 1999) 45 p.

5.1.3 Conference lectures

Berg, R.H.; Rasmussen, P.H.; Hvilsted, S.; Ramanujam, P.S., Optical holographic data storage using peptides. In: Peptides. Frontiers of peptide science. Proceedings. 15. American peptide symposium, Nashville, TN (US), 14-19 Jun 1997. Tam, J.P.; Kaumaya, P.T.P. (eds.), (Kluwer Academic Publishers, Dordrecht, 1999) p. 88-90.

Fleck, B.; Wenke, L.; Ramanujam, P.S., A nonlinear optical element for incoherent image processing based on photoanisotropy. In: Technical digest. 18. Congress of the International Commission for Optics, San Francisco, CA (US), 2-6 Aug 1999. Glass, A.J.; Goodman, J.W.; Chang, M.; Günther, A.H.; Asakura, T. (eds.), (International Society for Optical Engineering, Bellingham, WA, 1999) (Proceedings of SPIE, v. 3749) p. 354-355.

Hvilsted, S.; Ramanujam, P.S., Azobenzene side-chain liquid crystalline polyesters - A prodigious potential for optical information storage. In: Abstract book and general information. 6. International Bayreuth polymer and materials research symposium (BPS'99), Bayreuth (DE), 11-13 Apr 1999. (Universität Bayreuth, Bayreuth, 1999) 3 p. (L20).

Limeres, J.; Carrascosa, M.; Andersen, P.E.; Petersen, P.M., Experimental observation of nonlinear grating cross talk in multibeam photorefractive recording. In: Advances in photorefractive materials, effects, and devices. 7. Topical meeting on photorefractive materials, effects and devices (PR'99), Elsinore (DK), 27-30 Jun 1999. Andersen, P.E.; Johansen, P.M.; Pedersen, H.C.; Petersen, P.M.; Saffman, M. (eds.), (Optical Society of America, Washington, DC, 1999) (OSA trends in optics and photonics series, v. 27) p. 394-400.

Lyuksyutov, S.F.; Buchhave, P.; Vasnetsov, M.V.; Andersen, P.E.; Petersen, P.M., Reduction of photoexcited carriers modulation due to a long distance photoelectron pass in photorefractive $Bi_{12}SiO_{20}$. In: Advances in photorefractive materials, effects, and devices. 7. Topical meeting on photorefractive materials, effects and devices (PR'99), Elsinore (DK), 27-30 Jun 1999. Andersen, P.E.; Johansen, P.M.; Pedersen, H.C.; Petersen, P.M.; Saffman, M. (eds.), (Optical Society of America, Washington, DC, 1999) (OSA trends in optics and photonics series, v. 27) p. 96-100.

Petersen, P.M.; Juul Jensen, S.; Johansen, P.M., Phase locking of laser diode arrays using a photorefractive Rh:$BaTiO_3$ crystal (Invited paper). In: Proceedings. Laser resonators 2, San José, CA (US), 23-29 Jan 1999. Kudryashov, A.V. (eds.), (International Society for Optical Engineering, Bellingham, WA, 1999) (Proceedings of SPIE, v. 3611) p. 142-146.

Ramanujam, P.S.; Holme, N.C.R.; Berg, R.H.; Hvilsted, S., Holographic memory. In: Selected papers from Photonics India '98. International conference on fiber optics and photonics, New Delhi (IN), 14-18 Dec 1998. Sharma, A.; Gupta, B.D.; Ghatak, A.K.; (eds.), (International Society for Optical Engineering, Bellingham, WA, 1999) (Proceedings of SPIE, v. 3666) p. 611-617.

Rasmussen, P.H.; Ramanujam, P.S.; Hvilsted, S.; Berg, R.H., Improved peptides for holographic data storage. In: Peptides. Frontiers of peptide science. Proceedings. 15. American peptide symposium, Nashville, TN (US), 14-19 Jun 1997. Tam, J.P.; Kaumaya, P.T.P. (eds.), (Kluwer Academic Publishers, Dordrecht, 1999) p. 168-169.

Sahlén, F.; Geisler, T.; Hvilsted, S.; Holme, N.C.R.; Ramanujam, P.S.; Petersen, J.C., Combined main- and side-chain azobenzene polyesters: A potential for photoinduced nonlinear waveguides. In: Proceedings. Symposium on organic nonlinear optical materials and devices, San Francisco, CA (US), 6-9 Apr 1999. Kippelen, B.; Lackritz, H.S.; Claus, R.O. (eds.), (MRS, Warrendale, PA, 1999) (Materials Research Society symposium proceedings, 561) p. 57-62.

5.1.4 Publications for a broader readership

Sundstrøm, M., Øjet og de fysiologiske farver. DOPS-Nyt (1999) v. 14 (no.1) p. 9-15.

Thestrup, B.; Schou, J., AZO - et nyt optisk materialer. DOPS-Nyt (1999) v. 14 (no.4) p. 17-19.

5.1.5 Unpublished Danish lectures

Andersen, T.N.; Jessen, N.C., The use of a CO_2 laser in the study of the human pain system. In: Abstracts. Annual meeting of the Danish Optical Society, Lyngby (DK), 18-19 Nov 1999. (Technical University of Denmark. Research Center COM, Lyngby, 1999) p. 17.

Ellegaard, O.; Schou, J.; Urbassek, H.M., Gasflow and collision dynamics in a thermally laser ablated plume of silver atoms described by Monte Carlo simulations. In: Programme. Abstracts. List of participants. Annual meeting of the Danish Physical Society, Nyborg (DK), 3-4 Jun 1999. (HCØ Tryk, København, 1999) p. AF16P.

Holmelund, E.; Thestrup, B.; Schou, J.; Nordskov, A., Production of films of transparent semiconductors by laser ablation. In: Abstracts. Annual meeting of the Danish Optical Society, Lyngby (DK), 18-19 Nov 1999. (Technical University of Denmark. Research Center COM, Lyngby, 1999) p. 40.

Imam, H., Refractive index sensing using waveguides. Symposium on biomedical optics, Technical University of Denmark, Lyngby (DK), 21 Sep 1999. Unpublished.

Johansen, P.M., Risø - et moderne forskningscenter. Møde i Aalborg "Stigsborg" Rotary Klub, Aalborg (DK), 15 Feb 1999. Unpublished.

Johansen, P.M., Optical materials: Linear and non-linear effects. Coloquium på Fysisk Institut, Odense Universitet, Odense (DK), 1 Dec 1998. Unpublished.

Juul Jensen, S.; Løbel, M.; Petersen, P.M., Single mode laser diode array with external feedback. In: Programme. Abstracts. List of participants. Annual meeting of the Danish Physical Society, Nyborg (DK), 3-4 Jun 1999. (HCØ Tryk, København, 1999) p. AF14P.

Lindvold, L., Laserpincetter. Temamøde om biomedicinsk optik, Risø (DK), 22 Jun 1999. Unpublished.

Petersen, P.M., High-power lasers for photodynamic therapy. Symposium on biomedical optics, Technical University of Denmark, Lyngby (DK), 21 Sep 1999. Unpublished.

Ramanujam, P.S., Optical techniques for analysis of polymers. Danish Society for Polymer Technology (PTS) thematic meeting, Risø (DK), 5 Oct 1999. Unpublished. Abstract available.

Schou, J., Laser ablation of solids: Fundamental problems and applications. Meeting at Institute of Physics, Odense University, Odense (DK), 2 Mar 1999. Unpublished. Abstract available.

Sundstrøm, M., Construction of a flourometer for the detection and analysis of flourescence from the lens and retina of the human eye. In: Abstracts. Annual meeting of the Danish Optical Society, Lyngby (DK), 18-19 Nov 1999. (Technical University of Denmark. Research Center COM, Lyngby, 1999) p. 35.

Thestrup, B.; Schou, J.; Larsen, N.B., Pulsed laser deposition of transparent, conducting AZO and ITO films. In: Programme. Abstracts. List of participants. Annual meeting of the Danish Physical Society, Nyborg (DK), 3-4 Jun 1999. (HCØ Tryk, København, 1999) p. KF09P.

Toftmann Christensen, B.; Schou, J., Laser ablation from radiation-produced or artificial craters. In: Programme. Abstracts. List of participants. Annual meeting of the Danish Physical Society, Nyborg (DK), 3-4 Jun 1999. (HCØ Tryk, København, 1999) p. AF17P.

Toftmann, B.; Schou, J., Laser ablation at different angles of incidence. In: Abstracts. Annual meeting of the Danish Optical Society, Lyngby (DK), 18-19 Nov 1999. (Technical University of Denmark. Research Center COM, Lyngby, 1999) p. 46.

5.1.6 Unpublished international lectures

Busson, P.; Hult, A.; Hvilsted, S.; Ramanujam, P.S., Synthesis and characterization of azobenzene functionalized dendritic macromolecules for holographic storage applications. In: Nordic polymer days 1999. Nordic polymer days, Danish Society for Polymer Technology, Copenhagen (DK), 31 May - 2 Jun 1999. (Ingeniørforeningen i Danmark, Copenhagen, 1999) 1.4.

Ellegaard, O.; Schou, J.; Urbassek, H.M., Monte Carlo description of gasflow from a thermally ablated silver surface. COLA 99, 5. International conference on laser ablation, Göttingen (DE), 19-23 Jul 1999. Unpublished. Abstract available.

Hansen, T.N.; Lunney, J.G.; Toftmann, B.; Schou, J., Langmuir probe study of plasma expansion in pulsed laser ablation. COLA 99, 5. International conference on laser ablation, Göttingen (DE), 19-23 Jul 1999. Unpublished. Abstract available.

Hvilsted, S.; Ramanujam, P.S., Light induced surface relief in azobenzene materials. In: 2. Symposium on phthalocyanines and related compounds. Abstracts. COST action 518. Molecular materials and functional polymers for advanced devices. First Working Group 2 meeting, Madrid (ES), 28-29 May 1999. (Cost Action 518, Madrid, 1999) 1 p.

Hvilsted, S.; Ramanujam, P.S., Azobenzene side-chain LC polyesters for optical information storage. SICL '99 workshop: Applications of liquid crystals, Portonovo di Ancona (IT), 23-26 Jun 1999. Unpublished. Abstract available.

Johansen, P.M.; Nikolajsen, T., New aspects of optical storage in photorefractive $La_3Ga_5SiO_{14}:Pr^{3+}$ crystals. Workshop on applications of nonlinear optical phenomena and related industrial perspectives, joined to the 2. Annual meeting of the COST Action P2, Amalfi (IT), 6-9 Oct 1999. Unpublished.

Johansen, P.M.; Petersen, P.M., Photorefractive holographic storage: Fundamental limits and new materials. Møde i WG1 under COST Action P2 'Application of non-linear optical phenomena' Technische Universität Berlin, Fachbereich Physik, Berlin (DE), 12 Feb 1999. Unpublished.

Lindvold, L., Projection display based on an optically addressed spatial light modulator using bacteriorhodopsin as a photochromic material. Information meeting, Scientific Generics, Cambridge (GB), 20 Apr 1999. Unpublished.

Lindvold, L., Polymer optics at Risø. Information meeting, Institute of Biotechnology, Cambridge (GB), 19 Apr 1999. Unpublished.

Lindvold, L.; Lausen, H., Projection display using a bacteriorhodopsin thin film as a spatial light modulator. 6. International display workshops, Sendai (JP), 1-3 Dec 1999. Unpublished.

Nikolajsen, T., Nonvolatile holographic storage in photorefractive materials: Theory. Nonlinear science festival 2, Risø (DK), 1-4 Dec 1999. Unpublished.

Nikolajsen, T., Fixing of holograms in photorefractive crystals - $La_3Ga_5SiO_{14}$. Meeting at California Institute of Technology (CalTech), Pasadena, CA (US), 3 Jun 1999. Unpublished.

Nikolajsen, T.; Johansen, P.M.; Yue, X.; Kip, D.; Krätzig, E., Optical fixing in a $La_3Ga_5SiO_{14}$ crystal doped with praseodymium. In: Post-deadline papers. 7. Topical meeting on photorefractive materials, effects and devices (PR'99), Elsinore (DK), 27-30 Jun 1999. (Risø National Laboratory, Roskilde, 1999) p. 43-46.

Pedersen, T.G.; Johansen, P.M., Nonlinear optical polymers for reversible optical data storage. Workshop on applications of nonlinear optical phenomena and related industrial perspectives, joined to the 2. Annual meeting of the COST Action P2, Amalfi (IT), 6-9 Oct 1999. Unpublished.

Pedersen, T.G.; Johansen, P.M.; Pedersen, H.C., Nonlinear optical properties of liquid crystalline polymers. Nonlinear science festival 2, Risø (DK), 1-4 Dec 1999. Unpublished.

Pedrys, R.; Krok, F.; Leskiewicz, P.; Schou, J., Time-of-fight studies of heavy water ice sputtering by Xe ion bombardment. 18. International conference on atomic collisions in solids, Odense (DK), 3-8 Aug 1999. Unpublished. Abstract available.

Pedrys, R.; Warczak, B.; Krok, F.; Schou, J.; Ellegaard, O., Sputtering of solid neon by keV He ions. 12. International workshop on inelastic ion-surface collisionsq, Padre Island, TX (US), 24-29 Jan 1999. Unpublished. Abstract available.

Petersen, P.M., A high power laser diode array with external phase conjugate feedback. Workshop on applications of nonlinear optical phenomena and related industrial perspectives,

joined to the 2. Annual meeting of the COST Action P2, Amalfi (IT), 6-9 Oct 1999. Unpublished. Abstract available.

Petersen, P.M., Progress in high brightness laser diode arrays. Meeting at Frunhofer Institut Lasertechnik, Aachen (DE), 12 Nov 1999. Unpublished.

Petersen, P.M., Phase locking and frequency doubling of laser diode arrays. Meeting at Thomson CSF, Orsay (FR), 29 Oct 1999. Unpublished.

Ramanujam, P.S., Optical storage in azobenzene polymers. LC Photonet meeting, Southampton (GB), 11-13 Feb 1999. Unpublished. Abstract available.

Ramanujam, P.S., Azobenzene polymers for optical information storage. 4. Mediterranean workshop and topical meeting: Novel optical materials and applications (NOMA '99), Cetraro (IT), 4-10 Jun 1999. Unpublished. Abstract available.

Ramanujam, P.S.; Hvilsted, S., Optical storage in azobenzene polymers. In: Nordic polymer days 1999. Nordic polymer days, Danish Society for Polymer Technology, Copenhagen (DK), 31 May - 2 Jun 1999. (Ingeniørforeningen i Danmark, Copenhagen, 1999) 2.2.

Rasmussen, P.H.; Ramanujam, P.S.; Hvilsted, S.; Berg, R.H., Remarkably efficient proline-based azobenzene peptides for optical information storage. In: Program and abstracts. 16. American peptide symposium: Peptides for the new millennium, Minneapolis, MN (US), 26 Jun - 1 Jul 1999. (American Peptide Society, Minneapolis, 1999) p. 275 (P438).

Schou, J.; Holmelund, E.; Thestrup, B.; Toftmann, B., Nonlinear phenomena in laser ablation. Nonlinear science festival 2, Risø (DK), 1-4 Dec 1999. Unpublished.

Schou, J.; Toftmann, B.; Hansen, T.N.; Thestrup, B.; Ellegaard, O., Low-energy ion-surface interactions in pulsed laser deposition. 12. International workshop on inelastic ion-surface collisions, Padre Island, TX (US), 24-29 Jan 1999. Unpublished. Abstract available.

Thestrup, B.; Dam-Hansen, C.; Schou, J.; Johansen, P.M., Holographic gratings induced in laser deposited AZO and ITO films. In: Post-deadline papers. 7. Topical meeting on photorefractive materials, effects and devices (PR'99), Elsinore (DK), 27-30 Jun 1999. (Risø National Laboratory, Roskilde, 1999) p. 31-34.

Thestrup, B.; Schou, J.; Larsen, N.B., Transparent, conducting AZO and ITO films produced by pulsed laser ablation at 355 nm. COLA 99, 5. International conference on laser ablation, Göttingen (DE), 19-23 Jul 1999. Unpublished. Abstract available.

Toftmann, B.; Schou, J., Ablation from flat or crater surfaces of silver induced by laser irradiation at 355 nm. COLA 99, 5. International conference on laser ablation, Göttingen (DE), 19-23 Jul 1999. Unpublished. Abstract available.

Toftmann, B.; Thestrup, B.; Schou, J.; Hansen, T.N.; Ellegaard, O., Ion-solid interactions in laser ablation of silver and nickel. 18. International conference on atomic collisions in solids, Odense (DK), 3-8 Aug 1999. Unpublished. Abstract available.

5.1.7 Internal reports

Andersen, P.E.; Lindvold, L., Lyskilder og detektorer i det midt-infrarøde bølgelængdeområde. (Forskningscenter Risø. Afdelingen for Optik og Fluid Dynamik, Roskilde, 1999) 12 p.

Andersen, P.E.; Lindvold, L.; Thrane, L., Bestemmelse af optiske parametre for DNP display skærme. Risø-Dok-617 (1999) 26 p.

5.2 Optical diagnostics and information processing

5.2.1 International publications

Andersen, P.E.; Johansen, P.M.; Pedersen, H.C.; Petersen, P.M.; Saffman, M. (eds.), Advances in photorefractive materials, effects, and devices. 7. Topical meeting on photorefractive materials, effects and devices (PR'99), Elsinore (DK), 27-30 Jun 1999. (Optical Society of America, Washington, DC, 1999) (OSA trends in optics and photonics series, v. 27) 675 p.

Andersen, F.; Kirkegaard, M., Resultatet af NIF audit "D1 digitaltermometer". In: Guttulsrød, G.F. (ed.), Sammenligningsmålinger i Norden 1998. NT-TR-443 (1999) 31 p.

Andersen, F.; Kirkegaard, M., Resultatet af NIF audit "D5 Pt 100 resistanstermometer". In: Guttulsrød, G.F. (ed.), Sammenligningsmålinger i Norden 1998. NT-TR-443 (1999) 30 p.

Andersen, F.; Kirkegaard, M., Resultatet af NIF audit "D6 digitaltermometer" (tørblokkalibrator). In: Guttulsrød, G.F. (ed.), Sammenligningsmålinger i Norden 1998. NT-TR-443 (1999) 21 p.

Angelsky, O.V.; Hanson, S.G.; Maksimyak, P.P., Use of optical correlation techniques for characterizing scattering objects and media. (SPIE Press, Bellingham, WA, 1999) 204 p.

Bak, J., Rapid method for simulating gas spectra using reversed PCR temperature calibration models based on Hitran data. Appl. Spectrosc. (1999) v. 53 p. 1375-1381.

Bak, J.; Clausen, S., Signal-to-noise ratio of FT-IR CO gas spectra. Appl. Spectrosc. (1999) v. 53 p. 697-700.

Bak, J.; Clausen, S., FTIR transmission-emission spectrometry of gases at high temperatures: Demonstration of Kirchhoff's law for a gas in an enclosure. J. Quant. Spectrosc. Radiat. Transfer (1999) v. 61 p. 687-694.

Clausen, S.; Bak, J., FTIR transmission emission spectroscopy of gases at high temperatures: Experimental set-up and analytical procedures. J. Quant. Spectrosc. Radiat. Transfer (1999) v. 61 p. 131-141.

Frandsen, S.; Lading, L.; Hansen, R.S.; Kristensen, L.; Miller, G.; Kjaer Hansen, J.; Sangill, O.; Lading, P., Laser anemometry for control and performance testing of wind turbines. 12-monthly progress report for the period 1 July 1998 to 1 July 1999. (European Commission, [s.l.], 1999) 73 p.

Helt-Hansen, J.; Larsen, H.E.; Christensen, P., Portable triple silicon detector telescope spectrometer for skin dosimetry. Nucl. Instrum. Methods Phys. Res. A (1999) v. 438 p. 523-539.

Jørgensen, T.M.; Linneberg, C., Theoretical analysis and improved decision criteria for the n-tuple classifier. IEEE Trans. Pattern Anal. Mach. Intell. (1999) v. 21 p. 336-347.

Limeres, J.; Carrascosa, M.; Agullo-Lopez, F.; Andersen, P.E.; Petersen, P.M., Nonlinear grating interactions in multibeam photoreactive recording: Theoretical investigation. J. Opt. Soc. Am. B (1999) v. 16 p. 414-419.

Yura, H.T.; Hanson, S.G.; Hansen, R.S.; Rose, B., Three-dimensional speckle dynamics in paraxial optical systems. J. Opt. Soc. Am. A (1999) v. 16 p. 1402-1412.

5.2.2 Danish publications

Mogensen, P.C.; Glückstad, J., Programmable phase optics. Progress report 1, 1st December 1998 - 30th May 1999. (Risø National Laboratory, Roskilde, 1999) 10 p.

Mogensen, P.C.; Glückstad, J., Programmable phase optics. Progress report 2, 1st June 1999 - 30th November 1999. (Risø National Laboratory, Roskilde, 1999) 16 p.

5.2.3 Conference lectures

Andersen, F., Framgångsrik kalibrering. Förbättra dina mätosäkerhetsberäkningar genom en ökad förståelse för alla led i kedjan. In: Dokumentation. Framgångsrik kalibrering, Stodkholm (SE), 20-21 Jan 1999. (Institute for International Research AB, Stockholm, 1999) 23 p.

Andersen, P.E.; Hanson, S.G.; Jacques, S.L., Photoacoustic imaging of buried objects using an all-optical detection scheme. In: Proceedings. Laser-tissue interaction 10: Photochemical, photothermal, and photomechanical, San José, CA (US), 23-29 Jan 1999. Jacques, S.L.; Müller, G.J.; Roggan, A.; Sliney, D.H. (eds.), (International Society for Optical Engineering, Bellingham, WA, 1999) (Proceedings of SPIE, v. 3601) p. 303-309.

Battuello, M.; Clausen, S.; Hameury, J.; Bloembergen, P., The spectral emissivity of surface layers, currently applied in blackbody radiators, covering the spectral range from 0,9 to 20 μm. An international comparison. In: Proceedings. Vol. 2. 7. International symposium on temperature and thermal measurements in industry and science (TEMPMEKO '99), Delft (NL), 1-4 Jun 1999. Dubbeldam, J.F.; Groot, M.J. de (eds.), (NMi Van Swinden Laboratorium, Delft, 1999) p. 601-606.

Glückstad, J., Image decrypting common path interferometer. In: Proceedings. Optical pattern recognition 10, Orlando, FL (US), 7-8 Apr 1999. (International Society for Optical Engineering, Bellingham, WA, 1999) (Proceedings of SPIE, v. 3715) p. 152-159.

Glückstad, J.; Mogensen, P.C.; Toyoda, H.; Hara, T., Binary phase image encryption method. In: Technical digest. Vol. 4. CLEO/Pacific Rim '99, Seoul (KR), 30 Aug - 3 Sep 1999. (Institute of Electrical and Electronics Engineers, Bellingham, WA, 1999) p. 1314-1315.

Glückstad, J.; Mogensen, P.C., Analysis of wavefront sensing using a common path interferometer architecture. In: Proceedings. 2. International workshop on adaptive optics for industry and medicine, Durham (GB), 12-16 Jul 1999. Love, G.D. (ed.), (World Scientific, Singapore, 1999) p. 45-51.

Hanson, S.G.; Hansen, R.S.; Hansen, B.H., Compact system for measuring rotational speed in two dimensions. In: Proceedings. Optical measurement systems for industrial inspection, Munich (DE), 16-17 Jun 1999. Kujawinska, M.; Osten, W. (eds.), (International Society for Optical Engineering, Bellingham, WA, 1999) (Proceedings of SPIE, v. 3824) p. 115-123.

Jørgensen, T.M.; Linneberg, C., Boosting the performance of weightless neural networks by using a post-processing transformation of the output scores. In: Proceedings. 1999 IEEE international joint conference on neural networks (IJCNN'99), Washington, DC (US), 10-16 Jul 1999. (IEEE, Washington, DC, 1999) Paper 126.

Jørgensen, T.M.; Linneberg, C., The hidden continuous weights of the standard n-tuple neural net. In: Proceedings. 3. International workshop on weightless neural networks (WNNW 99), York (GB), 30-31 Mar 1999. (University of York, Department of Computer Science, York, 1999) 10 p.

Kaiser, N.E., Accurate temperature measurements using Pt 100 resistance thermometers. In: Proceedings. Vol. 1. 7. International symposium on temperature and thermal measurements in industry and science (TEMPMEKO '99), Delft (NL), 1-4 Jun 1999. Dubbeldam, J.F.; Groot, M.J. de (eds.), (NMi Van Swinden Laboratorium, Delft, 1999) p. 365-370.

Kaiser, N.E., Temperature calibration in block calibrators. In: Proceedings. Vol. 1. 7. International symposium on temperature and thermal measurements in industry and science (TEMPMEKO '99), Delft (NL), 1-4 Jun 1999. Dubbeldam, J.F.; Groot, M.J. de (eds.), (NMi Van Swinden Laboratorium, Delft, 1999) p. 320-325.

Kaiser, N.E., Uncertainty budgets in theory and practice. Applications to thermometry. In: Proceedings. 21. Nordic conference on measurements and calibration, Gardemoen (NO), 22-23 Nov 1999. (NIF, Oslo, 1999) 16 p.

Limeres, J.; Carrascosa, M.; Andersen, P.E.; Petersen, P.M., Experimental observation of nonlinear grating cross talk in multibeam photorefractive recording. In: Advances in photorefractive materials, effects, and devices. 7. Topical meeting on photorefractive materials, effects and devices (PR'99), Elsinore (DK), 27-30 Jun 1999. Andersen, P.E.; Johansen, P.M.; Pedersen, H.C.; Petersen, P.M.; Saffman, M. (eds.), (Optical Society of America, Washington, DC, 1999) (OSA trends in optics and photonics series, v. 27) p. 394-400.

Linneberg, C.; Jørgensen, T.M., Discretization methods for encoding of continuous input variables for Boolean neural networks. In: Proceedings. 1999 IEEE international joint conference on neural networks (IJCNN'99), Washington, DC (US), 10-16 Jul 1999. (IEEE, Washington, DC, 1999) Paper 2155.

Linneberg, C.; Jørgensen, T.M., A statistical framework for analysing and improving the behaviour of the standard n-tuple classifier. In: Proceedings. 3. International workshop on weightless neural networks (WNNW 99), York (GB), 30-31 Mar 1999. (University of York, Department of Computer Science, York, 1999) 10 p.

Lyuksyutov, S.F.; Buchhave, P.; Vasnetsov, M.V.; Andersen, P.E.; Petersen, P.M., Reduction of photoexcited carriers modulation due to a long distance photoelectron pass in photorefractive $Bi_{12}SiO_{20}$. In: Advances in photorefractive materials, effects, and devices. 7. Topical meeting on photorefractive materials, effects and devices (PR'99), Elsinore (DK), 27-30 Jun 1999. Andersen, P.E.; Johansen, P.M.; Pedersen, H.C.; Petersen, P.M.; Saffman, M. (eds.), (Optical Society of America, Washington, DC, 1999) (OSA trends in optics and photonics series, v. 27) p. 96-100.

Mogensen, P.C.; Glückstad, J.; Toyoda, H.; Hara, T., Experiments with new phase image encrypting method. In: Technical digest. 18. Congress of the International Commission for Optics, San Francisco, CA (US), 2-6 Aug 1999. Glass, A.J.; Goodman, J.W.; Chang, M.; Güenther, A.H.; Asakura, T. (eds.), (International Society for Optical Engineering, Bellingham, WA, 1999) (Proceedings of SPIE, v. 3749) p. 274-275.

Rose, B.; Ibsen, P.E.; Hanson, S.G.; Hansen, R.S., Compact optical sensors for measuring linear and angular velocities. In: Proceedings. Optical measurement systems for industrial inspection, Munich (DE), 16-17 Jun 1999. Kujawinska, M.; Osten, W. (eds.), (International Society for Optical Engineering, Bellingham, WA, 1999) (Proceedings of SPIE, v. 3824) p. 20-29.

5.2.4 Publications for a broader readership

Clausen, S.; Bak, J., Måling af forbrændingsgasser fra fly; Simulering af IR-gasspektre. Industriel IR-analyse. Nyhedsbrev (1999) (no.Marts) p. 1-2.

Clausen, S.; Bak, J., AEROPROFILE - Risø-målinger i München og Napoli. Industriel IR-analyse. Nyhedsbrev (1999) (no.December) p. 1-2.

Sundstrøm, M., Øjet og de fysiologiske farver. DOPS-Nyt (1999) v. 14 (no.1) p. 9-15.

5.2.5 Unpublished Danish lectures

Andersen, T.N.; Jessen, N.C., The use of a CO_2 laser in the study of the human pain system. In: Abstracts. Annual meeting of the Danish Optical Society, Lyngby (DK), 18-19 Nov 1999. (Technical University of Denmark. Research Center COM, Lyngby, 1999) p. 17.

Glückstad, J., Recent activities in the programmable phase optics project. Meeting at Research Center COM, Technical University of Denmark, Lyngby (DK), 6 Dec 1999. Unpublished.

Hanson, S.G., Speckles. Why they appear, how they are treated analytically, and what they can be used for. Colloquium på Fysisk Institut, Odense Universitet, Odense (DK), 9 Nov 1999. Unpublished. Abstract available.

Hanson, S.G.; Hansen, R.S.; Hansen, B.H.; Eilertsen, E., FreePen, a miniaturized optical system. In: Abstracts. Annual meeting of the Danish Optical Society, Lyngby (DK), 18-19 Nov 1999. (Technical University of Denmark. Research Center COM, Lyngby, 1999) p. 22.

Jensen, P.S., FT-IR as a tool for non-invasive measurements on biological materials. In: Abstracts. Annual meeting of the Danish Optical Society, Lyngby (DK), 18-19 Nov 1999. (Technical University of Denmark. Research Center COM, Lyngby, 1999) p. 18.

Mogensen, P.C.; Glückstad, J., Phase-only optical encryption. In: Abstracts. Annual meeting of the Danish Optical Society, Lyngby (DK), 18-19 Nov 1999. (Technical University of Denmark. Research Center COM, Lyngby, 1999) p. 10.

Sundstrøm, M., Construction of a flourometer for the detection and analysis of flourescence from the lens and retina of the human eye. In: Abstracts. Annual meeting of the Danish Optical Society, Lyngby (DK), 18-19 Nov 1999. (Technical University of Denmark. Research Center COM, Lyngby, 1999) p. 35.

Thrane, L., Modeling light propagation in OCT systems. Symposium on biomedical optics, Technical University of Denmark, Lyngby (DK), 21 Sep 1999. Unpublished.

5.2.6 Unpublished international lectures

Andersen, P.E., Biomedical imaging modalities (invited lecture). European Commission Summer School: Low dimensional semiconductors for optoelectronic devices and communication systems, Aveiro (PT), 27 Jun - 4 Jul 1999. Unpublished.

Bak, J.; Clausen, S., High temperature gas analysis in industrial environments. Pittcon '99, Orlando, FL (US), 7-12 Mar 1999. Unpublished.

Clausen, S., Non-contact measurements of temperature and gas composition from infrared spectra. Case studies in industrial radiation thermometry. A one-day meeting of the Non-contact Temperature Measurement Group of TPAC (Thermophysical Properties Awareness Club), Warwick (GB), 18 Nov 1999. Unpublished.

Glückstad, J., PAL-SLMs for optical cryptizing technologies. Meeting at Hamamatsu Photonics Central Research Laboratories, Hamakita (JP), 6 Sep 1999. Unpublished.

Glückstad, J., Photonic encryption technologies (Invited lecture). Meeting at Kochi University of Technology, Kochi (JP), 9 Sep 1999. Unpublished.

Hansen, R.S.; Yura, H.T.; Hanson, S.G.; Rose, R., Three-dimensional speckles: Static and dynamic properties. 4. International conference on correlation optics (CorrOpt 99), Chernivtsy (UA), 11-14 May 1999. Unpublished.

Hanson, S.G., Angular displacement measurement based on speckle displacement. Interferometry '99. International conference on optical metrology, Pultusk (PL), 20-23 Sep 1999. Unpublished.

Hanson, S.G.; Hansen, R.S.; Hansen, B.H., Simple low-cost optical system for measuring 2D rotation of reflective ball. EOS/SPIE international symposia on industrial lasers and inspection: Conference on optical measurement systems for industrial inspection, München (DE), 14-18 Jun 1999. Unpublished.

Hanson, S.G.; Hansen, R.S.; Rose, B., The use of Fourier plane filters and common path interferometers in vibrometers and electronic speckle interferometers (invited lecture). 4.

International conference on correlation optics (CorrOpt 99), Chernivtsy (UA), 11-14 May 1999. Unpublished.

Lading, L.; Hansen, R.S.; Miller, G., Long-range laser anemometry: Heterodyne versus autodyne. 8. EALA International conference on laser anemometry - advances and applications, Rome (IT), 6-9 Sep 1999. Unpublished.

Linneberg, C.; Höskuldsson, A., RAM based neural networks and principal components for classification. 6. Scandinavian symposium on chemometrics (SSC6), Porsgrunn (NO), 16-19 Aug 1999. Unpublished.

Mogensen, P.C.; Glückstad, J.; Toyoda, H.; Hara, T., Phase encryption applying parallel-aligned liquid crystal spatial light modulators. In: Optoelectronic information processing. 3. Euro American workshop, Colmar (FR), 31 May - 2 Jun 1999. (Université de Haute-Alsace, Mulhouse, 1999) p. 31.

Mogensen, P.C.; Glückstad, J., Wavefront sensing experiments using an optimised common path interferometer. International workshop on wavefront sensing and its applications, Canterbury (GB), 19-22 Jul 1999. Unpublished. Abstract available.

Rose, B.; Ibsen, P.E.; Hanson, S.G., Compact optical sensors for measuring linear and angular velocities. In: Abstract book. EOS/SPIE international symposia on industrial lasers and inspection: Conference on optical measurement systems for industrial inspection, München (DE), 14-18 Jun 1999. (European Optical Society, München, 1999) p. 56.

Thrane, L.; Yura, H.T.; Andersen, P.E., Optical coherence tomography: New analytical model and the shower curtain effect. Saratov Fall meeting '99. Workshop on optical technologies in biophysics and medicine, Saratov (RU), 5-8 Oct 1999. Unpublished.

5.2.7 Internal reports

Andersen, P.E.; Lindvold, L., Lyskilder og detektorer i det midt-infrarøde bølgelængdeområde. (Forskningscenter Risø. Afdelingen for Optik og Fluid Dynamik, Roskilde, 1999) 12 p.

Andersen, P.E.; Lindvold, L.; Thrane, L., Bestemmelse af optiske parametre for DNP display skærme. Risø-Dok-617 (1999) 26 p.

Hanson, S.G.; Lindvold, L.; Larsen, H.E.; Hansen, B.H.; Glückstad, J.; Stensborg, J., RUKO. Hologram key demonstrator project report. Risø-Dok-573 (1999) 24 p.

Larsen, H.E., Portable silicon beta spectrometer. Technical system description. Risø-I-1429(EN) (1999) 46 p.

5.3 Plasma and fluid dynamics

5.3.1 International publications

Bang, O.; Bergé, L.; Juul Rasmussen, J., Fusion, collapse, and stationary bound states of incoherently coupled waves in bulk cubic media. Phys. Rev. E (1999) v. 59 p. 4600-4613.

Chakrabarti, N., Steady state drift vortices in plasmas with shear flow in equilibrium. Phys. Plasmas (1999) v. 6 p. 417-419.

Chakrabarti, N.; Juul Rasmussen, J., Shear flow effect on ion temperature gradient vortices in plasmas with sheared magnetic field. Phys. Plasmas (1999) v. 6 p. 3047-3056.

Denz, C.; Juul Jensen, S.; Schwab, M.; Tschudi, T., Stabilization, manipulation and control of transverse optical patterns in a photorefractive feedback system. J. Opt. B (1999) v. 1 p. 114-120.

Dinesen, P.G.; Hesthaven, J.S.; Lynov, J.P.; Lading, L., Pseudospectral method for the analysis of diffractive optical elements. J. Opt. Soc. Am. A (1999) v. 16 p. 1124-1130.

Hesthaven, J.S.; Dinesen, P.G.; Lynov, J.P., Spectral collocation time-domain modeling of diffractive optical elements. J. Comput. Phys. (1999) v. 155 p. 287-306.

Konijnenberg, J.A. van de; Nielsen, A.H.; Juul Rasmussen, J.; Stenum, B., Shear-flow instability in a rotating fluid. J. Fluid Mech. (1999) v. 387 p. 177-204.

Korsholm, S.B.; Michelsen, P.K.; Naulin, V., Resistive drift wave turbulence in a three-dimensional geometry. Phys. Plasmas (1999) v. 6 p. 2401-2408.

Korsholm, S.B.; Michelsen, P.K.; Pécseli, H.L., Nonlinear dynamics of resistive electrostatic drift waves. Phys. Scr. (1999) v. T82 p. 12-16.

Królikowski, W.; Denz, C.; Saffman, M.; Luther-Davies, B.; Holmstrom, S.H., Interaction of coherent and incoherent photorefractive spatial solitons. Asian J. Phys. (1998) v. 7 p. 698-712.

Lodahl, P.; Saffman, M., Pattern formation in singly resonant second-harmonic generation with competing parametric oscillation. Phys. Rev. A (1999) v. 60 p. 3251-3261.

Naulin, V.; Juul Rasmussen, J., Vortex dynamics in inhomogeneous plasmas. Phys. Scr. (1999) v. T82 p. 28-31.

Naulin, V.; Nielsen, A.H.; Juul Rasmussen, J., Dispersion of ideal particles in a two-dimensional model of electrostatic turbulence. Phys. Plasmas (1999) v. 6 p. 4575-4585.

Schwab, M.; Denz, C.; Saffman, M., Multiple-pattern stability in a photorefractive feedback system. Appl. Phys. B (1999) v. 69 p. 429-433.

Schwab, M.; Saffman, M.; Denz, C.; Tschudi, T., Fourier control of pattern formation in an interferometric feedback configuration. Opt. Commun. (1999) v. 170 p. 129-136.

Wang, P.Y.; Saffman, M., Selecting optical patterns with spatial phase modulation. Opt. Lett. (1999) v. 24 p. 1118-1120.

5.3.2 Danish publications

Jensen, V.O., Fusionsenergi - hvor langt er vi nået?. Nat. Verden (1999) v. 82 (no.4) p. 14-25.

Lynov, J.P.; Singh, B.N (eds.), Association Euratom - Risø National Laboratory annual progress report for 1998. Risø-R-1136(EN) (1999) 46 p.

5.3.3 Conference lectures

Jessen, T.; Michelsen, P.K., Spectral time series analysis of plasma turbulence. In: Contributed papers. 26. European Physical Society conference on controlled fusion and plasma physics, Maastricht (NL), 14-18 Jun 1999. Schweer, B.; Oost, G. Van; Vietzke, E. (eds.), (European Physical Society, Mulhouse, 1999) (Europhysics conference abstracts, vol. 23J) p. 557-560.

Konijnenberg, J.A. van de; Nielsen, A.H.; Nijs, R. de; Juul Rasmussen, J.; Stenum, B., Shear flow instability in a rotating fluid layer. In: Simulation and identification of organized structures in flows. IUTAM symposium, Lyngby (DK), 25-29 May 1997. Sørensen, J.N.; Hopfinger, E.J.; Aubry, N. (eds.), (Kluwer Academic Publishers, Dordrecht, 1999) (Fluid mechanics and its applications, v. 52) p. 119-128.

Korsholm, S.B.; Michelsen, P.K., Density and temperature gradient driven drift waves. In: Contributed papers. 26. European Physical Society conference on controlled fusion and plasma physics, Maastricht (NL), 14-18 Jun 1999. Schweer, B.; Oost, G. Van; Vietzke, E. (eds.), (European Physical Society, Mulhouse, 1999) (Europhysics conference abstracts, vol. 23J) p. 59-552.

Michelsen, P.K.; Korsholm, S.B.; Pécseli, H.L., Three dimensional studies of a modified Hasegawa-Wakatani model. In: Contributed papers. 26. European Physical Society conference on controlled fusion and plasma physics, Maastricht (NL), 14-18 Jun 1999. Schweer, B.; Oost, G. Van; Vietzke, E. (eds.), (European Physical Society, Mulhouse, 1999) (Europhysics conference abstracts, vol. 23J) p. 553-556.

Naulin, V., Structure detection in driven drift wave turbulence. In: Simulation and identification of organized structures in flows. IUTAM symposium, Lyngby (DK), 25-29 May 1997. Sørensen, J.N.; Hopfinger, E.J.; Aubry, N. (eds.), (Kluwer Academic Publishers, Dordrecht, 1999) (Fluid mechanics and its applications, v. 52) p. 409-418.

Naulin, V.; Juul Rasmussen, J.; Nycander, J., Transport barriers in a model for turbulent equipartition. In: Contributed papers. 26. European Physical Society conference on controlled fusion and plasma physics, Maastricht (NL), 14-18 Jun 1999. Schweer, B.; Oost, G. Van; Vietzke, E. (eds.), (European Physical Society, Mulhouse, 1999) (Europhysics conference abstracts, vol. 23J) p. 545-548.

Naulin, V.; Korsholm, S.; Michelsen, P.K., Three-dimensional simulations of drift-wave turbulence. In: Theory of fusion plasmas. International School of Plasma Physics "Piero Caldirola": Joint Varenna-Lausanne international workshop (ISSP 18), Varenna (IT), 31 Aug - 4 Sep 1998. Connor, J.W.; Sindoni, E.; Vaclavik, J. (eds.), (Editrice Compositori, Bologna, 1999) p. 505-510.

Schwab, M.; Denz, C.; Saffman, M., Multiple stability and pattern control in a photorefractive feedback system. In: Advances in photorefractive materials, effects, and devices. 7. Topical meeting on photorefractive materials, effects and devices (PR'99), Elsinore (DK), 27-30 Jun 1999. Andersen, P.E.; Johansen, P.M.; Pedersen, H.C.; Petersen, P.M.; Saffman, M. (eds.), (Optical Society of America, Washington, DC, 1999) (OSA trends in optics and photonics series, v. 27) p. 424-431.

5.3.4 Unpublished Danish lectures

Juul Rasmussen, J., Collaps and coherent structures in nonlinear optical media. Ph.D. course on nonlinear waves, coherent structures and stochastic dynamics, Technical University of Denmark (4 lectures), Lyngby (DK), 11-12 Nov 1999. Unpublished.

Korsholm, S.B.; Lynov, J.P.; Michelsen, P.K., Fusion energy research. In: Programme. Abstracts. List of participants. Annual meeting of the Danish Physical Society, Nyborg (DK), 3-4 Jun 1999. (HCØ Tryk, København, 1999) p. AF18P.

Lodahl, P., Generation and characterization of single-photon fock states. Atomic physics and quantum optics seminar, University of Århus, Århus (DK), 20 May 1999. Unpublished.

Lodahl, P.; Saffman, M., Pattern formation in intracavity second harmonic generation. In: Programme. Abstracts. List of participants. Annual meeting of the Danish Physical Society, Nyborg (DK), 3-4 Jun 1999. (HCØ Tryk, København, 1999) p. AF12.

Michelsen, P.K., Fusionsenergi - er det en mulighed?. Foredrag på Danmarks Tekniske Universitet, Lyngby (DK), 25 Oct 1999. Unpublished.

Michelsen, P.K., Fusionsenergi - er det en mulighed?. Foredrag på Danmarks Tekniske Universitet, Lyngby (DK), 7 Oct 1999. Unpublished.

Nielsen, A.H.; Stenum, B., 2D coherent structures in rotating flows. Lecture in the DTU hydrodynamic lecture series, Lyngby (DK), 25 Nov 1999. Unpublished.

Stenum, B., Undersøgelser af mikroflow på Risø. Seminar at Dantec Measurement Technology, Skovlunde (DK), Aug 1999. Unpublished.

5.3.5 Unpublished international lectures

Bache, M.; Lodahl, P.; Saffman, M., Instabilities and localized structures in cavity enhanced $\chi^{(2)}$-nonlinear processes. Nonlinear science festival 2, Risø (DK), 1-4 Dec 1999. Unpublished.

Bache, M.; Lodahl, P.; Saffman, M., Influence of competing parametric oscillation on pattern formation in second harmonic generation. Euroconference on control of complex behaviour in optical systems (COCOS), Munster (DE), 7-10 Oct 1999. Unpublished.

Clercx, H.J.H.; Nielsen, A.H., Vortex statistics for decaying 2D turbulence in containers with periodic and with no-slip boundaries. In: Vortical structures in rotating and stratified fluids. Book of abstracts. EUROMECH colloquium 396 with ERCOFTAC and TAO workshops, Cortona (IT), 22-25 Jun 1999. ([s.n.], [s.l.], 1999) 1 p.

Hansen, H.; Lodahl, P.; Schiller, S.; Mlynek, J., Quantenzustandstomographie eines optischen 1-Photon Fock-Zustandes. Frühjahrstagung der Deutschen Physikalischen Gesellschaft, Heidelberg (DE), 15-19 Mar 1999. Unpublished.

Jensen, V.O., The physics behind diffusion caused by collision between like particles. 34. Nordic plasma and gas discharge symposium, Geilo (NO), 24-27 Jan 1999. Unpublished.

Juul Rasmussen, J., Statistical properties of cross-field plasma transport: Vortices, avalanches and self-organization. Fluctuations in fusion and non-fusion plasmas. TTF Turbulence Working Group, Padova (IT), 3-4 Mar 1999. Unpublished.

Juul Rasmussen, J., Vortex dynamics and particle transport in electrostatic turbulence of magnetized plasmas. 1999 plasma Easter meeting on nonlinear phenomena in fluids and plasmas, Turin (IT), 7-9 Apr 1999. Unpublished.

Juul Rasmussen, J., Turbulent equipartition in plasma and fluid. International workshop on solitons, collapses and turbulence: Achievements, developments and perspectives, Chernogolovka (RU), 3-10 Aug 1999. Unpublished.

Juul Rasmussen, J., Introduction to the Study Centre: Coherent structures. 1999 TAO Study Centre, Palma de Mallorca (ES), 6 Sep - 1 Oct 1999. Unpublished.

Juul Rasmussen, J.; Naulin, V.; Konijnenberg, J.A. van de; Stenum, B., Vortex dynamics and turbulence in the β-plane. 24. General Assembly of the European Geophysical Society, The Hague (NL), 19-23 Apr 1999. Geophys. Res. Abstr. (1999) v. 1 p. 810.

Juul Rasmussen, J.; Naulin, V., Cross-field plasma transport, avalanches, self-organized criticality and vortex dynamics. 34. Nordic plasma and gas discharge symposium, Geilo (NO), 24-27 Jan 1999. Unpublished.

Juul Rasmussen, J.; Nycander, J.; Naulin, V., Transport barriers in a model for turbulent equipartition. In: Programme and abstracts. 8. European fusion theory conference, Como (IT), 27-29 Oct 1999. (Istituto di Fisica del Plasma "Piero Caldirola", Milano, 1999) OW 7.

Konijnenberg, J. van de; Naulin, V.; Stenum, B.; Juul Rasmussen, J., Formation of a polar vortex by oscillatory forcing in a rotating fluid. In: Vortical structures in rotating and stratified fluids. Book of abstracts. EUROMECH colloquium 396 with ERCOFTAC and TAO workshops, Cortona (IT), 22-25 Jun 1999. ([s.n.], [s.l.], 1999) 2 p.

Konijnenberg, J.A. van de; Naulin, V.; Juul Rasmussen, J.; Stenum, B.; Heijst, G.J.F. van, Spin-up in a circular tank with a sloping bottom. 24. General Assembly of the European Geophysical Society, The Hague (NL), 19-23 Apr 1999. Geophys. Res. Abstr. (1999) v. 1 p. 786.

Konijnenberg, J.A. van de; Stenum, B.; Juul Rasmussen, J., The shallow-water approximation versus the Taylor-Proudman theorem in a curved geometry. 24. General Assembly of the European Geophysical Society, The Hague (NL), 19-23 Apr 1999. Geophys. Res. Abstr. (1999) v. 1 p. 794.

Korsholm, S.B.; Michelsen, P.K.; Naulin, V.; Juul Rasmussen, J., Poloidal flows and transport in non-periodic 3D simulations of the Hasegawa-Wakatani model. IAEA Technical Committee meeting on first principle-based transport theory, Monestery Seeon (DE), 21-23 Jun 1999. Unpublished. Abstract available.

Korsholm, S.B.; Michelsen, P.K.; Naulin, V., Three dimensional drift wave simulations. In: Programme and abstracts. 8. European fusion theory conference, Como (IT), 27-29 Oct 1999. (Istituto di Fisica del Plasma "Piero Caldirola", Milano, 1999) PT 12.

Korsholm, S.B.; Naulin, V., Plasma transport, zonal flows and Reynolds stress in 2 and 3D models of drift wave turbulence. Nonlinear science festival 2, Risø (DK), 1-4 Dec 1999. Unpublished.

Lodahl, P.; Bache, M.; Saffman, M., Pattern formation in second harmonic generation with competing parametric oscillation. Nonlinear science festival 2, Risø (DK), 1-4 Dec 1999. Unpublished.

Lomholt, S.; Stenum, B., Numerical and experimental investigations of magnetic particle separation. 4. Annual meeting of the Nordic ERCOFTAC Pilot Center, Brekstad (NO), 25-27 Aug 1999. Unpublished.

Mamaev, A.V.; Saffman, M.; Mezentsev, V.K., Optical patterns in a passive ring cavity containing a photorefractive crystal. In: Post-deadline papers. 7. Topical meeting on photorefractive materials, effects and devices (PR'99), Elsinore (DK), 27-30 Jun 1999. (Risø National Laboratory, Roskilde, 1999) p. 51-54.

Naulin, V., Vortex dynamics and Reynolds stress in dift-wave simulations. Fluctuations in fusion and non-fusion plasmas. TTF Turbulence Working Group, Padova (IT), 3-4 Mar 1999. Unpublished.

Naulin, V., Role of polarization drift in drift wave simulations. TTF turbulence workshop, Madrid (ES), 24-26 Mar 1999. Unpublished.

Naulin, V., Cross field plasma transport and poloidal flows. IAEA Technical Committee meeting on first principle-based transport theory, Monastery Seeon (DE), 21-23 Jun 1999. Unpublished.

Naulin, V., Closing the gap between numerics and experiment. 28. Steering Committee meeting, Risø (DK), 26. Apr 1999. Unpublished.

Naulin, V., Homogenization of potential vorticity. 1999 TAO Study Centre, Palma de Mallorca (ES), 6 Sep - 1 Oct 1999. Unpublished.

Naulin, V.; Juul Rasmussen, J.; Nycander, J., Zonal flow and transport barriers in turbulent equipartition. 34. Nordic plasma and gas discharge symposium, Geilo (NO), 24-27 Jan 1999. Unpublished.

Naulin, V.; Juul Rasmussen, J.; Nycander, J., Transport barriers in a model for turbulent equipartition. Seminar at Düsseldorf University, Düsseldorf (DE), Dec 1999. Unpublished.

Naulin, V.; Korsholm, S.B.; Michelsen, P.K.; Juul Rasmussen, J., Plasma transport, zonal flows, and Reynolds stress in 2 and 3D models of drift wave turbulence. In: Programme and abstracts. 8. European fusion theory conference, Como (IT), 27-29 Oct 1999. (Istituto di Fisica del Plasma "Piero Caldirola", Milano, 1999) PT 14.

Naulin, V.; Nielsen, A.H.; Juul Rasmussen, J., Transport und Disposition idealer Teilchen in 2-dimensionaler Turbulenz. Kolloquium at Kiel University, Kiel (DE), Dec 1999. Unpublished.

Nielsen, A.H.; Clercx, H., Two-dimensional turbulence in a bounded domain. 1999 TAO Study Centre, Palma de Mallorca (ES), 6 Sep - 1 Oct 1999. Unpublished.

Nielsen, A.H.; Coutsias, E.A.; Clercx, H.J.H., Forced and decaying 2D turbulence in circular containers. In: Vortical structures in rotating and stratified fluids. Book of abstracts. EUROMECH colloquium 396 with ERCOFTAC and TAO workshops, Cortona (IT), 22-25 Jun 1999. ([s.n.], [s.l.], 1999) 1 p.

Saffman, M., Atomic pattern formation. Nonlinear science festival 2, Risø (DK), 1-4 Dec 1999. Unpublished.

6. Personnel

Scientific Staff

Andersen, Peter E.
Bak, Jimmy
Clausen, Sønnik
Glückstad, Jesper
Hanson, Steen Grüner
Imam, Husian Gulam (until 31 October)
Jensen, V.O. (until 31 January)
Jessen, Niels Christian
Johansen, Per Michael
Jørgensen, Thomas Martini
Kaiser, N.E.
Kirkegaard, Mogens
Lading, Lars (until 31 September)
Larsen, Henning
Lindvold, Lars R.
Lynov, Jens-Peter
Michelsen, Poul K.
Naulin, Volker (from 1 April)
Nielsen, Anders H.
Pedersen, Henrik Chresten
Petersen, Paul Michael
Ramanujam, P.S.
Rasmussen, Jens Juul
Saffman, Mark (until 30 September)
Schou, Jørgen
Stenum, Bjarne

Post Docs

Dinesen, Palle
Hansen, Rene Skov
Konijnenberg, Johan Antoon van de (until 31 July)
Mogensen, Paul Christian
Naulin, Volker (until 31 March)

Industrial Post Docs

Løbel, Martin
Nielsen, Steen Arnfred (from 1 July)

PhD Students

Andersen, Anders (from 1 September)
Andersen, Thim Nørgaard (from 1 October)
Bache, Morten (from 1 April)
Basse, Nils
Jensen, Peter Snoer (from 1 July)

Jensen, Sussie Juul
Jessen, Thomas (until 30 September)
Korsholm, Søren Bang
Lodahl, Peter
Lomholt, Sune
Nielsen, Birgitte Thestrup (until 15 December)
Nikolajsen, Thomas
Okkels, Fridolin
Thrane, Lars
Tycho, Andreas

Industrial PhD Students

Kitchen, Steven R.
Linnebjerg, Christian

Technical Staff

Andersen, Finn
Eilertsen, Erik
Hansen, Bengt Hurup
Nordskov, Arne
Jessen, Martin
Petersen, Torben D.
Rasmussen, Erling
Sass, Bjarne
Stubager, Jørgen
Thorsen, Jess

Secretaries

Astradsson, Lone
Carlsen, Heidi
Skaarup, Bitten

Students Working for the Master's Degree

Andersen, Eva Samsøe (from 2 August)
Christensen, Bo Toftmann
Clausen, Thomas
Holmelund, Evy (from 1 August)
Sundstrøm, Martin

Student Assistant

Truelsen, Jimi (18-22 October)

Guest Scientists

Baragiola, Raul, University of Virginia, USA
Dridi, Kim, Technical University of Denmark, Denmark
Haglund, Richard, Vanderbilt University, USA
Hesthaven, Jan S., Brown University, Rhode Island, USA
Horvath, Robert, ELTE University, Budapest, Hungary

Karpman, Vladimir, Racah Institute of Physics, Hebrew University, Jerusalem, Israel
Limeres, Josefa, Universidad Autónoma de Madrid, Spain
Lushnikov, Pavel, Landau Institute, Moscow, Russia
Mamaev, Alexander, Russian Academy of Sciences, Moscow, Russia
Marian, Mihaela-Anca, National Institute for Laser, Plasma and Radiation Physics, Romania
Pedrys, Roman, Jagellonian University, Poland
Podivilov, Evgeny V., Institute of Automation and Electrometry, Novosibirsk, Russia
Popov, Ivan, Vavilov Institute, St. Petersburg, Russia
Ruban, Victor P., Landau Institute for Theoretical Physics, Moscow, Russia
Saffman, Mark, University of Wisconsin-Madison, USA
Schwab, Michael, Technische Universität Darmstadt, Germany
Shagalov, Arkadi G., Institute of Metal Physics, Ekaterinburg, Russia
Sturman, Boris I., International Institute for Nonlinear Studies, Novosibirsk, Russia
Wyller, John, Agricultural University of Norway, Norway
Yura, Harold T., The Aerospace Corporation, Los Angeles, USA

Short-term Visitors

Antar, Ghassan, Association Euratom-CEA, DRFC, CEA/Cadarache, France
Bergé, Luc, Commissariat à l'Energie Atomique, Centre d'Etudes de Limeil-Valenton, France
Germaschweski, Kai, University of Düsseldorf, Germany
Gonzalo, Luis Garcia, University Carlos III, Madrid, Spain
Grauer, Rainer, University of Düsseldorf, Germany
Konijnenberg, Johan van de, Eindhoven, Holland
Krane, Bård, University of Oslo, Norway (10-12/2)
Mezentsev, Vladimir K., Aston University, United Kingdom
Milligen, Boudewijn van, Ciemat, Madrid, Spain
Paulsen, Jim-Viktor, University of Tromsø, Norway
Pasmanter, Ruben, Royal Dutch Meteorological Institute, Holland
Rubahn, Horst-Günter, Odense University, Denmark
Schäfer, Tobias, University of Düsseldorf, Germany
Skryabin, Dmitry, University of Strathclyde, Glasgow, United Kingdom

Bibliographic Data Sheet **Risø-R-1157(EN)**

Title and author(s)

Optics and Fluid Dynamics Department

Annual Progress Report for 1999

Edited by S. G. Hanson, P. M. Johansen, J. P. Lynov and B. Skaarup

ISBN	ISSN
87-550-2650-8 (Internet)	0106-2840 0906-1797

Dept. or group	Date
Optics and Fluid Dynamics Department	May 2000

Pages	Tables	Illustrations	References
93	1	52	215

Abstract (max. 2000 char.)

The Optics and Fluid Dynamics Department performs basic and applied research within the three programmes: (1) optical materials, (2) optical diagnostics and information processing and (3) plasma and fluid dynamics. The department has core competences in: optical sensors, optical materials, biooptics, numerical modelling and information processing, non-linear dynamics and fusion plasma physics. The research is supported by several EU programmes, including EURATOM, by research councils and by industry. A summary of the activities in 1999 is presented.

Descriptors INIS/EDB

DYNAMICS; FLUIDS; LASERS; NONLINEAR OPTICS; NONLINEAR PROBLEMS; NUMERICAL SOLUTION; PLASMA; PROGRESS REPORT; RESEARCH PROGRAMS; RISOE NATIONAL LABORATORY; THERMONUCLEAR REACTIONS